Dissertation

Effects of Lysophosphatidic Acid-mediated Signaling Cascades on Microglia Inflammation and Metabolism

submitted by

Lisha JOSHI

for the Academic Degree of

Doctor of Philosophy

(PhD)

at the

Medical University of Graz

Gottfried Schatz Research Center

for Cell Signaling, Metabolism and Aging

under the Supervision of

Prof. Dr. Wolfgang SATTLER

2021

Declaration

I hereby declare that this thesis is my own original work and that I have fully acknowledged by name all of those individuals and organizations that have contributed to the research for this thesis. Due acknowledgement has been made in the text to all other material used. Throughout this thesis and in all related publications I followed the “Guidelines of the Medical University of Graz on Good Scientific Practice“.

Graz, 15.07.2021

Lisha Joshi

Disclosures

Parts of my dissertation have been published in:

Joshi L, Plastira I, Bernhart E, Reicher H, Koyani CN, Madl T, Madreiter-Sokolowski C, Koshenov Z, Graier WF, Hallström S, Sattler W. Lysophosphatidic Acid Induces Aerobic Glycolysis, Lipogenesis, and Increased Amino Acid Uptake in BV-2 Microglia. International Journal of Molecular Sciences. 2021 Jan; 22(4):1968. doi: 10.3390/ijms22041968. PMID: 33671212 Free PMC article.

Joshi L, Plastira I, Bernhart E, Reicher H, Triebl A, Köefeler H, Satler W. Inhibition of Autotaxin and Lysophosphatidic acid receptor 5 Attenuates Neuroinflammation in LPS-activated BV-2 microglia and a Mouse Endotoxemia Model. International Journal of Molecular Sciences. (Submitted; manuscript number ijms-1309314)

All of the above-mentioned co-authors have explicitly agreed to the use of their data in this thesis.

Other co-authored publications:

MAPK signaling determines lysophosphatidic acid (LPA)-induced inflammation in microglia. Plastira I, Bernhart E, **Joshi L**, Koyani CN, Strohmaier H, Reicher H, Malle E, Sattler W. J Neuroinflammation. 2020 Apr 23;17(1):127. doi: 10.1186/s12974-020-01809-1. PMID: 32326963 Free PMC article.

Small-Molecule Lysophosphatidic Acid Receptor 5 (LPAR5) Antagonists: Versatile Pharmacological Tools to Regulate Inflammatory Signaling in BV-2 Microglia Cells. Plastira I, **Joshi L**, Bernhart E, Schoene J, Specker E, Nazare M, Sattler W. Front Cell Neurosci. 2019 Nov 29;13:531. doi: 10.3389/fncel.2019.00531. eCollection 2019. PMID: 31849616 Free PMC article.

Microglial metabolism is a pivotal factor in sexual dimorphism in Alzheimer's disease. Guillot-Sestier MV, Araiz AR, Mela V, Gaban AS, O'Neill E, **Joshi L**, Chouchani ET, Mills EL, Lynch MA. Commun Biol. 2021 Jun 10;4(1):711. doi: 10.1038/s42003-021-02259-y. PMID: 34112929 Free PMC article.

Acknowledgement

I take this opportunity to express my heartfelt gratitude to my supervisor, Prof. Wolfgang Sattler, for his continuous guidance and support throughout the project and materialization of the thesis. I am extremely grateful to him for helping me realize my potential and for the constant words of encouragement.

Next, I would like to thank the Austrian Science Fund (FWF), Doctoral College in Molecular Inflammation (DK-MOLIN) and Medical University of Graz for the financial support and for giving me the opportunity to be part of such dynamic PhD program.

My experience in the lab has been home away from home. My special thanks go to Ioanna, for being my mentor, and for believing in me more than I believe in myself. A special mention to Eva and Helga for sharing their knowledge and experience. I am grateful to all my lab family Jürgen, Celina, Vishwa and Anja for creating such a wonderful environment to work together. Working with them is a pleasure every single day. They have truly made my PhD life so much easier. I appreciate Chintan for all the positivity and charm that he brings. Also I would like to thank Niroj for being such a wonderful friend. I am grateful to all the colleagues at molecular biology and biochemistry department and all my collaborators. I am grateful to my mentor, Prof. Kathrin Eller for all her support and guidance.

I highly appreciate my PhD dissertation committee members, Peter Holzer and Roland Malli for their valuable suggestion and discussion during the project.

I am grateful to Prof. Jerold Chun at Sanford Burnham Prebys Medical Discovery Institute, La Jolla, USA for providing us with $LPA5^{-/-}$ mice.

Further, I would like to express my gratitude to Prof. Marina Lynch and her research group at Trinity College Dublin for accepting me at her lab for six months and proving me an opportunity to grow both professionally and personally.

Finally, I would like to thank my family and friends for being the rock solid support in pursuing my PhD.

Lisha Joshi

Table of Content

Abbreviations

ACLF	Acute-On Chronic Liver Failure
AD	Alzheimer's Disease
AIDS	Acquired Immunodeficiency Syndrome
AKT	Protein Kinase B
ALS	Amyotrophic Lateral Sclerosis
ATP	Adenosine Triphosphate
ATX	Autotaxin
Aβ	Amyloid beta
BALF	Bronchoalveolar Lavage Fluid
BBB	Blood Brain Barrier
BCA	Bicinchoninic acid
BDNF	Brain-Derived Neurotrophic Factor
Ca2+	Calcium
CE	Cholesteryl Esters
CNS	Central Nervous System
COX-2	Cycloxygenase-2
CPT1	Carnitine Palmitoyltransferase I
CX3CR1	C-X3-C Motif Chemokine Receptor 1
DAG	Diacylglycerol
DAMPs	Damage-Associated Molecular Patterns
DMSO	Dimethyl Sulfoxide
EDG	Endothelium Differentiation Gene
ERK1/2	Of Extracellular-Regulated-Kinase1/2
FA	Fatty Acid
FAO	Fatty Acid Oxidation
FGF	Fibroblast Growth Factor
FID	Flame Ionization Detection
GAPDH	Glyceraldehyde 3-Phosphate Dehydrogenase
GDNF	Glial Cell–Derived Neurotrophic Factor
GLS	Glutaminase
GLUD1	Glutamate Dehydrogenase
GLUT	Glucose Transporter
HD	Huntington's Disease
HIF1 α	Hypoxia Inducible Factor α
HTT	Huntington Gene
IFN- γ	Interferon Gamma
IGF-1	Insulin-like Growth Factor 1
IL	Interleukin
iNOS	Inducible Nitric Oxide Synthase
LDH	Lactate Dehydrogenase
LPA	Lysophosphatidic Acid
LPAAT	LPA Acyltransferase
LPAR	Lysophosphatidic Acid Receptor
LPL	Lipoprotein Lipase
LPPs	Lipid Phosphate Phosphatases
LPS	Lipopolysaccharide
MAPK	Mitogen-Activated Protein Kinase

MD2	Myeloid Differentiation Factor 2
MS	Multiple Sclerosis
mTOR	mechanistic Target of Rapamycin
MTT	(3-(4,5-Dimethylthiazol-2-yl)-2,5-Diphenyltetrazolium Bromide)
NADP	Nicotinamide Adenine Dinucleotide Phosphate
NADPH	Nicotinamide Adenine Dinucleotide Phosphate Reduced
NF-kB	Nuclear Factor 'Kappa-Light-Chain-Enhancer'
NGF	Nerve Growth Factor
NO	Nitric Oxide
NPC	Neuro Progenitor Cell
OCR	Oxygen Consumption Rate
OXPHOS	Oxidative phosphorylation
PAMPs	Pathogen-Associated Molecular Patterns
PBS	Phosphate Buffered Saline
PCr	Phospho Creatine
PD	Parkinson's Disease
PDE	Phosphodiesterase
PDL	Poly D-Lysine
PFKFB3	6-Phosphofructo-2-Kinase/Fructose-2,6-Biphosphatase 3
PGE2	prostaglandin E2
PKD	Protein Kinase D
PL	Phospholipid
PLC	Phospholipase C
PLD	Phospholipase D
PMM	Primary Murine Microglia
ROS	Reactive Oxygen Species
SNAT	Sodium-Coupled Neutral Amino Acid Transporter
TAG	Triacylglycerol
TAM	Tyro3, Axl and Mertk
TCA	Tricarboxylic Acid Cycle
TGF-β	Transforming Growth Factor beta
TLC	Thin Layer Chromatography
TLR4	Toll Like Receptor 4
tMCAO	transient Middle Cerebral Artery Occlusion
TNF-α	Tumour Necrotic Factor Alpha
TREM2	Triggering Receptor Expressed On Myeloid Cells 1
TRIF	TIR-Domain-Containing Adapter-Inducing Interferon-B
VEGF	Vascular Endothelial Growth Factor

Zusammenfassung

Mikroglia, die immunkompetenten Zellen des ZNS, tragen in ihrer Doppelfunktion als Glia- und Immunzellen wesentlich zu Entwicklung und Homöostase des Gehirns bei. Über eine Reihe von Rezeptoren führen sie eine ständige Kontrolle des sie direkt umgebenden Parenchyms durch, was als Mikroglia-Sensom bezeichnet wird. Abhängig von den Stimuli des sie umgebenden Gewebes nehmen Mikrogliazellen ein breites Spektrum an Aktivierungszuständen ein, das von einem pro-inflammatorischen bis zu einem anti-inflammatorischen Phänotyp reichen kann. Diese Polarisierung der Mikroglia führt zu Veränderungen in ihrer Morphologie, ihrer phagozytotischen Kapazität, sowie zur Aktivierung des sogenannten Inflammasoms, das von der Sekretion von Zytokinen, Chemokinen und anderen Entzündungsmediatoren begleitet wird. Die genannten Reaktionen werden durch eine Kombination von komplexen epigenetischen, transkriptionellen, funktionellen und metabolischen Veränderungen reguliert, die schließlich den neurotoxischen oder neuroprotektiven Phänotyp der Mikroglia bestimmen.

Eines der extrinsischen Signale, die Mikroglia aktivieren, ist Lysophosphatidsäure (LPA). LPA ist ein bioaktives Lipid, das über G-Protein-gekoppelte Rezeptoren (LPA1-6) ein breites Spektrum an zellulären Reaktionen auslöst. Die Hauptquelle für LPA ist die Autotaxin (ATX)-abhängige Hydrolyse von Lysophospholipiden, die hauptsächlich von Membranphospholipiden stammen. Immer mehr Hinweise deuten darauf hin, dass die Pathogenese zahlreicher Erkrankungen mit einer dysfunktionalen Expression und Aktivität von ATX und daraus resultierenden Veränderungen in der LPA-Signalgebung zusammenhängt.

Die Ergebnisse der vorliegenden Studie zeigten, dass eine systemische Entzündung neuro-inflammatorische Prozesse induzieren kann, an welchen Mikrogliazellen maßgebliche beteiligt sind. Pro-inflammatorische Stimuli, wie z.B. LPS, initiieren eine nachgeschaltete Signalkaskade zur Aktivierung der ATX-LPA-LPAR-Achse, die wiederum Entzündungsmediatoren in Mikroglia induzieren. Die Hemmung von ATX (PF8380) und LPA5 (AS2717638) zeigte eine vielversprechende Abschwächung der neuroinflammatorischen Reaktion in LPS-stimulierten Mikroglia in vitro (BV-2 Zelllinie) und in einem akuten Sepsis-Mausmodell in vivo. Diese Daten zeigen, dass eine pharmakologische Intervention in die ATX-LPA-LPAR-Achse eine mögliche Strategie gegen neuro-inflammatorische Prozesse sein kann.

Neue Studien deuten darauf hin, dass eine metabolische Umprogrammierung ein grundlegender Faktor in der Regulation der Immunfunktion von Mikroglia ist. In der vorliegenden Studie konnte nachgewiesen werden, dass LPA die Entzündungsreaktion von primären Mikrogliazellen der Maus über den LPA-Rezeptor 5 vermittelt. Diese entzündlichen Prozesse werden von Veränderungen des metabolischen Phänotyps der primären Mikrogliazellen begleitet. In BV-2-Mikrogliazellen wiederum induziert LPA die aerobe Glykolyse, die Lipogenese und eine erhöhte Aminosäureaufnahme. Weiterhin bedingt LPA die Nutzung des Pentosephosphatweges zur Erzeugung von NADPH, einem Reduktionsäquivalent, das vor allem im Fettsäurestoffwechsel von Bedeutung ist. Alle diese metabolischen Veränderungen wurden über LPA5 vermittelt, wie mittels genetischer Deletion des Rezeptors gezeigt werden konnte.

Die Ergebnisse dieser Studie liefern uns ein besseres Verständnis der LPA-vermittelten Effekte in Mikroglia und zeigen neue Wege der Entstehung neuro-inflammatorischer Prozesse auf. Eine Intervention in den LPA-Signalweg könnte ein bedeutendes Target zur Modulation des Entzündungs- und Stoffwechselprofils von Mikrogliazellen darstellen und somit wesentlich zur Entwicklung gezielter Therapien für neurodegenerative Erkrankungen beitragen.

Abstract

Microglia are the resident immune cells of the CNS and contribute to brain development and homeostasis. They serve dual functions as glial cells and immune cells. They perform constant surveillance of the brain micro environment via a set of receptors termed as microglia sensome. Depending on the environmental stimuli, microglia adopt wide spectrum of activation state ranging from a pro-inflammatory to an anti-inflammatory phenotype. The polarization of microglia leads to changes in morphology, alterations in its phagocytic capacity, inflammasome activation, accompanied by the secretion of cytokines, chemokines and other inflammatory mediators. These responses are regulated through a combination of complex epigenetic, transcriptional, functional and metabolic changes that determine the neurotoxic or neuroprotective phenotype of microglia.

One of the extrinsic signals which activate microglia is Lysophosphatidic acid (LPA). LPA is a bioactive lipid, which acts via G-protein coupled receptors (LPA1-6) to elicit a wide range of cellular responses. The major source of LPA is autotaxin (ATX)-dependent hydrolysis of lysophospholipids, primarily derived from membrane phospholipids. There is growing evidence suggesting that the pathogenesis of numerous diseases is linked to dysfunctional expression and activity of ATX, with subsequent changes in LPA signaling.

The results of the present study demonstrated that systemic inflammation has a profound effect on neuroinflammation that involve the contribution of microglia activation. Pro-inflammatory stimuli such as LPS, initiates downstream signaling cascade to activate the ATX-LPA-LPAR axis to mediate inflammation in microglia. The inhibition of ATX (PF8380) and LPA5 (AS2717638) in endotoxemia showed promising effect in attenuating the neuroinflammatory response in LPS stimulated microglia in vitro (BV-2) and in an in vivo acute mouse model of sepsis. Hence, I provide proof that pharmacological intervention along the ATX-LPA-LPAR axis can be a potential strategy against neuroinflammation.

Emerging studies indicate that metabolic reprograming acts as an underlying factor for the regulation of immune function of microglia. In the present study, I provide evidence that LPA mediates the inflammatory response of primary murine microglia via LPA5. In addition, this inflammatory response in microglia is accompanied by changes in the metabolic phenotype of the cells. LPA induces aerobic glycolysis, lipogenesis, and increased amino acid uptake in BV-2 microglia. Further, LPA increases the utilization of pentose phosphate pathway to generate

NADPH, a reducing equivalent of the primary microglia. All of these metabolic alterations were mediated via LPA5 as supported by genetic deletion of the receptor.

The outcomes of this study provide us with a better understanding of LPA-mediated effects in microglia. These results build a foundation for understanding neuroinflammation in a different light. Interfering with LPA signaling can be a possible target in modulating the inflammatory and metabolic profile of microglia, and hence contribute to develop targeted therapies for neurodegenerative diseases.

1. Introduction

1. 1 Microglia

Over the past few decades, the historic neuro-centric view of the brain has seen quite some advancement to appreciate functions of other important cell types in the nervous system. One of such non-neuronal cell type is microglia, first discovered by Nissl in 1899. Since then, microglia have been well established for its role in the interplay between immunology and nervous system.

1.1.1. Origin

Microglia originate from mesodermal yolk sac progenitor cells and colonize the brain at E8.5 before the closure of blood brain barrier, proliferate in the parenchyma and then undergo a dieback phase until adult numbers of these cells are reached (1). This endogenous microglial population generated during early stages of embryonic development is maintained through adulthood by the virtue of its self-renewal property in physiological conditions (2,3).

1.1.2. Microglia function

Despite accounting for approximately 10% of cells in the CNS, microglia serve as universal sentinel cells in the CNS, and performs a wide range of function to maintain brain homeostasis.

1.1.2.1. Neurogenesis

Microglia produce neurotropic factors for neuronal survival and axonal growth, such as insulin-like growth factor 1 (IGF-1) to promote neurogenesis (4) during early development process. Microglia create a neurogenic microenvironment during the early development phase to assemble complex neural networks (5).

1.1.2.2. Synaptogenesis and synaptic plasticity

Microglia shapes neuronal synapses by eliminating redundant neurons that do not establish functional circuits during postnatal development. Microglia exhibits synaptic pruning via CX3CR1 to structure synaptic density and hence connectivity (6). Also, microglia release brain-derived neurotrophic factor (BDNF), prostaglandin E2 (PGE2), and IL-10 to impact synapse strength and plasticity (7).

1.1.2.3. Phagocytosis

Microglia phagocytose apoptotic neural stem cells and apoptotic neurons mediated by TAM receptors. Upon recognition of cells marked for removal or cell death, microglia engulf cells and debris by opsonisation (8).

1.1.2.4. Efferocytosis

Persistent exposure to dead or dying cells or cell debris drives inflammatory process in the CNS. Hence, in an attempt to resolve inflammation, microglia contribute to efferocytic activities, or phagocytic clearance of dead/dying cells through a reciprocal interaction between the dead/dying cells and phagocytes (9)

1.1.2.5. Immune function

Microglia perform constant surveillance of the CNS to detect subtle alterations in brain microenvironment to function in host defence and homeostasis. Microglia express a unique cluster of transcripts encoding proteins that make them competent to sense the endogenous ligands and microbes, collectively termed as microglia sensome (10,11). The sensome proteins include pattern recognition receptors to detect pathogen-associated molecular patterns (PAMPs) or tissue damage-associated molecular patterns (DAMPs). In response to inflammatory stimuli, microglia undergo activation via complex transcriptional, epigenetic, metabolic and functional changes (12–14).

1.1.2.6. Neurotransmitter release

Microglia constantly monitor neuronal activity and co-ordinate neuro-glia communication by expressing multiple receptors for neurotransmitters (15). Microglia are also shown to impart protection against excitotoxicity.

1.1.3. Heterogeneous activation states of microglia

Recent studies on microglia ontogeny combined with extensive transcriptomic analysis and novel tools to study microglia biology have deepened existing knowledge to characterize the spectrum of microglial phenotypes during development, homeostasis and disease (5).

1.1.3.1. Resting vs. activated microglia

Resting state microglia have ramified morphology with multiple branches and processes. These processes are in continuous movement, extending and retracting to inspect all areas of brain. Microglia processes constantly monitor neurons, astrocytes, and blood vessels to maintain

homeostasis (5). In response to exogeneous signals, microglia takes amoeboid shape with shortened processes directed towards the site of injury to phagocytose damaged tissue and induce appropriate effector functions (5). Multiple studies suggest that depending on external stimuli, age and disease condition, microglia activation occurs in varying degree, progressing from a mild reactive phenotype to severe neurotoxic phenotypes, in a context dependent manner (16,17).

Microglial activation is often categorized in two functional categories, a classical activation, M1 phenotype and an alternative M2 phenotype, following the prototypic nomenclature used for macrophages (18).

1.1.3.2. M1 polarization

The M1 response is induced by endotoxins, such as LPS or signals associated with infection such as IFN- γ (19). In response to injury, resident microglia become polarized toward a pro-inflammatory phenotype to release inflammatory cytokines (such as TNF-α, IL-6, IL-1β), and chemokines (such as CXCL10 and CXCL2) and induce iNOS for NO production (20). In addition, microglia activate M1 associated defence response such as altered redox homeostasis via NADPH oxidase to generate ROS, and co-stimulatory proteins like CD40 (13,15,21). This activation plays a critical role in host defence against pathogens and tumor cells yet can also damage resident healthy bystander cells by inducing inflammation and neurotoxicity (22).

1.1.3.3. M2 polarization

M2 activation is characterized by anti-inflammatory and healing activities of microglia. In response to stimuli such as IL-4, IL-13 and IL-10, microglia undergo M2 activation to promote the release of anti-inflammatory cytokines, such as IL-10 and TGF-β and induces Arginase 1 to promote the generation of polyamines. In addition, M2 microglia secrete growth factors such as insulin-like growth factor I (IGF-I), fibroblast growth factor (FGF), and CSF1, as well as neurotrophic factors such as nerve growth factor (NGF), brain-derived neurotrophic factor (BDNF), neurotrophins (NT) 4/5, and glial cell–derived neurotrophic factor (GDNF) (5) to promote tissue repair and reduce inflammation.

Although M1 and M2 categorization have been helpful for understanding microglia biology, however it is considered an oversimplification of the wide range of microglia response (23). Transcriptome studies of microglia gives a strong evidence that microglia activation is varied and context dependent. Microglia in neurodegenerative models indeed express both

neurotoxic and neuroprotective factors (24). Furthermore, recent transcriptional analysis of microglia from different regions of the healthy adult brain demonstrated remarkable regional diversity of microglia. Understanding the causes and physiological impact of spatiotemporal heterogeneity of microglia can unravel mysteries of microglia (5).

1.1.4. Effect of systemic inflammation in microglia

The peripheral immune system has a profound effect on the brain as evident by high incidence of altered consciousness and long term cognitive deficits in patients with sepsis (25). Animal studies demonstrate that systemic challenge with endotoxin such as LPS initiate a complex immunological response in the brain resulting in microglial activation, priming and/or tolerance, memory deficits and loss of brain synapses and neurons (26).

It is not entirely clear how systemic inflammation affects microglial activation. Several pathophysiological mechanisms appear to contribute to this process. The highly restrictive blood brain barrier was found to be disrupted in an LPS-induced sepsis model of mice as indicated by extravasation of sodium fluorescein (27). This increase in BBB permeability allows plasma components to infiltrate the brain including transport of pro inflammatory chemo- and/or cytokines, and peripheral immune cell infiltration and potentially allowing the entry of endotoxin into the brain (26,28,29). However, intravenous injection of radioactive I^{125}-labelled LPS is barely detected in the brain, indicating low brain uptake of LPS. Hence most effects of LPS is possibly mediated through LPS receptors located outside the BBB which stimulates afferent nerves acting at circumventricular organs to alter BBB permeability and function (30). A single systemic LPS challenge activates microglia 6h after challenge and the activation remains for at least 3 days (31).

The neuro-inflammatory hypothesis explaining the association of systemic infection and chronic central nervous system inflammation is supported by clinical evidence. For example, brain endotoxin levels are elevated two-three fold in Alzheimer's disease (AD), with LPS colocalised with Aβ1-40/42 in amyloid plaques and around vessels in AD brain (31,32). Endotoxin aggravates amyloid beta production and aggregation (33,34) and TAU hyperphosphorylation (35,36). An early attribute in patients with Parkinson's disease is intestinal permeability and increased LPS binding protein (37). Mean blood endotoxin levels are also elevated in amyotrophic lateral sclerosis (ALS) patients possibly as a result of gut inflammation and microbiome changes (38). Furthermore, peripheral diseases that elevate blood endotoxin, such as sepsis and AIDS, are known to lead to neurodegeneration (26). In addition, systemic

inflammation is reported to alter microglia morphology and its function of amyloid-beta clearance in an NLRP3-dependent manner (39). Hence, LPS has been used to study neuroinflammation in experimental models of Parkinson's disease, Alzheimer's disease as well as ALS (13,40,41).

1.1.5. Metabolic flexibility of microglia

The brain is a privileged organ protected by the blood brain barrier (BBB). This interface is formed mainly by endothelial cells and astrocytes, and strictly regulates the entry of energy substrates and other nutrients, thus creating a unique metabolic environment in the brain. Nearly 20 % of the blood flow is required to maintain the high metabolic demands of neurons and neural circuit. Glial cells support this high energy consuming neurons and neural circuits. Astrocytes are well studied for their role in rapid uptake of glutamate and their conversion to glutamine, and as a potential source of lactate production to maintain the neuron energy metabolism in a process termed astrocyte to neuron lactate shuttle (42,43). The focus has since then shifted to other glia including microglia to elucidate their contribution to energy homeostasis of neurons.

Immune cells such as macrophages and T-cells are known to react to their environment by flexibly reprogramming their intracellular metabolic pathways, that subsequently support coordinated immune functions, in a process called immunometabolism (44,45). In a similar manner, microglia as resident immune cells of the brain, possess remarkable metabolic flexibility to vary their energy substrate when changes occur in their microenvironment in order to control the microglial response. Transcriptional studies indicate that microglia express genes for transporters and enzymes involved in metabolism of the three major energy substrates (46,47). This imparts metabolic adaptability in microglia between glycolysis, oxidative phosphorylation, amino acid, and/or fatty acid metabolism to support changing cellular activities. It is conceivable that intracellular metabolites themselves can possibly serve as signalling molecules to alter immune cells phenotype and their response (44).

1.1.1.5.1. Glucose

Of the three major energy substrates, glucose is the main source of energy in brain. Microglia express multiple glucose transporters and enzymes involved in glucose metabolism. They transcribe most of the genes necessary for OXPHOS and glycolysis, indicating that microglia has an inclination towards oxidative glucose metabolism to fulfill the energy demands of these cells. Glucose uptake in microglia is mediated via five main glucose transporters (GLUT1-5). High affinity glucose transporter, GLUT3 is transcribed in both neurons and

microglia, to maintain sufficient glucose influx. Specific fructose transporter, GLUT5, is reported to be present only in microglia within the CNS, however its role in microglial function is unclear due to the low fructose content in the brain under normal physiological conditions (48,49).

The glycolytic enzyme, glyceraldehyde 3-phosphate dehydrogenase (GAPDH) was reported to be a moonlighting protein, i.e. to exhibit more than one biochemical functions. In monocytes, when GAPDH is inactive in glycolysis, it binds with TNFα mRNA to prevent its translation. This suggests increased glycolytic flux decrease TNFα mRNA – GAPDH interaction to allow production of TNFα pro-inflammatory cytokine (50).

Microglia activation interferes with glucose metabolism in a context dependent manner. LPS and IFN-γ stimulated microglia was reported to upregulate GLUT1 at mRNA and protein level (51). In contrast, mRNA level for microglia specific fructose transporter GLUT5 was decreased in inflammatory conditions, indicating its role in resting microglia (44,52). Inflammatory stimulation (LPS and/or amyloid beta) induced HIF1α, a major glycolytic transcriptional factor along with two key rate-limiting enzymes in the glycolytic pathway, hexokinase and PFKFB3. This led to increased glycolytic flux in microglia (52–54). Similar microglial shifts to glycolysis were observed in AD human patients induced pluripotent stem cell derived microglia (55) and in aging mice (56). This knowledge helps us understand disease pathology in a different light.

1.1.5.2. Fatty acids

Fatty acids are carboxylic acids with a long aliphatic chain (saturated or unsaturated). In the periphery these energy substrates are generated by means of lipoprotein lipase (LPL)-mediated hydrolysis of chylomicron- and lipoprotein-associated triglycerides (57). Once internalized, fatty acids undergo mitochondrial beta oxidation to generate ATP (58). However, the role of fatty acids as a source of energy in CNS is controversial, notably due to poor transport across the BBB, slow ATP generation, and the potential for superoxide generation (59–61).

The expression of the fatty acid translocase CD36 in microglia potentially mediates FA uptake in the cells (62). However, CPT1, which is an important enzyme for FAs import into mitochondria, is not expressed in microglia (44,63). Based on that, it would be logical to assume that under normal conditions FAO does not contribute to mitochondrial energy production in microglia.

A disrupted TCA cycle is a hallmark of microglia inflammation. The TCA metabolite citrate is reported to accumulate in response to pro-inflammatory stimuli. Mitochondrial citrate can be exported into the cytoplasm, and is converted to acetyl-CoA to be used for fatty acid biosynthesis, including inflammatory prostaglandins (64).

1.1.5.3. Amino acids

Synaptic communication between neurons is mediated by numerous amino acids and amino acid-derived metabolites (glutamate, glycine, GABA), which is closely regulated by glial cells (65,66). Astrocytes are well studied for their role of rapid uptake of excess glutamate, the primary excitatory neurotransmitter in the CNS. In this process, internalized glutamate is converted into glutamine and released back into the extracellular space in order to protect neurons against glutamate-induced excitotoxicity.

In addition to glucose, glutamine serves as an anaplerotic energy substrate in microglia. The released glutamine can be taken up by microglia and processed through glutaminolyis. Appreciable levels of mRNA transcripts of glutamine transporter SNAT (Slc38a1) are expressed in microglia (44). Studies indicate that microglia shift its metabolism to glutaminolysis under aglycemia, in mTOR dependent manner (59). In glutaminolytic cells, when glutamine is taken up, it is broken down to glutamate and subsequently α-ketoglutarate via glutaminase (GLS) and glutamate dehydrogenase (GLUD1), which are highly expressed in human and murine microglia. The intermediate α-ketoglutarate may feed the TCA cycle to support mitochondrial respiration when glucose availability is insufficient.

Consideration has to be made that the majority of studies are based on in vitro metabolic assessment and that the metabolic states of microglia in vivo is still unclear. Recent novel tools such as hippocampal slice cultures, have added value in our understanding of microglia biology (67). In situ microglia metabolism studies suggest the role of metabolites to induce microglial activation by fine-tuning metabolic pathways. This in turn alters microglial effector function, in an attempt to regulate neuronal communication (44). A clear understanding of the intersection of microglia metabolism and neuroinflammation is required to target immunometabolism for clinical/therapeutic purpose.

1.1.6. Microglia bioenergetics in physiology

Comparative transcriptomic analyses indicate microglia express the full complement of genes required for both glycolytic and oxidative energy metabolism. That confirms microglia's ability to generate ATP by both glycolytic and oxidative pathways (68). Glucose appears to be

the essential energy fuel for microglia, although they are capable of utilizing alternative substrates for energy production (69).

Quiescent microglia have been suggested to rely mainly on oxidative phosphorylation for ATP production (70,71). On the other hand, activated microglia has been shown to shift towards aerobic glycolysis by increasing lactate production and decreasing mitochondrial respiration, a paradigm similar to macrophages (72). Under normoglycemic condition, naïve microglia appear to undergo fatty acid metabolism for energy production however with minimal contribution. However, under low energy state, fatty acid metabolism could be increased (59). Glutamine appears to be main alternate carbon source for microglia (59).

1.1.7. Microglia bioenergetics in pathology

In response to pro-inflammatory stimuli such as LPS, IL-1β and IFN-γ, microglia favour aerobic glycolysis, decrease mitochondrial function and induces glutaminolysis and pentose phosphate pathway (73). The glycolytic flux then influences the pro-inflammatory gene expression at both transcriptional and post translational levels (68). In addition, microglia utilizes glucose metabolism pathway for production of superoxide by NADPH oxidase (68).

The acute phase of microglia activation, marked by release of several inflammatory mediators as well as oxidative stress, is thought to be beneficial to the CNS. Conversely, chronic stimulation of microglia may result in deleterious effects to induce neuronal damage (69).
Deficits in energy metabolism, particularly glucose hypometabolism, along with mitochondrial dysfunction are regarded as early indicators of neurodegenerative diseases (69). Moreover, the contribution of microglial activation and microglia metabolism has gathered focus of research in the context of neurodegenerative diseases (44).

1.1.8. Microglia in pathology

Microglia play a critical role in many acute and chronic disorders such as oxidative stress, neuropathic pain, traumatic injury, stroke/ischemia, immunological diseases, tumour, neurodegenerative disease and psychiatric disorder. Impairment of microglia function leads to the creation of an environment in the CNS for acute or chronic pathological processes. Recent genetic and functional studies implicate involvement of microglia in determining progression of almost all CNS diseases. However, whether microglia have detrimental or beneficial function or is context dependent in diseased condition is currently under investigation (5).

1.1.8.1. Alzheimer's disease

AD is a progressive neurological disorder characterized by extracellular amyloid β (Aβ) aggregates infiltrated with reactive microglia and astrocytes, and intracellular bundles of Tau tangles. Initial phagocytosis of Aβ plaques by microglia might prove to be beneficial. However chronic exposure of microglia to Aβ, can induce neuroinflammation to exhibit detrimental neurotoxic effects (74). Recent genetic analysis has identified variants of TREM2, expressed by microglia, as an important risk factor for AD, further instigating the role of microglia in the pathogenesis of AD (75).

Compromised brain energy metabolism is a notable attribute in AD pathology and in aging (76). Brains of AD patients revealed decreased levels of GLUT-1 and -3, leading to diminished brain glucose uptake and a subsequent cognitive decline (69,77). A remarkable loss of activity of glycolytic enzymes was observed in brain tissue of AD patients (78). Hence instead of a metabolic shift, a metabolic crisis has been associated with chronic AD progression (67,79). In a similar manner, in vitro studies with primary microglia exposed with Aβ was reported to drive metabolic changes to impair microglia function.

1.1.8.2. Parkinson's disease

PD is a brain disorder that mainly affects the motor system. It is characterized by misfolded α-synuclein, called Lewy bodies and loss of dopaminergic neurons in the substantia nigra. Studies indicate that α-Synuclein activates microglia via TLR1/2 signalling to induce proinflammatory responses (80). In addition, the disease progression is reported to be due to microglia mediated TAM (Tyro3, Axl and Mertk) -dependent phagocytosis of distressed spinal cord motor neurons (5).

PD patients are reported to display microglial activation in the cortex and basal ganglia and decreased brain glucose metabolism in initial stage of disease progression, as indicated by neuroimaging method (81). Metabolic analysis in cultured microglia revealed α-synuclein activated microglia induced modulation of the glutamate-glutamine cycle, with a decrease in intracellular glutamate (82). It is assumed that microglial mitochondrial reprograming, ROS production and proinflammatory cytokine, which together contribute to dopaminergic neurodegeneration as observed in PD (44).

1.1.8.3. Multiple Sclerosis

MS is a condition characterized by degradation of myelin sheaths. Active lesions are associated with the presence of high level of reactive microglia in the substantia nigra and

putamen (69). In MS, microglia is reported to degrade myelin debris by receptor mediated phagocytosis and lysosomal activity, thereby demyelinating brain and spinal cord (83). This process is mediated through NF-kB activation (84). Early studies indicate a substantial role of mitochondrial dysfunction and impaired energy metabolism in the progression of MS (85,86). Evident to this, dysfunctional pyruvate metabolism, with elevated blood level of pyruvate and other TCA metabolites such as α-ketoglutarate, citrate and succinate in patients with MS were reported (69,87).

1.1.8.4. Huntington's disease

HD is a mostly inherited neurodegenerative disease which occurs due to the mutation in the huntingtin gene (HTT). Studies indicate accumulation of activated microglia in targeted cerebral areas to induced neuronal degeneration(88). HD is strongly correlated with glucose hypometabolism and decreased striatal metabolism (89).

1.1.8.5. Psychiatric disorders

Psychiatric disorders, such as obsessive compulsive disorders and autism spectrum, and neurodevelopmental disorders are considered to be of neuronal origin. Growing evidence suggest the role of microglia in neurodevelopment by contributing to neurogenesis, phagocytosis, synaptic connectivity and pruning to shape neural wiring during development. This implies that microglia dysfunction could contribute to the pathogenesis of these diseases (5). In line, the evidence of microgliosis in patients with major depressive disorder (90,91), suggests the role of neuroinflammation in the pathophysiology of these psychiatric disorders.

1.1.8.6. Neuropathic pain

Peripheral nerve injury leads to the activation of purinergic receptors (P2Y12, P2X4 and P2X&) expressed by microglia (92). Recent studies indicate the role of LPA5, a sensome receptor expressed by microglia as a key mediator of neuropathic pain (93). Microglial activation is hence suggested to contribute to the pathogenesis of neuropathic pain.

1.1.8.7. Microglia and aging

Age is a major risk factor for several neurodegenerative diseases. Aging microglia display signs of dystrophy, with reduced ability to survey the brain and respond to insults (5,94). The microglia processes are short, tortuous and swollen with reduced ramification in microglia from aged mice (95). Proteomic analyses revealed alterations in proteins involved in inflammatory signalling, mitochondrial function and cellular metabolism in primary microglia from

aged mice in comparison to that of young mice (96). Aged mice showed impaired blood flow and reduced brain glucose consumption (97). Aging is reported to skew microglia towards a primed inflammatory state (16) with subsequent imbalances in the cellular levels of metabolic substrates (98).

1.2.1. The ATX-LPA-LPAR axis

The human brain is composed largely of lipids contributing to 60 – 70% of dry weight (99). The high lipid content of the brain highlights the essential roles of these diverse set of molecules in brain homeostasis and the abundance of different lipid species in the CNS underlines that their function goes beyond structural and energetic requirements of the cells (100). Lipids are important in cell signaling, energy homeostasis and tissue physiology (101) and include well known families such as cholesterol, sphingolipids, glycerol phospholipids as well as fatty acids eicosanoids, endocannabinoids or prostaglandin (102,103). Of note, lipids are recognized as ligands themselves, or form precursors for secondary messengers to initiate events of cellular signaling (102). Lysophosphatidic acid (LPA), belonging to the lysophospholipid family, is not only a single molecular entity but is comprised of small structurally different bioactive lipid species (103).

1.2.2. Autotaxin (ATX)

ATX is ecto-nucleotide pyrophosphatase/phosphodiesterase-2 enzyme, encoded by the ENPP2 gene, that hydrolyzes extracellular lysophospholipids into lysophosphatidic acid (LPA), a growth factor like signaling phospholipid. ATX is synthesized as pre-pro-enzyme and undergoes post translational modification (N-glycosylation) followed by proteolytic maturation (104,105). ATX is a secreted glycoprotein with lysophopholipase D properties. Probable sources of plasma ATX are lymphatic high endothelial venules and adipose tissue, which secrete ATX at high levels (106). ATX is widely expressed in the neuronal tissue, ovary, lung, intestine, adipose tissue, lymph nodes, including biological fluids such as blood (107–109).

ATX is a multi-domain proteins consisting of two N-terminal cystein-rich somatomedin B-like (SMB) domains, a central catalytic phosphodiesterase (PDE) domain and a catalytically inactive C-terminal nuclease-like (NUC) domain (110), with a strong affinity for LPC. The complexity of ATX-LPA signaling is further elaborated by alternative splicing of ATX mRNA to give distinct isoforms (α, β, γ, δ) which differs by the presence or absence of sequences encoded by exons 12 and 21. However the functions of isoform-specific ATX has not been

characterized. ATX α was the first melanoma-derived isoform. ATX β was originally cloned from teratocarcinoma cells and is the canonical and most predominant isoform (111,112). The brain specific ATX γ isoform is characterized by the presence of 25 AA insertions encoded by exon 21(110,113,114).

A fine-tuned regulation of ATX is required to contribute to development and various biological actions. Homozygous ATX genetic deletion and abrogation of LPA production manifested in embryonic lethality by affecting vasculature development, neural tube defects, allantois malformation, and asymmetric headfolds. Heterozygous ATX genetic deletion resulted in phenotypically normal mice with 50% reduction in ATX activity and LPA production (115,116). In addition, embryonic transgenic overexpression of ATX also resulted in lethality, asserting the importance of tightly regulating level of LPA during development (117) and also in adulthood. On the contrary, studies show that majority of ATX expression is dispensable during adult life, suggesting ATX as a potential drug target in ATX-induced pathogenic conditions (118).

The majority of biological functions of ATX are mediated via the extracellular production of LPA with a subsequent action on G protein coupled receptors to exert pleiotropic effects (107,119).

1.2.3. Lysophosphatidic acid (LPA)

The enzymatic product of ATX, LPA is a small glycerophospholipid (molecular mass: 430-480 Da). Primarily derived from membrane phospholipids, LPA consist of a glycerol backbone with an ester or ether - linked fatty acid chain (acyl or alkyl chain of varied length and saturation in position 1 or 2) and a polar phosphate group (120). 18:1 oleoyl-LPA (1-acyl-2-hydroxy-sn-glycero-3-phosphate) form is the most common laboratory agent used for signaling studies (103). LPA acts as bioactive lipid species and signals via six known G-coupled receptors (GCPRs), LPA1-6 (103).

1.2.4. Metabolism and distribution of LPA

Two major enzymatic pathways are responsible for the generation of LPA. The first pathway involves the enzyme Autotaxin (ATX), which cleaves lysophospholipids to form LPA (121). This pathway is considered quantitatively the most important since mice heterozygous for Enpp2 have 50% reduced LPA in plasma compared to wild type animals (115). The other pathway involves hydrolysis of phosphatidic acid (PA) by the action of Phospholipase PLA1 or PLA2 (122). Additionally, LPA can be generated through the acylation of glycerol-3-phosphate

by glycerophosphate acyltransferase and the phosphorylation of monoacylglycerol by monoacylglycerol kinase (123). Intracellular LPA contributes for de novo biosynthesis of complex glycerolipids, whereas, extracellular LPA mediates bioactive signaling.

LPA degradation is mediated by enzymes lipid phosphate phosphatases (LPPs) (124), LPA acyltransferase (LPAAT) and various other phospholipases (PLA1 or PLA2).

LPA is ubiquitously distributed, both intracellularly and extracellularly. Within the CNS, it is found in neural progenitor cells, astrocytes, microglia and oligodendrocytes (105,125). Significant concentrations of LPA are present in biological fluids such as plasma, saliva, tears, aqueous humor and cerebrospinal fluid (126). LPA is present in the blood at a range of 0.1 μM in plasma to 10 μM in serum (103).

1.2.5. LPA function

LPA signals through its cognate GPCR to elicit a wide range of cellular functions including but not limited to cell proliferation, migration, survival, morphological changes, and production of other lipids such as prostaglandins (127,128). Six LPA receptors (LPA1-6) are known to mediate the diverse effects of LPA. LPAR are subdivided according to their homology: LPA1-3 show high homology to the endothelium differentiation gene (EDG) receptor family, while LPA4-6 receptors belong to non-EDG receptor family with a long phylogenetic distance (129). These 7-transmembrane GPCRs activate heterotrimeric G proteins subunits G12/13, Gq/11, Gi/o, and Gs to initiate numerous signal transduction pathways. The diverse effects of LPA are linked to varying spatiotemporal and cell specific expression profiles of different LPA receptors and associated activation of specific G protein-mediated cellular pathways (107).

1.2.6. LPA receptors

1.2.6.1. LPA1

The first LPA receptor to be identified was LPA1 (130). LPA1 is widely expressed in both adult mice and humans in brain, uterus, testis, lung, small intestine, heart, stomach, kidney, spleen, thymus, placenta and skeletal muscle (126,131). LPA1 couples with Gi/o, Gq/11, and G12/13 to initiate downstream signaling cascade through PLC, AKT, MAPK and Rho to affect cell proliferation, survival, migration, adhesion and Ca2+ mobilization (126,127). $LPA1^{-/-}$ mice presented neonatal lethality attributed to defective olfaction leading to impaired suckling behavior (132).

1.2.6.2. LPA2

LPA2 is mostly expressed in kidney, uterus, testis and leukocytes. Similar to LPA1, LPA2 couples with Gαi/o, Gαq/11 and Gα12/13 to active Ras, MAPK, Rac, PLC, and generate diacygycerol (DAG) to modulate cell survival and migration (126). No evidence of phenotypic abnormality was found in LPA2 deficient mice (133).

1.2.6.3. LPA3

In the development process, LPA3 is mostly expressed in the heart, mesonephros and the three spots in the otic vehicles (134). In adult human, LPA3 is most prominent in heart, testis, prostate and pancreas, whereas the adult mouse expresses LPA3 in lung, kidney, uterus and testis (135,136). LPA3 mediates PLC activation, Ca^{2+} mobilization and adenylyl cyclase inhibition and activation by coupling with Gαi/o and Gαq of the heterotrimeric G protein (137). LPA3-deficient female mice presented with delayed embryonic implantation, embryonic crowding and reduced litter size (138). This indicates that LPA3 is closely associated with reproduction (129).

1.2.6.4. LPA4

The expression of LPA4 is most prominent in mouse heart, skin, ovary, thymus, developing brain and embryonic fibroblast (133). This receptor induces formation of stress fiber and neurite retraction by activating Rho/ROCK pathway by binding with Gαq, Gαi, Gα12/13 and Gαs subunits (139,140). Adult $LPA4^{-/-}$ mice exhibit increased volume, number and thickness of trabeculae, suggesting that LPA4 negatively regulates osteogenesis (141). LPA4 is also indicated for its role in circulatory and lymphatic system development during embryonic growth (142).

1.2.6.5. LPA5

LPA5 is the fifth 7-transmembrane GPCR identified through screening approaches that led to the deorphanization of GPR92 (143). LPA5 is highly expressed in the spleen, small intestine, and colon, but relatively low in most other tissues (129,144). Additionally, in the early embryonic stage of mouse, LPA5 is expressed in forebrain, rostral midbrain and hindbrain, suggesting a possible role of LPA5 in brain development (134).

LPA5 couples to G12/13 and Gq/11 to exhibit neurite retraction, stress fiber formation and receptor internalization in vitro, and also, Ca^{2+} mobilization by activating Gq (145). Within the CNS, LPA5 expression is most prominent in microglia. In addition, LPA5 was reported to be

involved in nociception in the dorsal root ganglia (93). LPA5 has also been studied for its role in secretion of MIP-1 in mast cells (146).

1.2.6.6. LPA6

The most recently identified receptor, LPA6 couples with Gαi and Gα12/13 and activates downstream pathways. LPA activates LPA6 to mediate morphological changes and cAMP accumulation to increase intracellular Ca^{2+} (147,148). LPA6 is reported to regulate hair follicles and loss of LPA6 was found to lead to congenital alopecia (149,150).

1.2.7. Lysophosphatidic acid signaling in nervous system

LPAR expression is widely distributed with varying spatiotemporal patterns throughout the stages of development ((103). One of the major locus of LPAR expressions is the nervous system, and relatively high expression of LPA is present in the brain (151). LPA signaling has been associated with effects on neural progenitor cell (NPC) function (152), synaptic transmission (153), myelination (154) and the brain immune response (155). LPA receptors are expressed in most of the cell type of nervous system, including neural progenitors, neurons, astrocytes, microglia, oligodendrocytes, and Schwann cells, the expression of which changes during development and adulthood (156).

1.2.7.1. Neurons

During development, LPA was shown to promote NPCs differentiation for cortical neurogenesis via LPA1 and Gi/o pathway (157,158). Neurite retraction and neurite branching, the essential functions of neurons are also mediated by LPA via ROCK and Rho pathway respectively (159,160). In addition, LPA mediated morphological changes in neurons by altering actin cytoskeleton and microtubule formation (125,161). The activation of LPA further mediated synapse formation/transmission, cell death/survival, synaptic plasticity and neuronal migration (105,162).

1.2.7.2. Astrocytes

In astrocytes, LPA induces intracellular calcium mobilization, generation of ROS, cytoskeletal rearrangement and proliferation during development (103,163–165). In addition, LPA induces the expression of nerve growth factor (NGF), immediate early genes and cytokine genes in astrocytes (166). Interestingly, astrocytes express mainly LPA1 in vivo, whereas in culture, LPA1-5 were expressed. LPA in cultured astrocyte decreased uptake of glutamate and glucose, which can eventually lead to neurodegeneration (167).

1.2.7.3. Microglia

Microglia are the resident immune cells of the brain, responsible for maintaining brain homeostasis. They play an important role in the regulation of inflammation and repair by undertaking wide spectrum of activation state (83). Murine microglia express LPAR-1, -3, -5 and -6 (168). The activation of these LPA receptors induced microglial proliferation, cell membrane hyperpolarization, intracellular calcium mobilization, enhanced chemokinesis, membrane ruffling and growth factor upregulation (155,169,170). Recent studies indicate LPA instigates metabolic reprograming in human C13NJ microglial cells and in murine BV-2 microglia (171,172). In addition, LPA induced the activation of PKD, MAPK and transcriptional factors to induce a pro-inflammatory phenotype in microglia (20,173).

1.2.7.4. Oligodendrocytes

Oligodendrocytes are the myelinating glia and express LPA1 in a spatiotemporal manner (174). LPA was reported to stimulate oligodendrocyte process formation and increase differentiating oligodendrocytes (175). In vitro studies indicate that LPA induces calcium mobilization, phosphorylation of ERK1/2, process retraction and cell rounding in mature oligodendrocyte (176).

1.2.7.5. Brain vasculature

Development of the vascular system is essential for the expansion of nervous system. Hence, this requires angiogenesis, vasculogenesis, vessel maturation and stability and the formation of the BBB (177,178). LPA is reported to induce VEGF expression via LPA1 expression in endothelial cells to affect vascular biology (103,179,180). The role of LPA in vascular development is further highlighted by embryonic lethality of ATX null mice due to vascular defects (115). In vitro endothelial cells express LPA1-6 (181–183). LPA signaling promoted ECs survival and proliferation, migration and influences the vascular tone (184). Studies indicate that LPA serves as a stimulus for vasodilation via LPA1, phospholipase C and endothelial nitric oxide synthase (185). Overexposure of LPA increased BBB permeability to induce pathological conditions (103,126).

1.2.8. Dysregulated ATX-LPA-LPAR signaling

Dysfunctional expression and activity of ATX and concomitant changes in LPA signaling have been implicated in the pathogenesis of a range of diseases, most notably neurodevelopmental and neuropsychiatric disorder, pain, cardiovascular disease, idiopathic pulmonary fibrosis, chronic liver disease, infertility, and cancer. (107,126). Atypical ATX-LPA-

LPAR signaling, due to altered LPA production/degradation, or changes in receptor expression, has been especially found to disrupt the nervous system to produce sequelae relevant to human brain disorders (103).

LPS, one of the commonly known endotoxins which causes sepsis, was reported to induce ATX expression in monocytic THP-1 cells via PKR, JNK and p38 MAPK mediated pathways, to induce a pro-inflammatory response by regulating LPA levels in the microenvironment (186). Also, an increase in ATX level in bronchoalveolar lavage fluid (BALF) in LPS inhaled mice, suggested the involvement of the ATX/LPA axis in a model of LPS induced inflammation (187).

1.2.9. ATX-LPA-LPAR modulators

Aberrant LPA signaling was implicated in tumorigenesis, fibrosis, autoimmune diseases, metabolic disorders, and neurodegenerative diseases. Hence there is a growing interest to target this signaling cascade as a potential treatment approach. A number of antagonists with varying potency and selectivity has been reported and are currently undergoing preclinical and clinical studies.

Given that ATX has an extracellular PDE binding domain; it is an attractive and druggable target. In addition, since its biological effects are mediated by the production of LPA, it may not be necessary for an ATX inhibitor to cross the BBB in order to exert its function in CNS (188). Hence, a lot of attention is directed towards developing specific ATX inhibitors. Non-lipid small-molecule inhibitors have shown promise as inhibitors of ATX. The ATX catalytic domains consist of a characteristic bimetallic active site followed by a shallow binding groove, a deep lipid binding pocket and an open tunnel adjacent to the active site (110). The tripartite ATX binding site, characterized by groove, pocket and surface, facilitates development of selective and specific inhibitors (110). Early ATX inhibitors based on substrate analogs showed weak ATX inhibition (189). Ferry and colleagues identified S32826 [[4-(tetradecanoylamino) benzyl] phosphonic acid disodium salt] as a potent ATX inhibitor in vitro and in whole blood, however, it was not suitable for in vivo studies because of their limited bioavailability (190).

High-throughput-screening has identified a number of potent ATX inhibitors. Boronic acid based ATX inhibitor (HA155) formed a reversible covalent bond with the threonine nucleophile in the lipid binding pocket of ATX (191), and showed a prominent decrease in plasma LPA levels. A high throughput screening assay followed by structure-activity-relationship exploration resulted in the identification of PF-8380. This tight-binding potent inhibitor of ATX appeared to be

competitive with substrate and titrate the enzyme active site (192). PF-8380 shows good oral bioavailability and potency in reducing LPA levels in the plasma and the inflammation site (192).

Despite the considerable number of studies supporting the diverse role of LPA and its receptors, not much has been explored regarding the structure of each receptor and the ligand recognition mechanism (193–195). Identification of the LPA1 structure has enhanced our understanding of the EDG family of LPA receptors and the structure-based drug design has led to identification of antagonists with varying degree of specificity and selectivity, along with other favorable parameters like BBB permeability and bioavailability (196). One of the output of HTS is LPA5 inhibitor AS2717638, with good oral bioavailability and high selectivity for LPA5 and potency with IC50 value of 0.038 μM, however how the compound binds to LPA5 receptor precisely is currently unknown (197). A brief overview about pharmacological compounds that target LPA synthesis or LPAR-mediated signaling cascades that are currently in clinical or preclinical evaluation is provided in Table 1.

Table 1: Pharmacological antagonists of the ATX-LPA-LPAR axis that are currently in clinical or preclinical studies

	Compound	**Company**	**Indications / Diseases**	**Phase**
Autotaxin	GLPG1690 (Ziritaxestat)	Galapagos	Idiopathic pulmonary fibrosis	Phase 3 (Terminated)
	BBT 877	Bridge Biotherapeutics	Pulmonary fibrosis	Phase 1
	Compound 1 (X-165)	X-chem Inc.	Lung fibrosis	Phase 1
	PF8380	Pfizer Netherlands	Nociception	Preclinical studies
	HA130	Proteomics Centre	Muscle development	Preclinical studies
	BI-2545	Boehringer Ingelheim	Osteoarthritis pain, inflammatory condition	Preclinical studies
LPA Ab	B3/Lpathomab	Lpath Inc.	Spinal cord injury, Traumatic brain injury	Preclinical studies
	LT3114/Lpathomab	Lpath Inc.	Allodynia, Neuropathic pain	Preclinical studies
	LT3015/Lpathomab	Lpath Inc.	Neuropathic pain	Phase 1a
Pan LPARs	BrP-LPA	University of Utah	Lung injury, Asthma, Arthritis, Gliomas	Preclinical studies
LPA1	AM966	Amira	Lung fibrosis, Inflammation	Preclinical

		Pharmaceuticals		studies
	AM095	Amira Pharmaceuticals	Lung fibrosis, Kidney fibrosis, Diabetic nephropathy	Preclinical studies
	Ki-16425	Kirin Brewery Company	Lung cancer, Gliomas, Hyperalgesia, Inflammation	Preclinical studies
	ONO-7300243	ONO Pharmaceuticals Co.	Lung cancer, Benign prostatic hyperplasia	Preclinical studies
	ASP6432	Astellas Pharma	Lower urinary tract symptoms	Early Phase
	BMS-986202	Bristol-Myers Squibb	Idiopathic pulmonary fibrosis	Phase 2
	SAR-100842	Sanofi	Systemic sclerosis	Phase 2
LPAR2	n/a	Amgen	Colorectal cancer	Preclinical studies
	n/a	Ceretek LLC	Ovarian cancer	Preclinical studies
	H2L5186303	University of Memphis	Fibrosarcoma	Preclinical studies
LPAR3	Ki-16425	Kirin Brewery Company	Lung cancer	Preclinical studies
	n/a	Ceretek LLC	Fibrosarcoma	Preclinical studies
LPAR4	n/a	Amgen	n/a	n/a
LPA5	TCLPA5 4	Sanofi – Aventis	Platelet aggregation, Itch, Ischemia, neuroinflammation	Preclinical studies
	Compound 3	Sanofi – Aventis	Neuroinflammation	Preclinical studies
	AS2717638	Astellas Pharma Inc.	Neuropathic pain, Inflammatory pain, Neuroinflammation	Preclinical studies
	Compound 7e	Astellas Pharma Inc.	Neuropathic pain	Preclinical studies
LPAR6	C75	University of Bari	Hepatocellular carcinoma	Preclinical studies
	XAA	University of Bari	Hepatocellular carcinoma	Preclinical studies

1.3. Aims of the dissertation

Microglia are specialized immune cell populations of the CNS that respond swiftly and vigorously to various types of external and cellular stress. Accumulating research has been focused on studying the immune function of these cells in response to various stimuli. Emerging studies indicate that cellular metabolism regulate effector functions and consequently influences the final outcome of the immune response of the immune cells.

Growing evidence indicate the association of LPA with numerous human diseases. Aberrant LPA signaling has been indicated in neuroinflammation, and subsequent neurodegeneration in mouse and in human.

Therefore, the aims of this thesis were as following:

Part I: To study potential protective effects of ATX and LPA5 inhibition in LPS-induced neuroinflammation in vitro and in vivo.

Part II: To scrutinize the impact of LPA as a modulator of immunometabolism in BV-2 microglia.

Part III: To investigate the consequences of LPA5 knockout on LPA-induced primary microglia polarization.

2. Materials and Methods

2.1. Materials

Complete list of all the materials, reagents, antibodies, and primers that have been used during the study are presented in the appendix I.

2.2 Methods

2.2.1. Animals and treatment

Mice were housed and bred in a clean environment and a 12h/12h light-dark cycle with chow diet and water ad libitum. All animal experiments were approved by the Austrian Federal Ministry of Education, Science and Research, (BMWF-66.010/0067-V/3b/2018 and 2020_0.547.884). The generation and genotyping protocols for $LPA5^{-/-}$ genetically modified mice have been described previously (198). Briefly, homozygous LPA5 null mutant mice were generated by targeted deletion of LPA5 gene to eliminate and replace most of the LPA5 coding region in C57BL/6J mice and were generously provided by Prof. Jerold Chun (Translational Neuroscience Program, Sanford Burnham Prebys Medical Discovery Institute, La Jolla, USA). The mice were bred with their genetic backgrounds (C57BL/6J) to get wildtype (+/+) and null mutant offspring (-/-). Genotypes of all cross offspring were confirmed by PCR genotyping with the following primers:

GFP Int Rev, 5-GTGGTGCAGATGAACTTCAGG- 3;
92GTFor, 5-CAGAGTCTGTATTGCCACCAG- 3; and
92GT Rev, 5-GTCCACGTTGATGAGCATCAG- 3.

All measures were taken to minimize animal suffering and distress.

2.2.2. Endotoxemia model of neuroinflammation in C57BL/6J mice

Male C57BL/6J mice were separated into different experimental groups (n=6-8)

Group I	DMSO control (3.33 ml/kg)
Group II	LPS (5 mg/kg) in PBS + DMSO (3.33 ml/kg)
Group III	PF8380 (30 mg/kg) in DMSO + LPS (5 mg/kg) in PBS
Group IV	AS2717638 (10mg/kg) in DMSO + LPS (5 mg/kg) in PBS

The substance was administered by intraperitoneal injections. At the end of 24 h, the animals were euthanized, perfused and the brains were harvested. Right half of the brain was collected in QIAzol Lysis Reagent (Qiagen, Hilden, Germany) for RNA isolation and left half of the brain was processed for protein analyses. One hundred mg of brain tissue was

homogenized with 1 ml of tissue extraction buffer (100 mM Tris pH 7.4, 150 mM NaCl, 1 mM EGTA, 1 mM EDTA, 1% Triton X-100) con-taining protease inhibitors (aprotinin, leupeptin, pepstatin: 1 µg/ml each), 10 µM PMSF, and phosphatase inhibitors (Thermo Scientific, Vienna, Austria). Brain tissue was homogenized in a Precellys homogenizer and centrifuged at 13,000 rpm for 20 min at 4 °C. The supernatant was collected to obtain soluble protein and its concentrations were determined using the BCA kit (Thermo Scientific). One hundred microgram of total cell protein was loaded per lane and further processed for western blot analyses.
200-300 µl of blood was collected by cardiac puncture. The tubes containing blood samples were kept at room temperature for 1 h and then centrifuged at 5,000 g for 10 min. Clear supernatant was collected. Serum was diluted 1:10 and used for ELISA analyses.

2.2.3. Primary microglia culture

Primary murine microglia (PMM) were isolated from cortices of neonatal (P0-P4) of $LPA5^{+/+}$ and $LPA5^{-/-}$ mice of C57BL/6 J background. Briefly, brain cortices were dissected from the whole brain, meninges were removed, and minced with scissors into small pieces. Tissues were trypsinized (0.1% trypsin, 25 min, 37 °C, 5% CO_2), and centrifuged at 1,700 rpm for 7min. Supernatant was aspirated and the pellet was suspended in DMEM medium. This cell suspension was cultured in poly-D-lysine (PDL; 5 µg/ml) coated 75 cm2 tissue culture flasks (4 brains per flask) in DMEM containing 15% FCS, 1% penicillin, 1% streptomycin, and 5 ml L-glutamine (stock 200 mM). The cells were cultured for another 10 to 14 days. Microglia were removed from the mixed glia cell cultures by vigorously tapping the culture flasks on the bench top and seeded onto PDL-coated cell culture plates for further use.

2.2.4. BV-2 microglia

The BV-2 murine microglia cell line was purchased from Banca Biologica e Cell Factory (Genova, Italy). Cells were grown and maintained in RPMI1640 medium supplemented with 10 % FCS, 100 units/ml penicillin, and 100 µg/ml streptomycin and 1 % L-glutamine (stock 200 mM) and cultured in a humidified incubator under 5 % CO_2 and 95 % air. The culture medium was changed to fresh medium every 2-3 days. When cells reached confluency, they were split in new flasks or processed for experiments.

2.2.5. CATH.a neurons culture

The murine neuronal cell line CATH.a was from ATCC (CRL-11179) and maintained in RPMI1640 medium supplemented with 10% horse serum, 5% FCS, 1% penicillin-streptomycin,

0.4 % HEPES, and 0.2% sodium pyruvate at 37 °C in a humified incubator (5% CO2 and 95% air). When cells reached confluency, they were split into new flasks (subcultivation ratio of 1:4) using 0.12% trypsin without EDTA or used immediately for the experiments.

2.2.6. Treatment with LPA

Aqueous LPA stock solution (5mM) was aliquoted and stored at -70 °C. Fresh aliquots were used for the experiments.

Cells were plated in 6, 12 or 24-well plates. Primary microglia were allowed to adhere for 2 days. BV-2 cells were used when they reached approx. 70% confluency. Before treatments, cells were incubated in serum free DMEM medium (primary microglia) or RPMI medium (BV-2) overnight. The following day, fresh serum free medium was added, and LPA was added.

2.2.7. Treatment with LPS

LPS stock solution of 1 mg/mL was prepared in water, aliquoted and stored at -20 °C. Cells were incubated with LPS 20 ng/mL with or without inhibitors.

2.2.8. Treatment with inhibitors

PF 8380, an autotaxin inhibitor and AS2717638, a specific LPA5 inhibitor were used. The inhibitors were dissolved in DMSO to get stock concentration of 10 mM each.

2.2.9. Cell counting

Viability of cells was detected using Guava ViaCount (Merck Millipore, MA, USA). Briefly, BV-2 cells were seeded at density of 5 x 10^4 cells per well in a 12-well plate. Following overnight serum starvation, the cells were treated with LPA for indicated concentration and time periods. At the end of the treatment, cells were washed with PBS, trypsinized, and equal amounts of serum containing medium was added. 50 µL of cell suspension was stained with 150 µL of Guava ViaCount reagent, incubated for 5 minutes at room temperature and measured using Guava easyCyte 8 Benchtop Flow Cytometer (Merck Millipore). Total viable and dead cells were analyzed (172).

2.2.10. MTT assay

The mitochondrial-dependent reduction of MTT to formazan was used to measure cellular metabolic activity. Briefly, BV-2 cells were seeded at 1 x 10^4 cells per well in a 48-well plate. Following overnight serum starvation, the cells were treated with different substance (as per the experiment) for indicated concentration and time periods. At the end of the treatment, MTT was added to the final concentration of 0.5 mg/mL and incubated for 30 min at 37 °C under

standard conditions. 200 µL of lysis buffer (isopropanol/1M HCl (25:1, v/v)) was added with vigorous shaking (1200 rpm, 15 min). 100 µL of it was transferred to 96 well-plate. Absorbance was measured at 570 nm on Victor 1420 multilabel counter (Wallac) and corrected for background absorption (650 nm).

2.2.11. Seahorse XF Analyzer Respiratory Assay

Metabolic analysis of cells was performed with extracellular flux analyzer XF96 (Seahorse, Agilent, CA, USA). The sensor cartridge for XF analyzer was hydrated in a 37°C non-CO_2 incubator a day before the experiment. Cells were seeded at a density of 6 x 10^3 cells (BV-2) or 6 x 10^4 cells (PMM) per well in Seahorse XFe96 FluxPaks. After overnight serum starvation, cells were treated with the indicated concentrations of LPA for indicated time periods. Prior to the assay, cells were washed and incubated with appropriate assay medium according to manufacturer's instructions for 1h in a 37°C non-CO_2 incubator. Cellular oxygen consumption rate (OCR) was detected using XF Cell Mito Stress Test (Agilent). According to the manufacturer's instructions, stressors concentrations were optimized and added as follows: 2 µM oligomycin, a complex V inhibitor (for both BV-2 and PMM), 0.5 µM carbonyl cyanide-4-(trifluoromethoxy) phenylhydrazone FCCP (for BV-2), 1.75 µM FCCP (for PMM), and 2.5 µM antimycin A, an inhibitor of complex I and III (for both BV-2 and PMM). OCR were normalized to protein content. Experiments were performed in triplicates (172).

2.2.12. Adenosine nucleotide and phosphocreatine analysis by HPLC

Briefly, the BV-2 cells were seeded at 1 x 10^5 per well in a 6-well plate. Following overnight serum starvation, the cells were treated with the indicated concentrations of LPA for indicated time periods. Cells were washed with ice-cold PBS, scrapped off the plates and transferred into Eppendorf tubes. After mild centrifugation the supernatant was discarded and the cells lysed with 200 µL 0.4 M perchloric acid (4°C). After vortexing and centrifugation at 12000g 150 µL of the supernatant was neutralized by addition of 15-18 µL of 2 mol/L K_2CO_3 at 4°C. The supernatant obtained after centrifugation was stored at -70°C until further analysis. Adenosine nucleotides and phosphocreatine (PCr) were measured by HPLC as previously described (199,200). In brief: Separation was performed with a Hypersil ODS column (5 µm, 250 × 4 mm I.D., equipped with a precolumn; Thermo Electron Corp. Runcorn, Cheshire, UK) using a L-2200 autosampler (injection volume: 40 µL), two L-2130 HTA pumps, and a L-2450 diode array detector (all VWR International, West Chester, PA, USA). Detector signals (absorbance at 214 nm for PCr and 254 nm) were recorded and the program EZchrom Elite (VWR) was used for

data acquisition and analysis. Energy charge (EC) was calculated as: EC = [ATP+ I/2ADP]/[ATP+ ADP + AMP]. The pellets of the acid extract were resuspended in 0.1 M NaOH for protein determination using the BCA kit (Thermo Scientific, San Jose, CA, USA) (172).

2.2.13. Immunoblotting

BV2 cells were seeded onto 6-well plates at a density of 1 x 10^5 per well and serum-starved overnight prior to experiment. Then, cells were treated with the indicated concentrations of substance (according to experiment) for the indicated time periods. At the end of the time points, the medium was removed and cells were washed twice with ice-cold PBS. The cells were lysed in RIPA buffer (50 mM Tris-HCl pH 7.4, 1% NP-40, 150 mM NaCl, 1 mM Na3VO4, 1 mM NaF, 1 mM EDTA) containing protease inhibitors (Sigma, Missouri, USA; aprotinin, leupeptin, pepstatin: 1 µg/ml each), 10 µM PMSF and phosphatase inhibitors cocktail (Thermo Scientific, Waltham, MA, USA), scraped and centrifuged at 13,000 rpm for 10 min. Protein content was determined using the BCA kit (Thermo Scientific) with BSA as standard. 50 µg (BV-2) of total protein were separated on 10% SDS-PAGE gels and transferred to polyvinylidene difluoride membranes using electrophoretic transfer (Bio-Rad, Berkeley, CA, USA). Membranes were blocked with 5% w/v low-fat milk in TBST and incubated with primary antibodies overnight at 4 °C. After removal of primary antibodies, the membranes were washed for 30 min in TBST and incubated for 2h at RT with HRP-conjugated secondary antibodies (anti-rabbit 1:5,000; anti mouse 1:5,000), followed by washes with TBST for 1h. Immunoreactive bands were visualized using chemiluminescence HRP substrate development (ECL or ECL plus reagents (Thermo Scientific)) and the Bio-Rad ChemiDoc MP Imaging System (Bio-Rad, Vienna, Austria). When necessary, the membranes were cut, stripped (70 µl β-mercaptoethanol in 10 ml 60 mM Tris/2 % SDS buffer, pH 6.8; 50 °C for 20 min) and re-probed. Anti-β-actin (1:5,000) was used as loading control (172).

2.2.14. RT - qPCR analysis

BV2 (6-well plate, 1 x 10^5 cells/well) were subjected to overnight serum starvation. Cells were treated with the indicated concentrations of substance (according to the experiment) for indicated time periods. Total RNA was extracted using the RNeasy Mini kit (BV-2) or RNeasy Micro kit (PMM) (QIAGEN, Hilden, Germany) according to manufacturer's protocol and quantified using NanoDrop (Thermo Fisher Scientific, Waltham, MA, USA). RNA was reverse-transcribed by using SuperScript® III reverse transcription kit (Invitrogen, Waltham, MA, USA). Quantitative real-time PCR (qPCR) was performed on Applied Biosystems 7900HT Fast Real-

Time PCR System using QuantifastTM SYBR® Green PCR kit (QIAGEN, Hilden, Germany). Relative gene expression levels were normalized to hypoxanthineguanine phosphoribosyltransferase (HPRT) and calculated using ΔΔCT method (201). Primer sequences are listed in appendix 1.

2.2.15. Lactate assay

Lactate content in the supernatant was measured using EnzyChrom™ Glycolysis Assay Kit (ENZO Life Sciences, Switzerland) according to manufacturer's protocol. Briefly, BV-2 (12-well plate, 5 x 10^4 cells per well) or PMM (96-well plate, 6 x 10^4 cells per well, were allowed to adhere, then incubated in serum-free medium and treated with LPA for indicated time periods. At the end of the treatment, the supernatant was collected and treated with enzyme mix with brief shaking, according to manufacturer's protocol. Optical density was measured at 565nm to quantify lactate content.

2.2.16. Fatty acid composition analysis by gas chromatography (GC)

Briefly, BV-2 microglia were seeded at 1 x 10^5 cells per well in a 6-well plate. Following overnight serum starvation, the cells were treated with the indicated concentrations of LPA for the indicated times. At the end of the treatment, the cells were washed with ice cold buffer containing 0.2% fatty acid free bovine serum albumin, sodium chloride (150 mM), Tris (50 mM), adjusted to pH 7.4. Lipids were then extracted twice with hexane/isopropanol (3:1, v/v), dried under a stream of nitrogen and dissolved in 1ml toluene. Lipid subclasses were fractionated by thin layer chromatography (TLC). After addition of the internal standard (pentadecanoic acid), lipids were trans-esterified (1.2 mL toluene and 1 mL boron trifluoride-methanol (20 %)) at 110 °C for 1 h. The derivatized lipids were analyzed on Agilent Technologies 5977B gas chromatograph with flame ionization detection (FID) as described previously (202). Fatty acid concentrations were quantified by peak area comparison with the internal standard and normalized to protein concentration (172).

2.2.17. Amino acid quantification by HPLC

Briefly, BV-2 microglia were seeded at 1 x 10^5 cells per well in a 6-well plate. Following overnight serum starvation, the cells were treated with LPA (1 μM) for indicated time periods. At the end of the treatment, the cells were washed with ice-cold PBS, scrapped off and sonicated in 70 μL H_2O. 50 μL of 1.5 M $HClO_4$ was added and the samples were left aside for 2 min. Then, 1.125 mL water and 25 μL of 2 M K_2CO_3 were added. After vortexing and centrifugation (10,000

g, 4 °C, 5 min), the supernatants were collected in glass vials and stored at -70 °C. Following o-phthalaldehyde (OPA) pre-column derivatization, HPLC analysis was performed as described (203) using a Waters 717 plus Autosampler equipped with a pump delivery system (Shimadzu, LC-20AD) and a scanning fluorescence detector (Waters 474). The amino acid concentrations (calculated by area comparison with external standard curves) were normalized to protein content (172).

2.2.18. ROS assay

Intracellular ROS levels were measured using the ROS-ID® Total ROS Detection Kit (ENZO Life Sciences, Switzerland) according to manufacturer's instructions. In brief, BV-2 cells were seeded in black clear bottom 96-well plates at a density of 5×10^3 cells per well. Cells were allowed to adhere overnight, then incubated in serum-free medium and treated with the indicated concentrations of LPA for the indicated times. Thirty minutes before the end of each treatment, the cells were loaded with the ROS detection solution. Fluorescence intensity was measured with excitation and emission wavelengths of 485 nm and 535 nm, respectively.

2.2.19. Glutathione assay

Intracellular glutathione content was measured using GSH-Glo™ Glutathione Assay Kit (Promega Corporation, United States) according to the manufacturer's protocol. Briefly, BV-2 (5×10^3 cells/well) or PMM (5×10^4 cells/well) were seeded in black clear bottom 96-well. Cells were allowed to adhere overnight, then incubated in serum-free medium and treated with LPA (1 or 5 µM as indicated) for indicated time periods. Then, GSH-Glo™ reagent was added to the plate and incubated for 30 min. After addition of luciferin detection reagent, luminescence was measured to quantify the glutathione content.

2.2.20. Lactate dehydrogenase assay (LDH)

LDH is a cytosolic enzyme released into the culture medium upon cell lysis or damage. The CyQUANT™ LDH Cytotoxicity Assay Kit was used to quantify cytotoxicity (Invitrogen, Waltham, MA, USA). BV-2 cells (6-well plate, 1×10^5 cells/well) were seeded. BV-2 cells were incubated in serum-free medium, and treated with indicated substance (according to experiment) for the indicated time periods. For each time point, the supernatants were collected and stored at -70 °C.

The CATH.a neurons were seeded in 96-well plates (1×10^5 cells per well) and allowed to adhere. Following overnight serum-starvation, the cells were incubated in the presence of

microglia-conditioned medium. Three wells containing only medium without cells were used as background control. As a positive control, cells were incubated with the LDH positive control solution (100% release). In order to measure maximum and spontaneous release, cells were incubated with 10% Triton X-100 and assay buffer, respectively. Cells were kept at 37 °C/5% CO_2 for 24 h and then the plate was centrifuged at 500 × g for 5 min. One hundred microliters of the supernatants was transferred to a new 96-well plate, and 100 µl of LDH reaction solution was added to each well. The plate was incubated at 37 °C/5% CO_2 for 30 min under gentle shaking and the absorbance at 490 nm was measured using a plate reader.

2.2.21. ELISA

Concentrations of cytokines like IL-1β, TNFα, IL-6, and chemokines like CCL5 (RANTES), CXCL2 (MIP-2), and CXCL10 (IP-10) were quantified using murine ELISA development kits (Peprotech, NJ, USA). Briefly, cells were seeded onto 6-well plates at a density of 1 x 10^5 (BV-2) or onto PDL-coated 12- well plates at a density of 5 x 10^5 (PMM) per well and serum-starved overnight prior to experiment. Then, cells were treated with the indicated concentrations of substance (according to experiment) for the indicated time periods. At the end of the time points, supernatant was collected and stored at − 80 °C until further use. The assays were performed using manufacturer's instructions. The concentration of cytokines and chemokines were determined using an external standard curve.

2.2.22. Determination of nitric oxide (NO)

The accumulated total nitrate levels were measured in the supernatant of cells that were incubated with indicated substance in serum-free medium using the total nitric oxide assay kit (ENZO Life Sciences, Switzerland). This assay is based on the enzymatic conversion of nitrate to nitrite by the enzyme nitrate reductase, followed by the Griess reaction to form a colored azo-dye product. The samples were processed according to manufacturer's protocol. A standard curve was generated in the range between 0–100 µM using nitrate as standard. The total nitrate concentration per sample was determined using external calibration.

2.2.23. Brain permeability detection of PF8380 by HPLC/MS

The brain permeability of PF 8380 was studied using HPLC/MS. Briefly, C57BL/6J mice were administered with PF8380 dissolved in oral formulation vehicle (Echelon), at a dose of 30 mg/kg (900 µg of PF8380 in 450 µL vehicle per mouse by gavage) for 30 min, 60 min, 120 min, 240 min (n=3). At the end of the treatment, Mice were transcardially perfused under anaesthesia

with ice-cold PBS, and the brains were dissected and snap frozen in liquid N2. Blood was collected and processed to obtain plasma which was extracted directly. Samples were processed by Bligh and Dyer HCl method as described previously (204,205). Brains were weighed, pulverised and extracted with 800 µL 1:1 (v/v) mixture of 0.1 M HCl and methanol and vortexed. 400 µL of chloroform was added and further vortexed for 1 min. The mixture was centrifuged for 3 min at 2,000 g, and the lower phase was collected. LPA 17:0 was used as internal standard (100 pmol/g for brain samples and 0.5 µM for plasma samples). External calibration was performed for PF8380 for the concentration of 0.1-2 µM. Quantitation of LPA and PF8380 was done by HPLC/MS. Chromatographic separation was performed on a Phenomenex Kinetex HILIC column (2.1 x 100 mm, 2.6 µm). Detection was performed on a Thermo Orbitrap Velos Pro (Thermo Fisher Scientific Inc., Waltham, MA) hybrid mass spectrometer, using a HESI II Probe in negative ionization mode. Identification and quantitation of LPA and PF8380 was performed by Lipid Data Analyzer, as previously reported (206).

2.2.24. NADPH/NADP assay

Nicotinamide nucleotides, NADP and NADPH were assayed using NADP/NADPH assay kit (Abcam, Cambride, UK) according to manufacturer's instruction. PMM were seeded onto PDL-coated 12- well plates at a density of 5 x 10^5 per well and serum-starved overnight prior to experiment. Cells were treated with the indicated concentrations of LPA for the indicated time periods. At the end of the time points, the medium was removed and cells were washed twice with ice-cold PBS, extracted with NADP/NADPH extraction buffer. The samples were deproteinised using 10 kD Spin Column (Abcam, Cambride, UK) before performing the assay. A part of the sample was used to measure total NADPt (total NADP and NADPH). Another part of the sample was heated at 60 °C for 30 min to decompose NADP for NADPH measurement. 10 µL of the sample was mixed with NADP cycling mix, to convert NADP to NADPH. 10 µL of NADPH developer into each well, mixed well, and incubated at room temperature for 1 – 4 h. Multiple readings were taken at OD 450 nm. The ratio of NADPH/NADP was calculated as:
NADPH/NADP ratio = NADPH / (NADPt – NADPH).

2.2.25. PLD activity

Autotaxin belonging to the ENPP family of enzymes display Phospholipase D (PLD) activity. PLD activity was measured using Phospholipase D Assay Kit (Sigma, Missouri, USA), according to manufacturer's instruction. Briefly, BV2 cells were seeded onto 6-well plates at a density of 1 x 10^5 cells/well and serum-starved overnight prior to experiment. Then, cells were

treated with the indicated concentrations of substance (according to experiment) for the indicated time periods. At the end of the time points, the medium was collected. 10 µL of the supernatant was mixed with 90 µL of the master reaction. After 10 min, initial absorbance, $(A_{570})_{initial}$ was measured at OD 570 nm. The plate was incubated at room temperature for 20 min and absorbance was measured again to determine $(A_{570})_{final}$. One unit of PLD catalyzes the formation of 1µmole choline per minute under the assay condition, and is calculated as follows:

Sample PLD activity = (B / (∆T x V)) x D

Where:

B = Amount of Choline in the sample (nmol).

∆T = Reaction time (minutes).

V = Sample volume added into the reaction well (ml).

D = Sample dilution factor.

2.2.26. Statistical analysis

Data are expressed as mean ± SEM from at least 3 independent experiments unless specified otherwise. Unpaired Student`s t-test (two groups), or one-way ANOVA followed by Bonferroni correction (more than two groups) was used for analysis of statistical significance (using the Graph Pad Prism6 package). All values of $p < 0.05$ were considered significant.

3. Results

3.1. Part I: Targeting the ATX-LPA axis in LPS-induced neuroinflammation

Effect of PF8380 and AS2717638 on BV-2 cell viability

In the first series of experiments, we determined non-toxic concentrations of the ATX (PF8380) and LPA5 (AS2717638) antagonists on BV-2 viability. Incubation with increasing concentrations of PF8380 indicated a decrease in MTT reduction by 70% at the highest concentration used (24 h; 30 µM; **Fig. 1A**). AS2717638 was without effect on MTT reduction at 0.1 and 1 µM, but compromised cell viability by 50 % when used at 10 µM for 24 h (**Fig. 1B**). For these reasons PF8380 was used at 1 and 10 µM while AS2717638 was used at 0.1 and 1 µM in the following experiments.

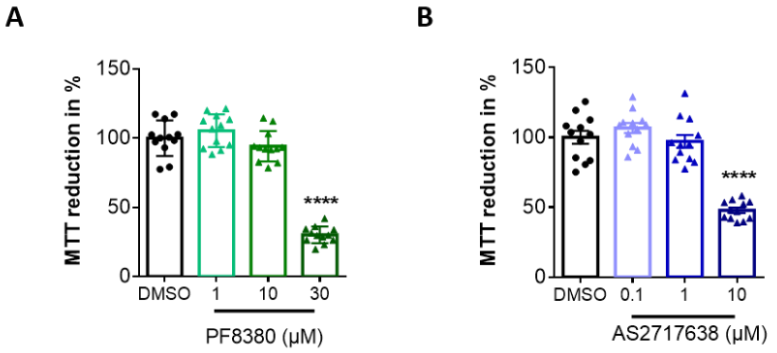

Figure 1. Evaluation of cytotoxicity of PF8380 and AS2717638 in BV-2 cells. BV-2 cells were treated with different concentration of (**A**) ATX inhibitor (PF8380) and (**B**) LPA5 inhibitor (AS2717638) for 24 h. DMSO was used as vehicle control. Dose dependent effect of the inhibitors on MTT reduction in cells was compared to control. Results are shown as mean ± SEM of 3 independent experiments. (****p < 0.0001, compared to control; one-way ANOVA with Bonferroni correction)

LPS induces the expression of ATX and PLD activity

To evaluate the effect of LPS on ATX protein expression, we performed western blot analyses. When compared to unstimulated cells, LPS significantly increased ATX protein level by about 1.7 fold after 8 and 24 h (**Fig. 2A**). ATX hydrolyzes lysophospholipids to produce LPA and choline. To get an indication about the effect of LPS on ATX activity and to determine the effectiveness of PF8380 we evaluated phospholipase D (PLD) activity (as surrogate readout for ATX activity) in supernatants collected from untreated, LPS- and LPS/PF8380-treated cells. These data indicate that LPS treatment significantly increased PLD activity in the supernatants (up to 2-fold; **Fig. 2B**). In contrast, PF8380 (10 and 1 μM) attenuated LPS-induced PLD activity almost back or below baseline levels.

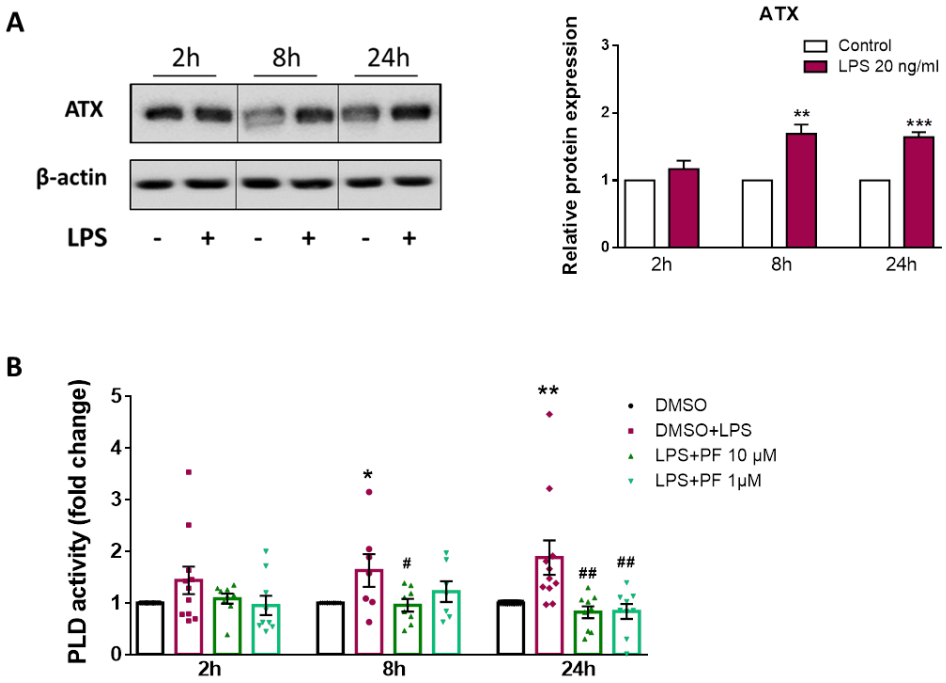

Figure 2. Effect of LPS on ATX protein expression and Phospholipase D (PLD) activity in BV-2 microglia. Cells were treated with LPS (20 ng/ml) for indicated time. Cell protein lysates were collected and ATX was detected by immunoblotting. β-actin was used as loading control. (**A**) One representative blot of ATX. Densitometric evaluation of immunoreactive bands. Values are expressed as mean ± SEM of three independent experiments. (** $p < 0.01$, ***$p < 0.001$, compared to control; unpaired Student's t test) (**B**) Cells were treated with LPS (20 ng/ml) in the absence or presence of PF8380 ('PF'; 10 and 1 µM) for indicated time. DMSO was used as vehicle control. PLD activity in the supernatant was measured by Phospholipase D kit (Sigma) and compared with their appropriate control. Results are presented as mean ± SEM of 3 independent experiments. (*$p < 0.05$, **$p < 0.01$ compared to control; # $p < 0.05$, ## $p < 0.01$ compared to LPS-treated cells; one-way ANOVA with Bonferroni correction)

LPS and IL4 induces the expression of LPARs

In a first series of experiments, we studied the impact of LPS or IL-4 priming (in macrophage terminology this would correspond to M1 and M2 polarization, respectively) on LPAR expression in BV-2 cells by Western blotting (representative blots are shown in **Fig. 3A**). These studies revealed that BV-2 cells express LPAR 2, -3, -5, and -6 immunoreactive protein while LPAR 1 and -4 were undetectable (as observed previously by qPCR analyses; (20). The bar graphs display relative protein expression of the individual LPA receptors in untreated or in LPS (20 ng/ml for 24 h) or IL-4 (50 ng/ml for 24 h) treated BV-2 cells. LPS treatment tended to upregulate LPA receptor expression and this reached statistical significance (2.2-fold up) for

LPA5. Also, IL-4 (50 ng/ml) treatment upregulated LPA-2,-3,-5 and -6 expression and this effect was most pronounced and statistically significant for LPA3 (11-fold).

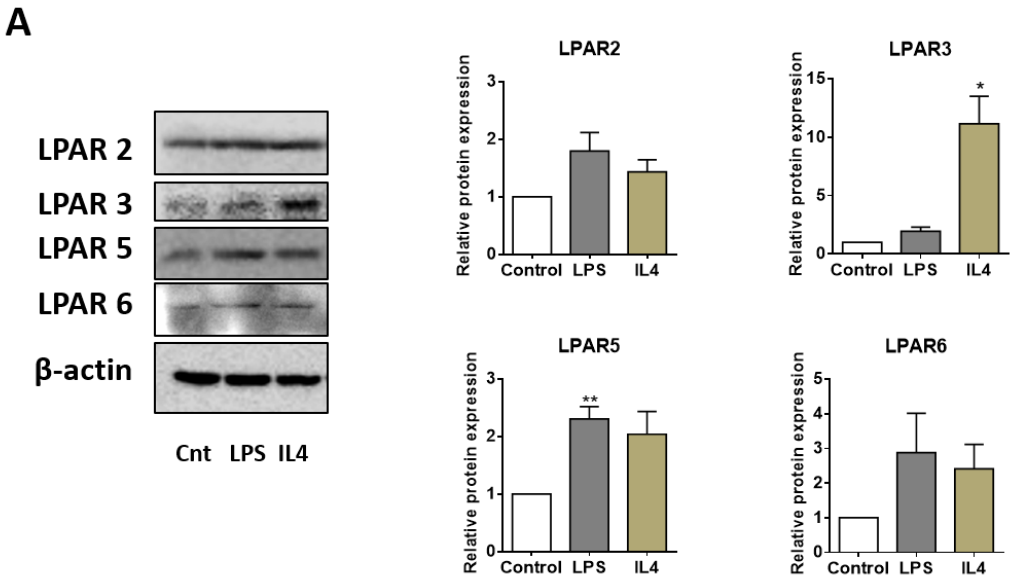

Figure 3. Immunoblot analyses of Lysophosphatidic acid receptors (LPARs) in LPS and IL4 primed BV-2 microglia. (**A)** Cells were incubated with LPS (20 ng/ml) or IL4 (50 ng/ml) for 24 h. Protein expression of LPAR 2, -3, -5 and -6 were detected by western blot analyses. β-actin was used as loading control. One representative blot for each protein. Densitometric evaluation of immunoreactive bands. Values are expressed as mean ± SEM of three independent experiments. (*p < 0.05, ** p < 0.01 compared to control; unpaired Student's t test)

ATX and LPA5 antagonism inhibits LPS induced markers of inflammation

Evidence suggests that LPS mediates its pro-inflammatory action mainly via TLR4. To investigate if the ATX antagonist impact TLR4 receptor expression, western blot analyses were performed. These studies showed LPS induced TLR4 protein at 8 h and 24 h (about 2-fold) in BV-2 cells while PF8380 treatment suppressed this increase (**Fig. 4A**). M1/M2 marker expression analysis revealed that LPS increased the expression of COX2 (M1 marker) at 24h. This effect was abrogated by PF8380. No significant changes were observed in the expression of Arg1 (M2 marker) in response to LPS or PF8380.

Qualitatively similar results were obtained in a second set of experiments to study the impact of AS2717638 on LPS-induced TLR4, COX2 and Arg1 expression. As expected, LPS induced TLR4 and COX2 protein and decreased Arg1 protein (**Fig. 4B**). TLR4 and COX2 protein levels were attenuated by LPA5 inhibition. Interestingly, AS2717638 at 1 μM elevated the

expression of Arg1 at 8 h while at 0.1 μM immunoreactive Arg1 was decreased below baseline levels at all time points studied.

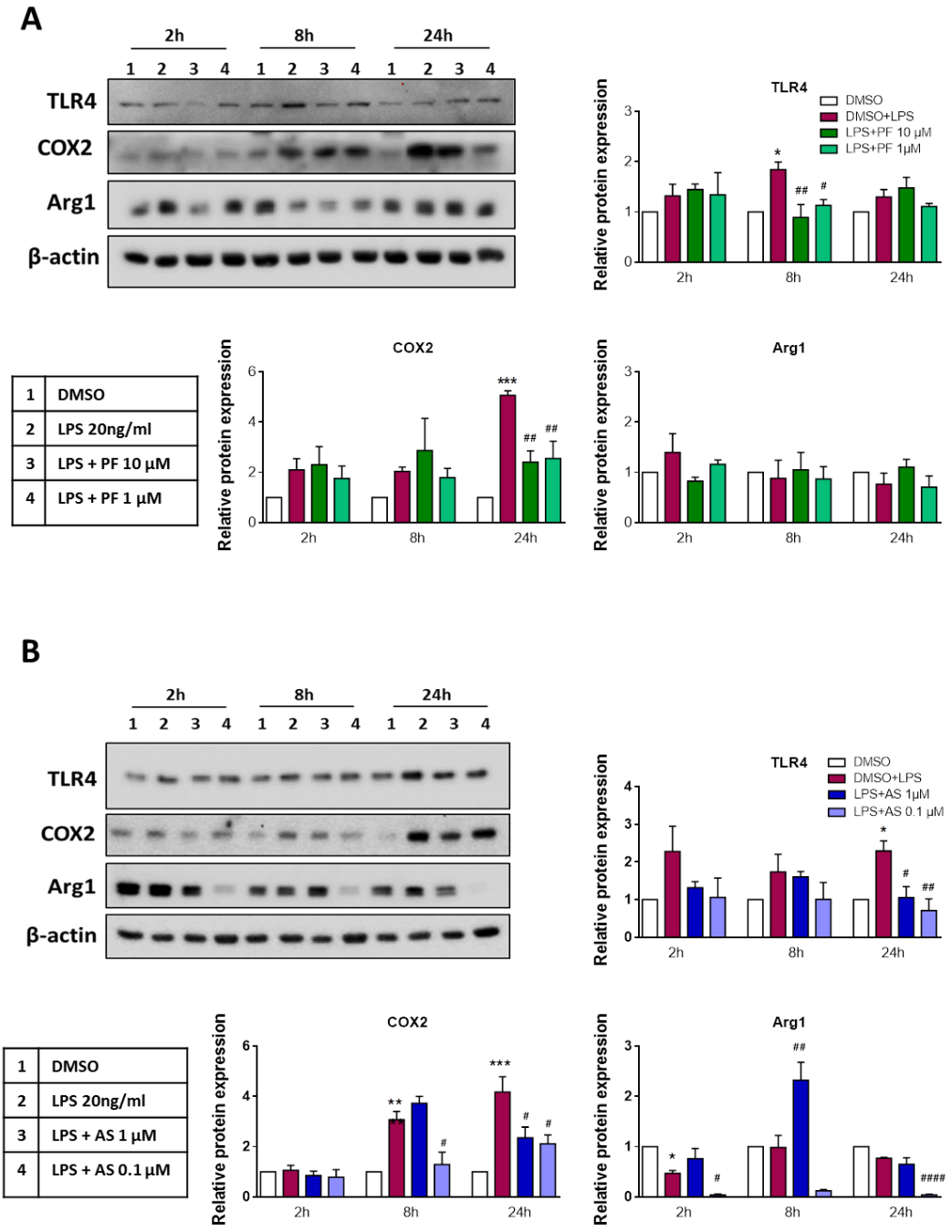

Figure 4. Inhibition of ATX and LPA5 regulates LPS-induced TLR4 expression and pro-inflammatory phenotype in BV-2 microglia. Cells were treated with DMSO control, LPS (20 ng/ml) plus DMSO, (**A**) LPS plus PF8380 ('PF'; 10 and 1 μM) or (**B**) LPS plus AS2717638 ('AS';

1 and 0.1 µM) for the indicated time. Cell lysate were collected and protein expression of TLR4, COX2 and Arg was monitored using western blot. β-actin was used as loading control. One representative blot for each protein. Densitometric evaluation of immunoreactive bands. Values are expressed as mean ± SEM of three independent experiments. (*p < 0.05, ** p < 0.01, ***p < 0.001 compared to DMSO control; # p < 0.05, ## p < 0.01, #### p < 0.0001 compared to LPS-treated cells; one-way ANOVA with Bonferroni correction)

ATX and LPA5 antagonism attenuates LPS induced NO production

We further examined the impact of PF8380 and AS2717638 on nitric oxide (NO) production in LPS-treated BV-2 cells. LPS increased NO production (detected as nitrate) and both, ATX and LPA5 inhibition reduced nitrate levels (**Fig. 5 A,B)**.

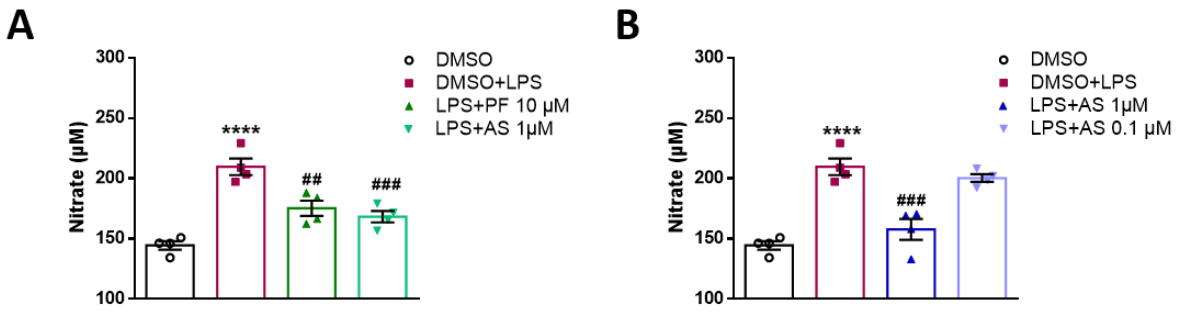

Figure 5: PF8380 and AS2717638 inhibits LPS-induced nitric oxide production in BV-2 microglia. Cells were treated with DMSO, LPS plus DMSO, and (**A**) LPS plus PF8380 ('PF'; 10 µM and 1 µM) or (**B**) LPS plus AS2717638 ('AS'; 1 µM and 0.1 µM) for 24 h. The production of NO was determined by measuring the total nitrate concentration in the supernatants. Values are expressed as mean ± SEM of three independent experiments. (**** p < 0.0001 compared to DMSO control; ## p < 0.01, ### p < 0.001 compared to LPS-treated cells; one-way ANOVA with Bonferroni correction

ATX and LPA5 antagonism attenuates LPS induced neurotoxicity

To determine potential cytotoxic properties of the LPS-induced secretome of BV-2 cells, CATH.a neurons were incubated with supernatants collected from LPS- or LPS/inhibitor-treated cells. These experiments revealed significant cytotoxicity of media collected from LPS-activated cells (**Fig. 6 A,B**). In contrast the pre-conditioned medium obtained from LPS/inhibitor treated cells did not affect neuronal viability and was slightly lower as compared to medium collected from untreated cells.

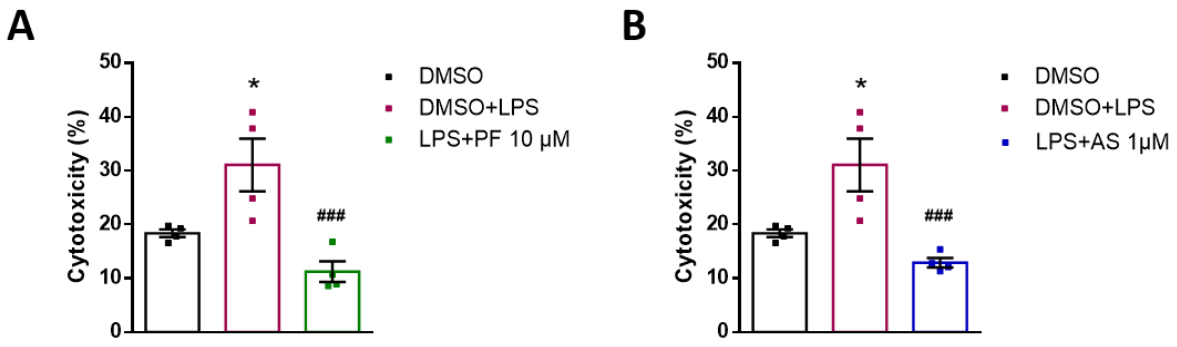

Figure 6: PF8380 and AS2717638 neuronal cytotoxicity in BV-2 microglia. CATH.a neurons were incubated for 24 h with conditioned media collected from LPS treated in absence or presence of (**A**) PF8380 ('PF'; 10 µM) or (**B**) AS2717638 ('AS'; 1 µM) for 24 h. LDH levels were detected and cytotoxicity was calculated according to manufacturer's protocol. Values are expressed as mean ± SEM of three independent experiments. (*$p < 0.05$ compared to DMSO control; ### $p < 0.001$ compared to LPS-treated cells; one-way ANOVA with Bonferroni correction)

ATX and LPA5 antagonism attenuates LPS induced inflammatory signaling pathway

To elucidate the mechanism of inhibition of these pro-inflammatory marker and cyto-/chemo-kines we studied pathways involved in inflammation. MAPK signaling pathways are key mediators of transcriptional response to extracellular signals (207). The effect of antagonists was studied in LPS stimulated MAPK signaling in BV-2 cells. In line, western blot analyses demonstrated LPS treatment significantly increased phosphorylation of p38 and JNK at one or more time points. In contrast, PF8380 remarkably reduced p38 (20 min) and JNK (120 min) phosphorylation (**Fig. 7A**). A similar immunoblot strategy was used to investigate the effect of the LPA5 antagonist AS2717638 (1 and 0.1 µM) on MAPK pathway. These results indicate AS2717638 attenuated the phosphorylation of p38 (120 min) and JNK (60 min) (**Fig. 7B**).

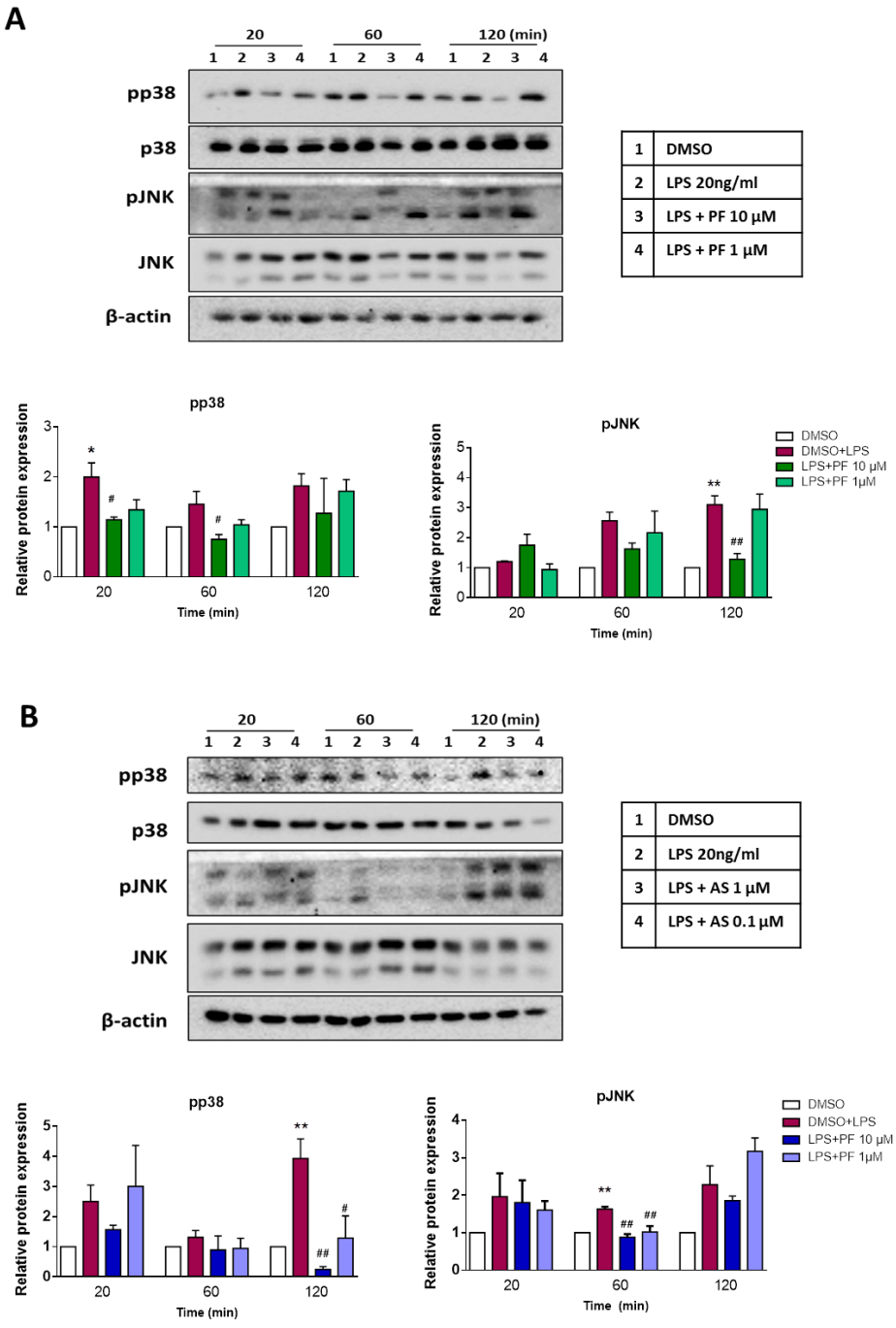

Figure 7: Inhibition of ATX and LPA5 regulates LPS-induced MAPK signaling pathway in BV-2 microglia. Cells were treated with DMSO control, LPS plus DMSO, and (A) LPS plus PF8380 ('PF'; 10 and 1 µM) or (B) LPS plus AS2717638 ('AS'; 1 and 0.1 µM) for the indicated times. Cell lysates were collected and protein expression of phosphorylated p38 and JNK along with their total protein was monitored by immunoblotting. β-actin was used as loading control. One representative blot for each protein is shown. Densitometric evaluation of immunoreactive bands

is shown in the bar graphs. Values are expressed as mean ± SEM of three independent experiments. (*p < 0.05, ** p<0.01 compared to DMSO control; # p < 0.05, ## p < 0.01 compared to LPS-treated cells; one-way ANOVA with Bonferroni correction)

TLR4 ligation results in activation of transcription factors (TF) that induce differential gene expression in response to LPS, a prerequisite for increased chemo-/cytokine secretion by microglia (168). To get an indication about effects of ATX and LPA5 inhibition we analyzed TF phosphorylation in response to LPS in the absence or presence of PF8380 or AS2717638. In response to LPS, phosphorylation of STAT1, p65, and cJun was significantly increased at one or more time points (**Fig. 8A**). Co-incubation of BV-2 cells with LPS/PF8380 significantly decreased STAT1 (24 h), p65 (2 h), and c-Jun (8 h) phosphorylation. The 10-fold increase in c-Jun phosphorylation in response to PF8380 (10 μM) at 2 h was unexpected. Phosphorylation of STAT6, associated with M2 subtype activation of macrophages was drastically decreased in response to LPS (0.05-fold at 24h). PF8380 could not alleviate the effect of LPS-induced STAT6 dephosphorylation.

A similar Western blot strategy was used to investigate the effect of the LPA5 antagonist AS2717638 (1 and 0.1 μM) on transcription factor phosphorylation in LPS-treated BV-2 cells (**Fig. 8B**). As expected from data in Fig. 9, LPS increased phosphorylation of STAT1, p65, and c-Jun, but decreased pSTAT6. AS2717638 effectively suppressed phosphorylation of STAT1, p65, and c-Jun at one or more time points. AS2717638 did not counteract LPS-mediated dephosphorylation of STAT6. In these experiments the lower concentration (0.1 μM) had a more pronounced inhibitory potential was as compared to the higher concentration (1 μM).

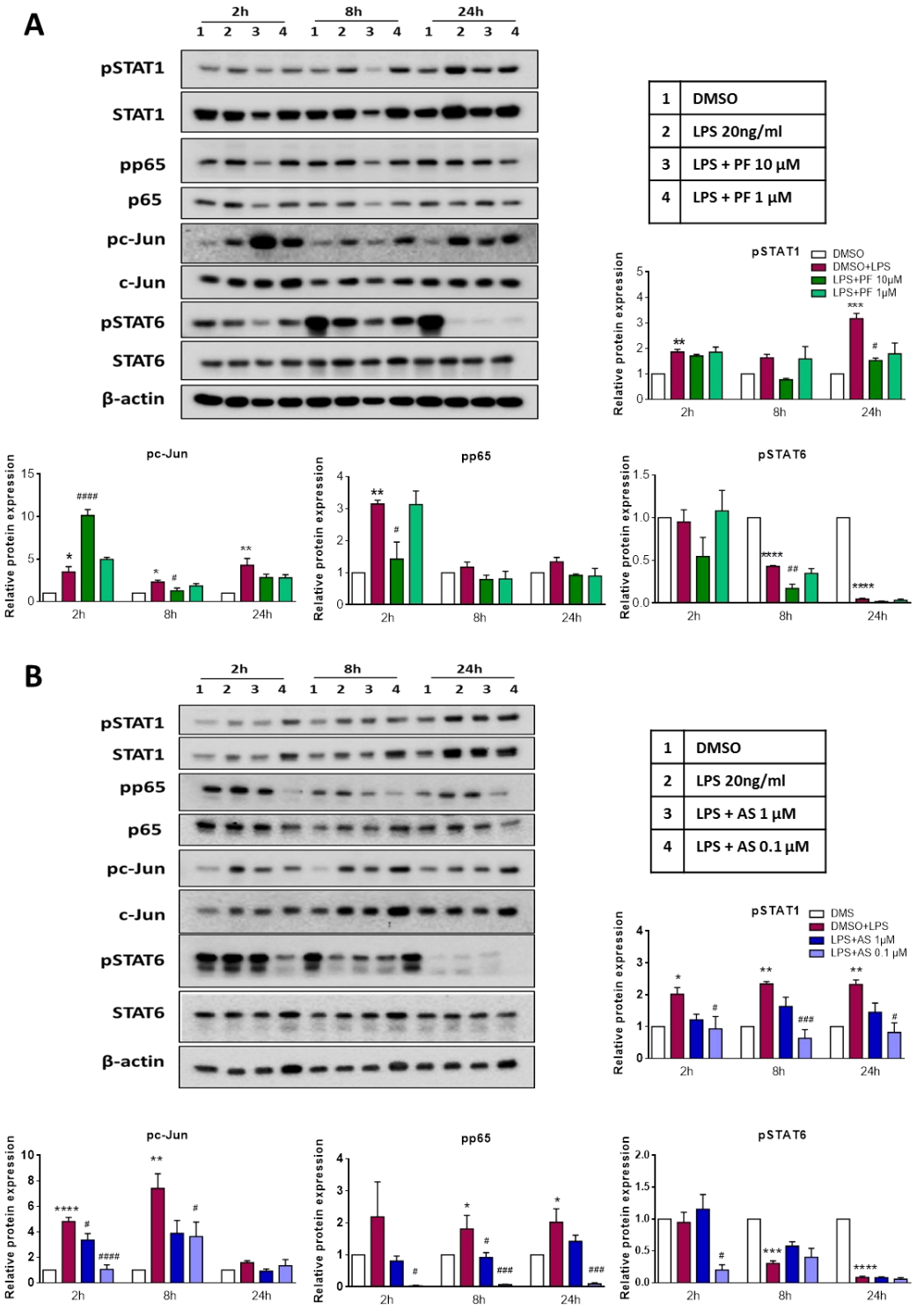
A
2h
8h
24h
1 2 3 4 1 2 3 4 1 2 3 4
pSTAT1
STAT1
pp65
p65
pc-Jun
c-Jun
pSTAT6
STAT6
β-actin
1 DMSO
2 LPS 20ng/ml
3 LPS + PF 10 µM
4 LPS + PF 1 µM
pSTAT1
DMSO
DMSO+LPS
LPS+PF 10µM
LPS+PF 1µM
Relative protein expression
pc-Jun
pp65
pSTAT6
B
1 DMSO
2 LPS 20ng/ml
3 LPS + AS 1 µM
4 LPS + AS 0.1 µM
DMS
DMSO+LPS
LPS+AS 1µM
LPS+AS 0.1 µM

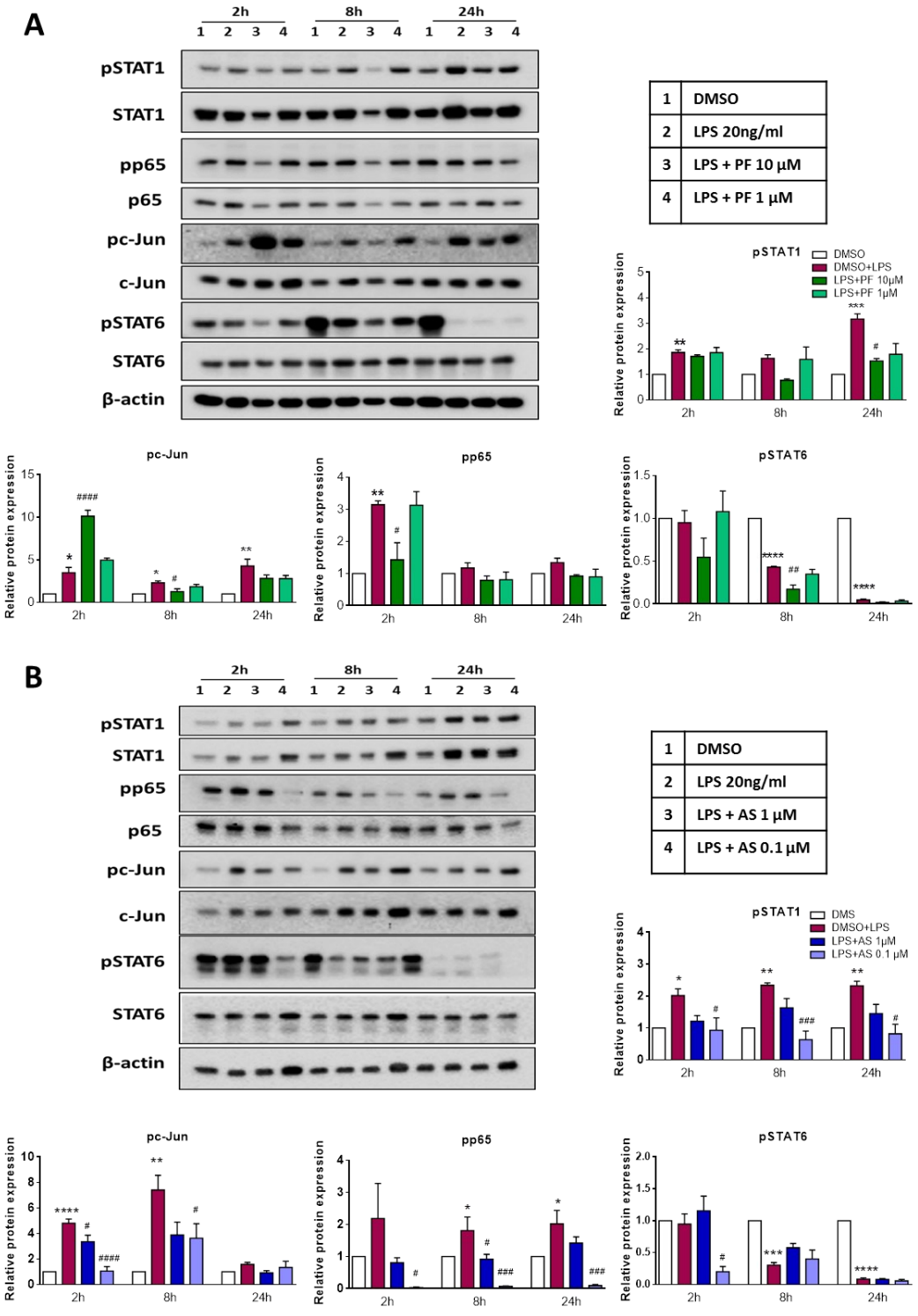

Figure 8: Inhibition of ATX and LPA5 regulates LPS-induced phosphorylation of pro-inflammatory transcriptional factors. Cells were treated with DMSO control, LPS (20 ng/ml) plus DMSO, and (**A**) LPS plus PF8380 ('PF'; 10 and 1 µM) or (**B**) LPS plus AS2717638 ('AS', 1

and 0.1 μM) for the indicated time. Cell lysate were collected and protein expression of phosphorylated STAT1, p65, cjun and STAT6 along with their total protein was monitored using western blot. β-actin was used as loading control. One representative blot for each protein. Densitometric evaluation of immunoreactive bands. Values are expressed as mean ± SEM of three independent experiments. (*p < 0.05, ** p<0.01, ***p<0.001, **** p < 0.0001 compared to DMSO control; # p < 0.05, ## p < 0.01, ### p<0.001, #### p<0.0001 compared to LPS-treated cells; one-way ANOVA with Bonferroni correction)

ATX and LPA5 antagonism attenuates LPS mediated secretion of cyto-/chemo-kines.

Next, we studied cyto-/chemokine secretion from LPS-stimulated BV-2 cells and the impact of the two inhibitors on extracellular accumulation of these analytes (**Fig. 9 and 10**). LPS significantly elevated TNFα concentrations at all time points and PF8380 significantly reduced secretion at 24 h **(Fig. 9A**). The same was true for IL6 (**Fig. 9B)** and IL-1β (**Fig. 9C**) at one or more time points. Results for chemokine secretion (CXCL10, CXCL2, and CCL5) were more clear-cut: LPS significantly increased extracellular accumulation of the three chemokines and in the presence of the ATX inhibitor this effect was significantly attenuated (**Figs. 9E-F**).

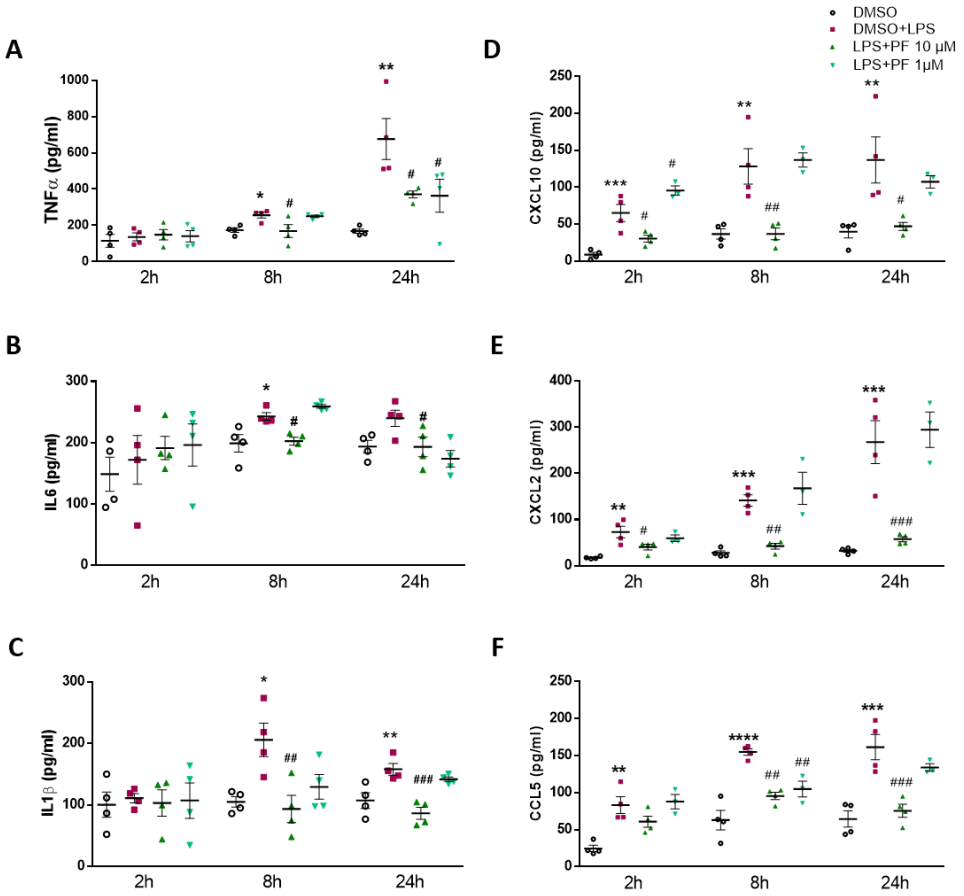

Figure 9: Inhibition of ATX by PF8380 attenuates LPS-induced secretion of cyto/chemokines in BV-2 microglia. Cells were treated with DMSO control, LPS (20 ng/ml) plus DMSO in absence or presence of PF8380 ('PF'; 10 and 1 µM) for the indicated time. Supernatants were collected. (**A-F**) Concentration of cytokines TNFα, IL6, and IL-1β and chemokines CXCL10, CXCL2, and CCL5 were quantified by ELISA. Values are expressed as mean ± SEM of three independent experiments. (*p < 0.05, ** p < 0.01, ***p < 0.001, **** p < 0.0001 compared to DMSO control; # p < 0.05, ## p < 0.01, ### p < 0.001 compared to LPS-treated cells; one-way ANOVA with Bonferroni correction)

Similar effects were observed for the LPA5 inhibitor which showed moderate inhibitory effects on cytokine secretion (**Fig. 10A-C**) but pronounced inhibitory potential for LPS-induced chemokine release (**Fig. 10D-F**).

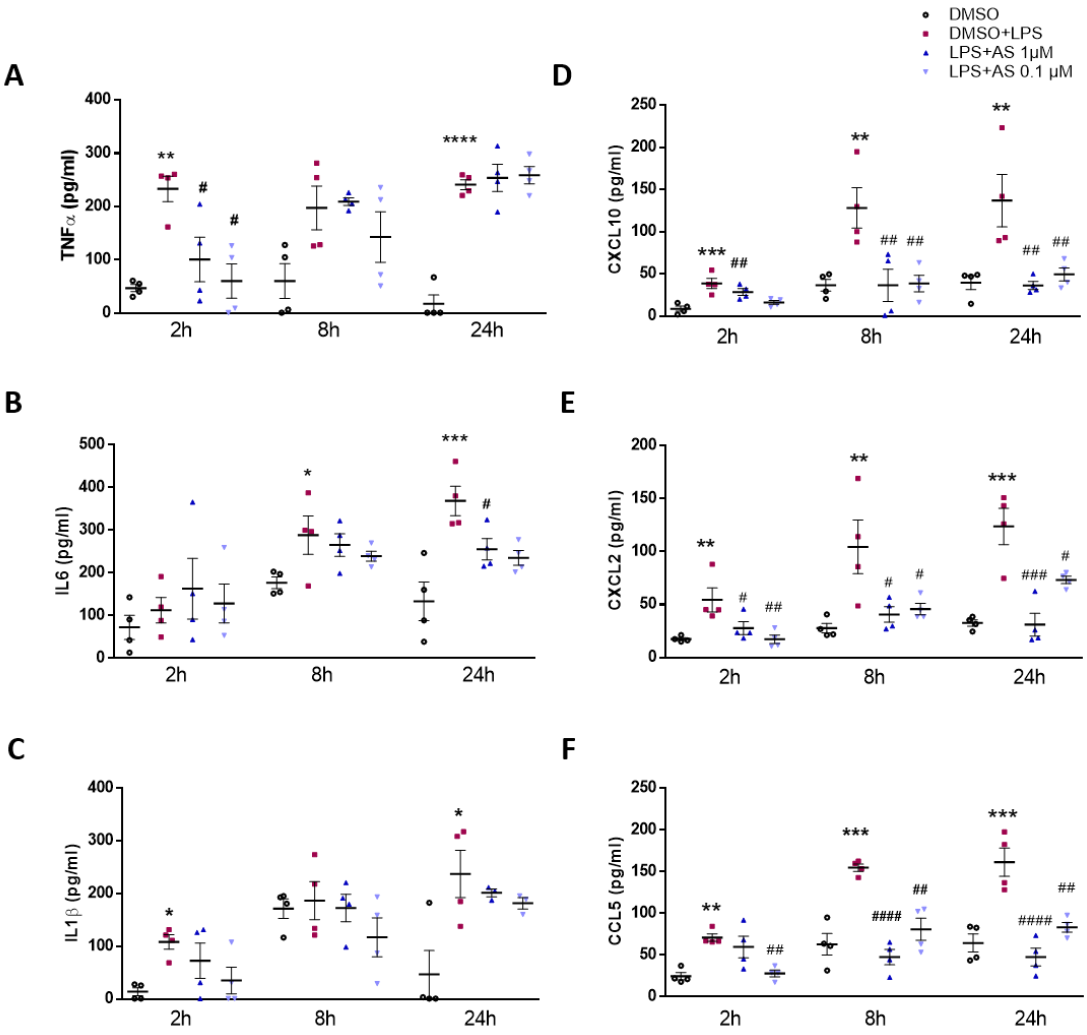

Figure 10: Inhibition of LPA5 by AS2717638 attenuates LPS-induced secretion of cyto/chemo-kines in BV-2 microglia. Cells were treated with DMSO control, LPS plus DMSO in absence or presence of AS2717638 ('AS'; 1 and 0.1 μM) for the indicated time. Supernatants were collected. (**A-F**) Concentration of cytokines TNFα, IL6, and IL-1β and chemokines CXCL10, CXCL2, and CCL5 were quantified by ELISA. Values are expressed as mean ± SEM of three independent experiments. (*p < 0.05, ** p<0.01, ***p<0.001, **** p < 0.0001 compared to DMSO control; # p < 0.05, ## p < 0.01, ### p < 0.001, #### p < 0.0001 compared to LPS-treated cells; one-way ANOVA with Bonferroni correction)

Oral administration of PF8380 crosses blood-brain-barrier (BBB)

We then asked whether PF8380 and AS1727638 would beneficially affect neuroinflammatory parameters *in vivo* in a murine endotoxin model. One of the main criteria for effective neurotherapeutic agents is their ability to cross the BBB. In a first step we determined BBB permeability of PF8380 in C57BL/6 mice. PF8380 was administered as a single dose (900 μg in 450 μL vehicle) by gavage. At the indicated time points animals (n=3) were anesthetized with 150 mg/kg pentobarbital and transcardially perfused with PBS. Subsequently, brains were removed, extracted, and PF8380 concentrations were quantitated by LC-MS/MS using external calibration (205). The maximal concentration was observed 60 min post application (0.21 ± 0.122 nmole/g brain; **Fig. 11A**). In PF8380-injected animals brain LPA levels dropped to concentrations below baseline at 120 min post application (**Fig. 11C**).

Transport of the AS2717638 compound across the BBB was demonstrated by Kawamoto and colleagues (208).

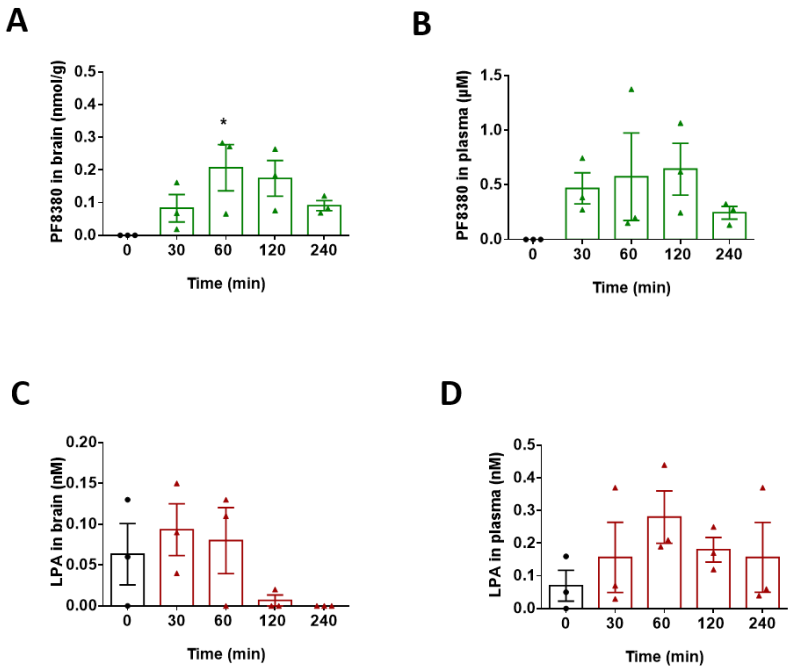

Figure 11: PF8380 crosses blood brain barrier to inhibit the concentration of LPA in the mice brain. Animals were administered with PF8380 dissolved in oral formulation vehicle, at a dose of 30 mg/kg PO. At the indicated times, mice were sacrificed and brain was dissected and snap frozen. Blood was collected and processed to obtain plasma. Tissue homogenate was extracted using modified Bligh & Dyer HCl method. Quantification of (**A-B**) PF8380 and (**C-D**) LPA in brain and plasma was done by LC-MS/MS. Results are presented as mean values ± SEM of 3 mice per group (*p < 0.05compared to control; one-way ANOVA with Bonferroni correction)

ATX and LPA5 antagonism attenuates LPS-induced neuroinflammation in vivo

Finally, we investigated whether ATX and LPA5 antagonism would affect LPS-induced neuroinflammation in vivo. Using a previously published model of acute LPS exposure mice were injected with LPS (5 mg/kg), perfused after 24 h, RNA was isolated from half a brain and gene expression analyzed by qPCR. Twenty-four hours following LPS application gene expression of iNOS, TNFα, IL6, IL1β, CXCL10, CXCL2, and CCL5 were significantly upregulated in comparison to DMSO (vehicle for inhibitors) injected animals (**Fig. 12**). Co-injection of LPS and PF8380 (30mg/kg) decreased iNOS (**Fig. 12A**), TNFα (**Fig. 12B)**, IL-6 (**Fig. 12C**), IL-1β (**Fig. 12D**) and CXCL2 (**Fig. 12F**). CXCL10 and CCL5 were not significantly regulated by PF8380 (**Fig. 12F and G**). Co-injection of LPS with the LPA5 antagonist AS2717638 (10 mg/kg) resulted in significantly decreased transcription of iNOS (**Fig. 12A**), TNFα (**Fig. 12B**), IL6 (**Fig. 12C**), and CXCL2 (**Fig. 11F**) in comparison to LPS. IL1β, CXCL10

and CCL5 showed only a non-significant downward trend (**Fig. 12D, E, G)**. No significant change was observed in Arg1 expression in LPS/+PF8380 treated animals (**Fig. 12H**). Interestingly, LPA5 antagonism showed an upward trend (**Fig. 12H**).

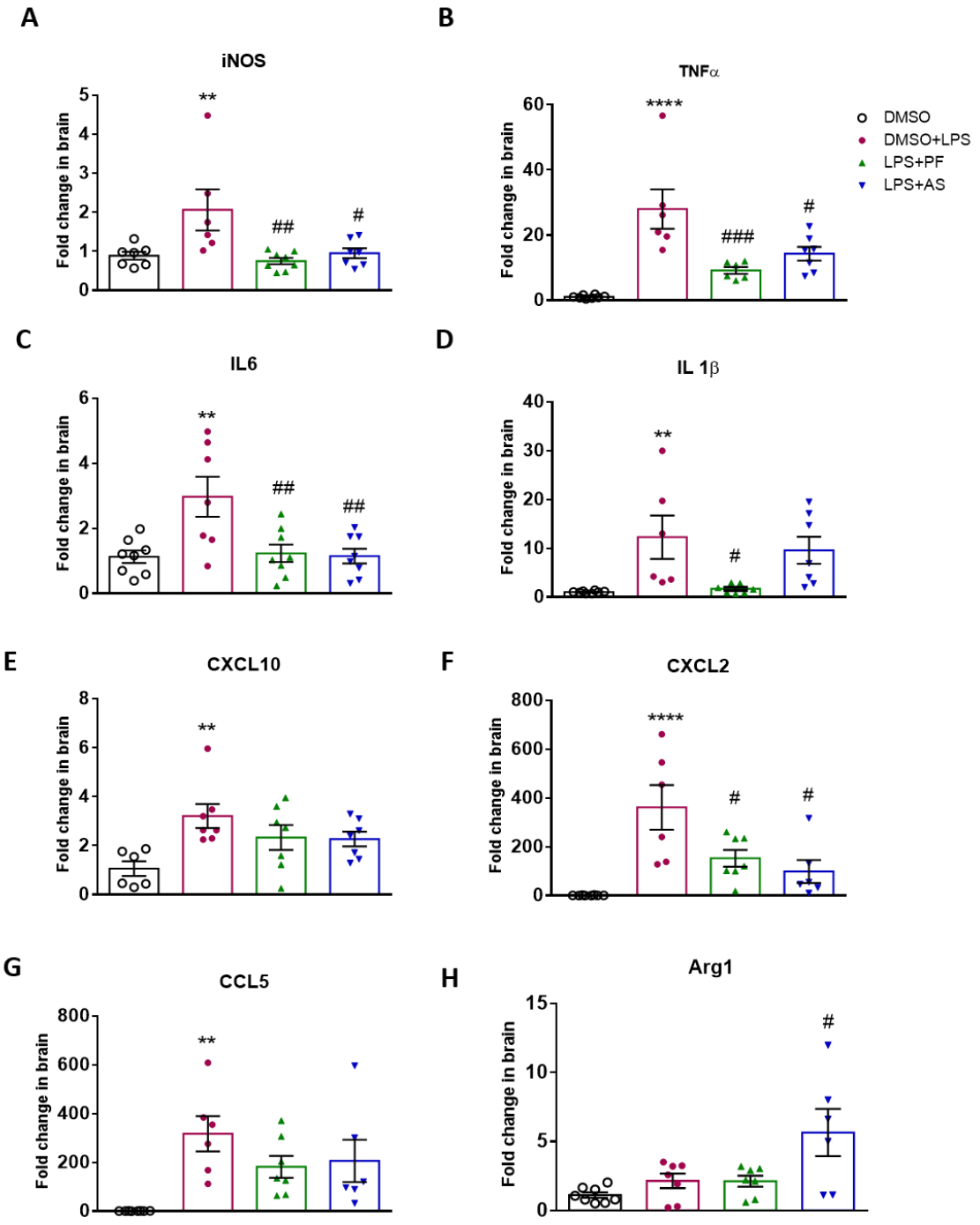

Figure 12: Inhibition of ATX and LPA5 regulates brain mRNA transcription of pro-inflammatory cyto/chemo-kines in acute inflammation model of mice. Mice (n = 6 - 8 per group) were injected intraperitoneally (i.p.) with DMSO, LPS (5 mg/kg) plus DMSO, in absence or presence of PF8380 ('PF'; 30 mg/kg) or AS2717638 ('AS'; 10 mg/kg). After 24 h, the animals were sacrificed and the brains were perfused. Right hemisphere from each mouse was processed for RNA isolation and gene expression of (**A**) iNOS, (**B**) TNFα, (**C**) IL6, (**D**) IL-1β, (**E**) CXCL10, (**F**) CXCL2, (**G**) CCL5 and (**B**) Arg were evaluated by qPCR. Hypoxanthine-guanine phosphoribosyltransferase (HPRT) was used as housekeeping gene. Expression was calculated using the 2−ddCt method. Results are presented as mean values ± SEM of 6-8 mice per group (*p < 0.05, **p<0.01, ***p<0.001 compared to DMSO control; # p < 0.05 compared to LPS-treated mice; one-way ANOVA with Bonferroni correction)

The other brain hemisphere of the corresponding animals was processed to study the expression of a set of proteins that are related to the severity of neuroinflammation. In these western blot analyses (**Fig. 13**) we assessed the expression of immunoreactive TLR4, IBA1 and GFAP (microglia and astrocyte activation marker, respectively), COX2 (M1 marker), synaptophysin (synaptic integrity marker), and Bax (inducer of apoptosis) and Bcl2 (repressor of apoptosis). LPS led to an increase of TLR4, Iba1, GFAP, COX2 and increased the Bax/Bcl2 ratio, while synaptophysin was decreased (**Fig. 13A and B**). LPS-mediated upregulation of TLR4, Iba1, GFAP, and COX2 were normalized in LPS/PF8380-injected mice (**Fig. 13A**). In a second set of experiments animals were injected with DMSO, LPS or LPS/AS2717638, LPS increased TLR4, Iba1, GFAP, COX-2, and Bax expression, while Bcl2 and synaptophysin were decreased (**Fig. 13B**). Co-administration of the LPA5 antagonist amended all of the neuroinflammatory parameters analyzed during these experiments (**Fig. 13B**).

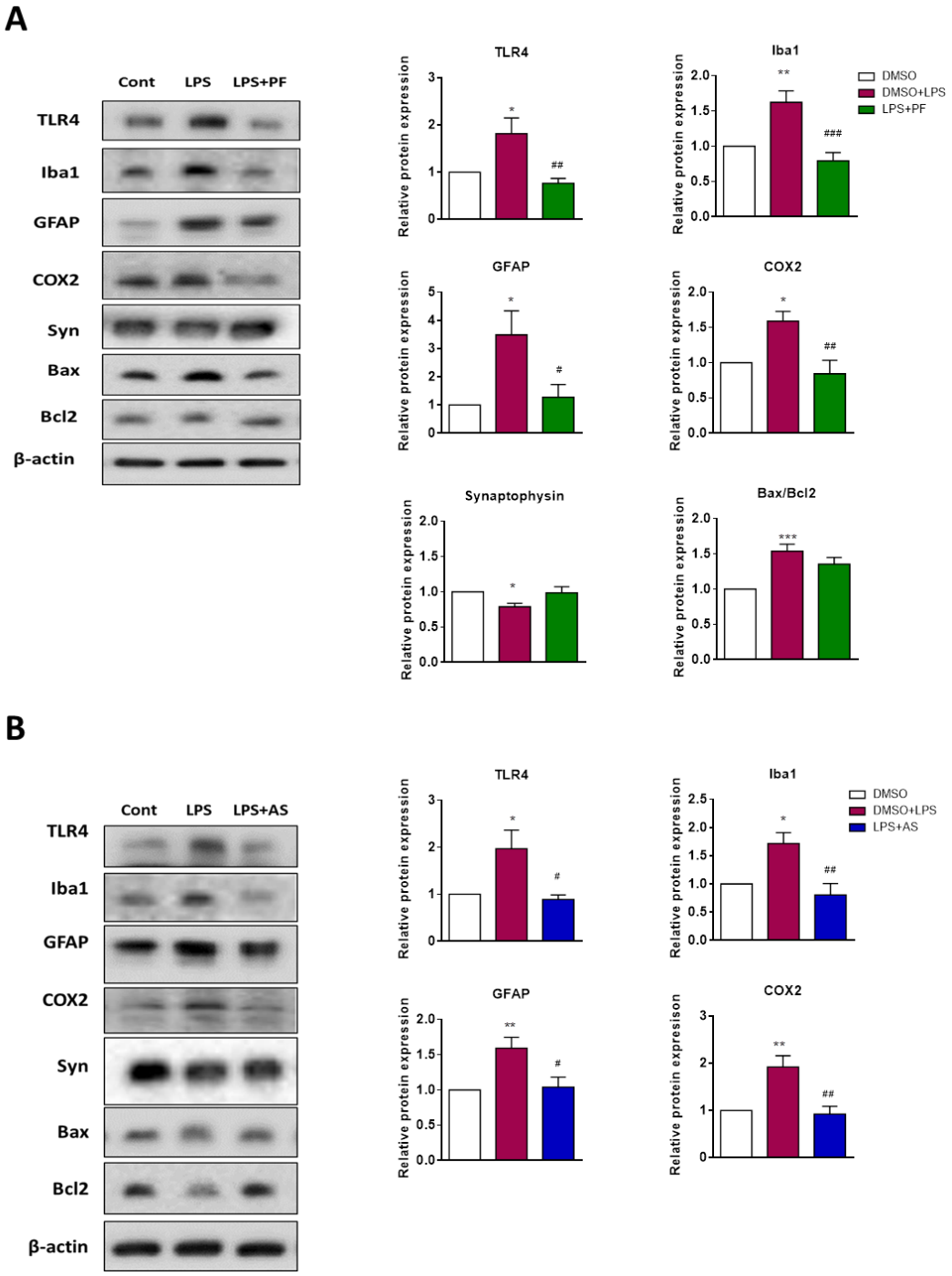

Figure 13: Inhibition of ATX and LPA5 regulates proteins involved in inflammation in the brain of mice subjected to acute inflammation. Mice (n = 6 - 8 per group) were injected intraperitoneally (i.p.) with DMSO, LPS (5 mg/kg) plus DMSO, in absence or presence of (**A**) PF8380 ('PF'; 30 mg/kg) or (**B**) AS2717638 ('AS'; 10 mg/kg). After 24 h, the animals were sacrificed and the brains were perfused. Left hemisphere from each mouse was processed for

protein analyses by immunoblot. Protein expression of TLR4, IBA1, GFAP, COX2, Syn, Bax, Bcl2 were monitored by western blot analyses. β-actin was used as loading control. One representative blot for each protein. Densitometric evaluation of immunoreactive bands. Values are expressed as mean ± SEM of 6-8 mice per group (*p < 0.05, **p<0.01 compared to DMSO control; # p < 0.05, ## p < 0.01, ### p < 0.001 compared to LPS-treated mice; one-way ANOVA with Bonferroni correction)

ATX and LPA5 antagonism inhibits LPS induced peripheral inflammation

To corroborate that the improvement of neuroinflammatory conditions in response to PF8380 and AS2717638 is also reflected in the periphery we performed ELISA measurement in serum. LPS administration significantly increased the serum concentrations of TNFα, IL6 and IL-1β (**Fig. 14**). PF8380 led to a significant reduction of LPS-mediated upregulation of TNFα, IL-6, and IL-1β while AS2717638 significantly attenuated TNFα (**Fig. 14A**) and IL-6 (**Fig. 14B**) but not IL-1β (**Fig. 14C**) concentrations.

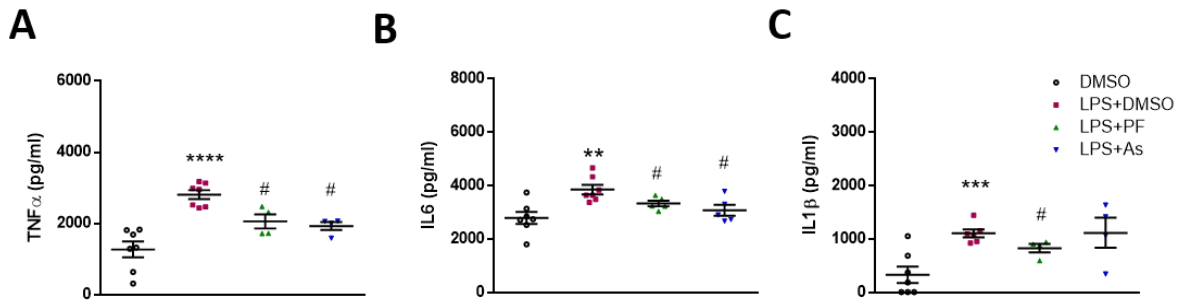

Figure 14: Inhibition of ATX and LPA5 regulates periphery cyto/chemo-kine concentration in acute inflammation model of mice. Mice (n = 6 - 8 per group) were injected intraperitoneally (i.p.) with DMSO, LPS (5 mg/kg) plus DMSO, in absence or presence of PF8380 ('PF'; 30 mg/kg) or AS2717638 ('AS'; 10 mg/kg). After 24 h, the animals were sacrificed and blood was collected and processed to obtain serum. Serum was diluted at 1:10 for further processing. (**A-C**) Concentration of cytokines TNFα, IL6 and IL-1β were quantified using ELISA. Values are expressed as mean ± SEM of 6-8 mice per group **p<0.01, ***p<0.001, **** p < 0.0001 compared to DMSO control; # p < 0.05 compared to LPS-treated mice; one-way ANOVA with Bonferroni correction)

Graphical summary

Key findings obtained during this part of my thesis are summarized in Figure 15.

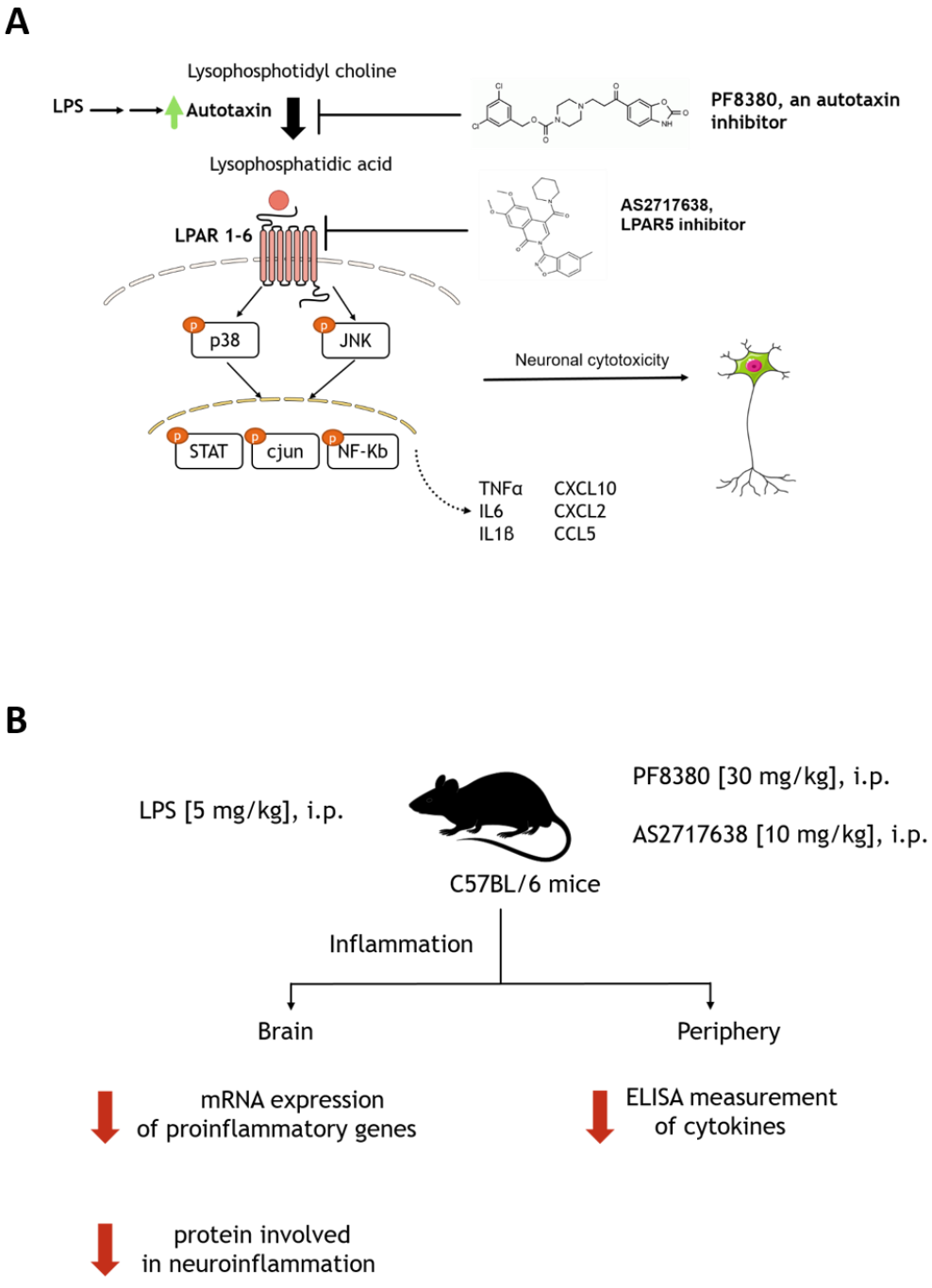

Figure 15 : Graphical summary of the findings obtained during this part of my thesis. (**A**) In vitro studies in BV-2 microglia indicate LPS activates ATX/LPA/LPAR axis. Antagonism of ATX (PF8380) and LPA5 (AS2717638) attenuates proinflammatory signaling cascade to inhibit secretion of cyto-/chemokines and neuronal cytotoxicity (**B**) In vivo studies indicate PF8380 (30 mg/kg, 24h) and AS2717638 (10 mg/kg, 24h) inhibits inflammation in the brain and periphery in endotoxemia model of mice (LPS 5 mg/kg, 24h).

3.2. Part II:. LPA induces metabolic reprograming in microglia

Immune cells reprogram intracellular metabolic pathways which subsequently alters effector function. In a similar manner, microglia are known to shift their bioenergetics pathways in response to external inflammatory stimuli to support changing cellular activities of phagocytosis, migration, proliferation and cytokine release. During this study, we addressed the question if LPA induces metabolic reprograming in microglia to support pro-inflammatory effects of LPA in microglia, as previously studied (20)

The three major energy substrates in microglia are glucose, amino acids and fatty acids. Hence, we investigated the effect of LPA on these metabolic pathways.

Effect of LPA on cell viability

The first set of experiments was performed to investigate cell proliferation and viability in untreated and LPA stimulated BV-2 cells using the Viacount system since LPA is a biomolecule with growth-factor-like activities (209). LPA (1 µM) increased the viable cell count (about 25 %) at 24 h (**Fig. 16A**). Approximately 20% of total cells were dead due to prolonged exposure to serum free conditions, and was unaffected upon treatment by LPA (**Fig. 16B**).

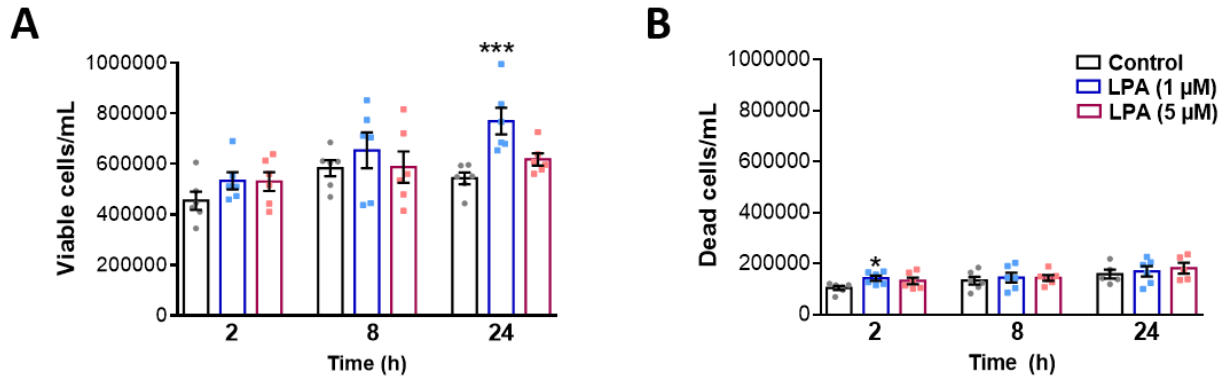

Figure 16: Effect of LPA on cell viability in BV-2 microglia. (**A**) Viable cells and (**B**) dead cells in the absence and presence of LPA for the indicated times and concentrations was measured by Guava ViaCount. Bar graph represents mean values ± SEM of 3 independent experiments; (*p < 0.05, *** p<0.001 compared to control; one-way ANOVA with Bonferroni correction) (172).

LPA impacts mitochondrial energy metabolism of BV-2 cells

Next, we characterized LPA-mediated effects on glucose utilization in microglia. As the main source of energy in brain and in microglia under normal conditions, glucose is metabolized mainly via oxidative phosphorylation to support the bioenergetics needs of the cells under normal conditions. To investigate the mitochondrial respiration of BV-2 cells in response to LPA, we analyzed oxygen consumption rate (OCR) using the real time Seahorse Extracellular Flux analyzer mitochondria stress test. This protocol employs the use of mitochondrial inhibitors, Oligomycin, FCCP and Antimycin to quantitate key parameters of mitochondrial respiration. LPA induced a time dependent change in mitochondrial energetics in the cells (**Fig. 17A**). An acute LPA exposure induced a transient increase in OCR, while at longer incubation times, basal and maximal OCR showed a downward trend (**Fig. 17B,C**). A similar pattern was observed for mitochondrial ATP production and spare respiratory capacity (**Fig. 17D,E**). This indicates a tendency for depression of mitochondrial respiration in response to LPS. In line, LPA (at 1 µM) diminished MTT reduction, a measure of mitochondrial activity, in BV-2 cells (**Fig 17F**).

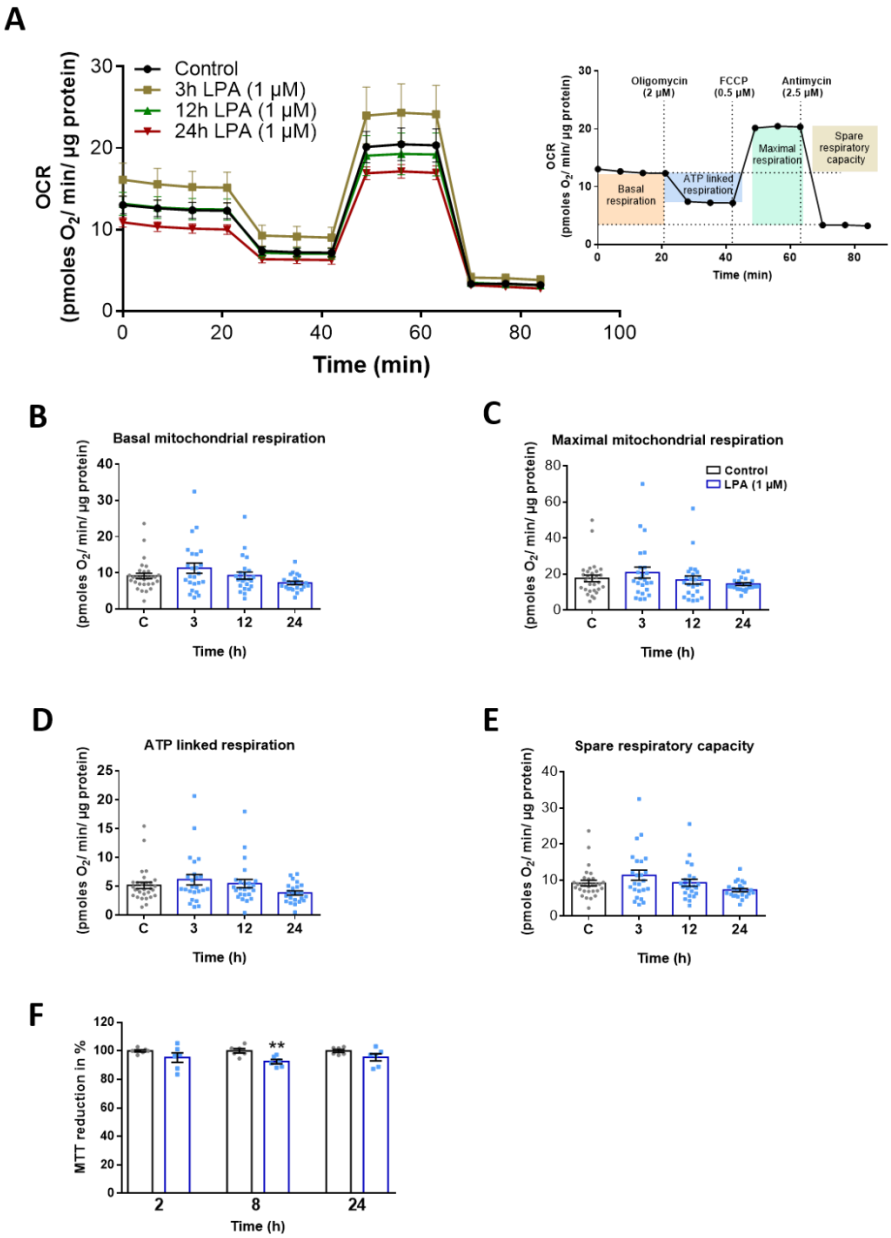

Figure 17: Effect of LPA on mitochondrial respiration in BV-2 microglia. (**A**) Oxygen consumption rate (OCR) in the absence and presence of LPA (1 µM) for the indicated times was detected using the XF Cell Mito Stress Test. Cells were treated with 2 µM oligomycin, 0.5 µM FCCP, and 2.5 µM antimycin A in XF assay medium to assess fundamental parameters of mitochondrial function (inset). Bar graphs show (**B**) basal mitochondrial respiration, (**C**) maximal mitochondrial respiration, (**D**) ATP linked respiration, and (**E**) spare respiratory capacity. (**F**) Effect of LPA (1 µM) on MTT reduction in cells was compared to control. Results are shown as mean values ± SEM; **p<0.01, compared to control; one-way ANOVA with Bonferroni correction) (172).

LPA impacts adenine nucleotide concentrations

To investigate the outcome of LPA-signaling on total cellular adenine nucleotide and phosphocreatine (PCr) concentration, HPLC analyses were performed. (**Fig. 18**) shows that LPA (1 µM) decreased ATP content (**Fig. 18A**), findings accompanied by an increase in low energy phosphate, ADP and AMP (**Fig. 18B, C**). A significant decrease in the ATD/ADP ratio and energy charge was seen at 24 h (**Fig. 18D,E**). Phosphocreatine, the ATP reservoir of the cell remained fairly unchanged (**Fig. 18F**).

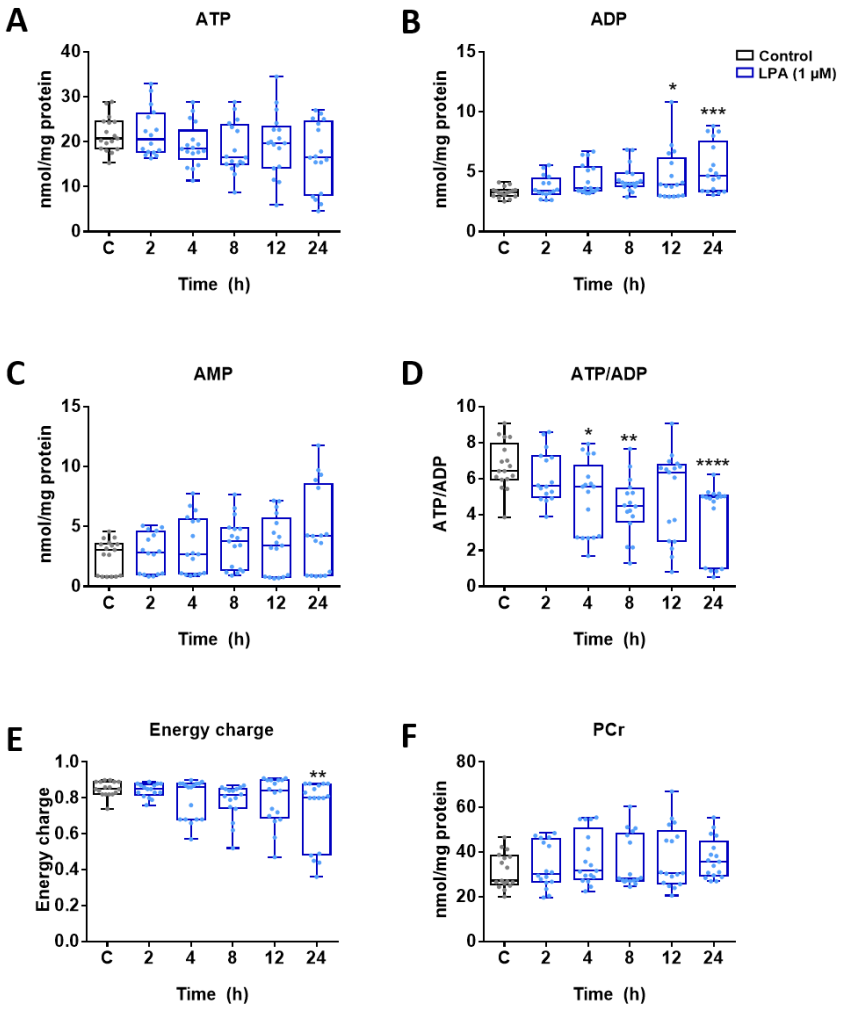

Figure 18: Effect of LPA on adenine nucleotide and phosphocreatine content in BV-2 microglia. Total cellular adenine nucleotide and phosphocreatine (PCr) content of BV-2 microglia in response to LPA treatment was quantified using HPLC. Graphs represent the concentration of (**A**) ATP, (**B**) ADP, (**C**) AMP, (**D**) ATP/ADP ratio, (**E**) the energy charge (EC) calculated as EC = ([ATP+1/2ADP]/[ATP+ADP+AMP]) and (**F**) phosphocreatine concentration.

Results are presented as mean values ± SEM of 3 independent experiments. (*p<0.05, **p<0.01, *** p<0.001, compared to control; one-way ANOVA with Bonferroni correction) (172).

LPA regulates the ATX-mTOR-HIF1α-PFKFB3 signaling pathway

Next, to determine intracellular signaling pathways that converge on glycolysis, I performed western blot analyses (**Fig 19A**). As Akt is a multifunctional kinase regulating a number of metabolic pathways, we aimed to examine Akt phosphorylation and its downstream signaling. The experiments revealed that LPA phosphorylated Akt at S472 and mTOR at Ser2448. HIF-1α (Hypoxia Inducible Factor), which functions as regulator of cellular and systemic homeostasis in response to hypoxia is driven by mTOR. LPA induced the expression of HIF1α under normoxic conditions, at incubation times >8h, which manifests into upregulation of HIF1α-dependent glycolytic genes like PFKFB3, a key regulator of glycolytic flux. Densitometric evaluations of band intensity from three independent biological replicates are shown in the bar graphs (**Fig. 19B-E**). These findings suggest that LPA activates a signaling axis in BV-2 cells that induces aerobic glycolysis.

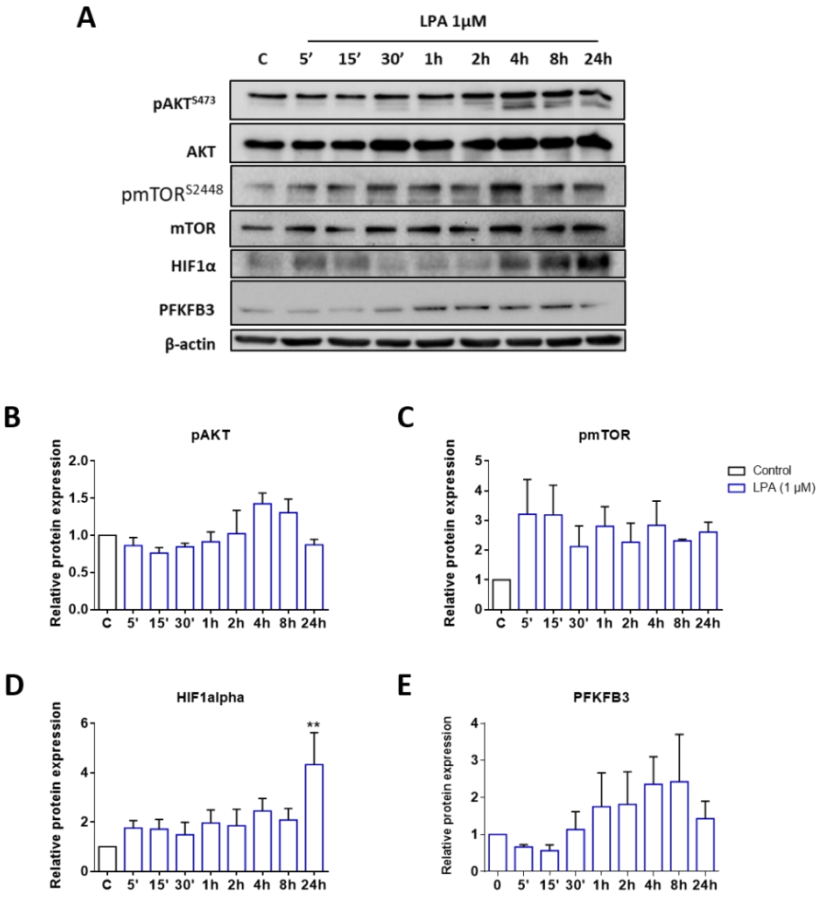

Figure 19: Immunoblot analysis of proteins involved in glycolysis upon treatment with LPA. Serum-starved BV-2 cells were incubated in the absence (c) and presence of 1 µM LPA for the indicated time points. Expression levels of energy/oxygen sensing proteins were examined by immunoblotting. (**A**) One representative blot out of three is shown. β-actin was used as loading control. Bar graphs represent densitometric analyses of immunoreactive bands of (**B**) phosphorylated AKT (pAKT), (**C**) phospho mTOR (pmTOR), (**D**) HIF1α, and (**E**) PFKFB3 relative to β-actin. Results are presented as mean values ± SEM of 3 independent experiments. (**p<0.01 compared to control; one-way ANOVA with Bonferroni correction) (172).

LPA regulates mRNA expression of glycolytic genes.

qPCR analyses were performed to analyze gene expression of glucose transporters in LPA stimulated BV-2 cells. LPA (1 µM) induced a transient upregulation of mRNA transcription of glucose transporters GLUT1, GLUT3, GLUT4, GLUT5, and hexokinase 2, a rate limiting enzyme in glycolysis however these effects were not statistically significant (**Fig. 20 A-E**).

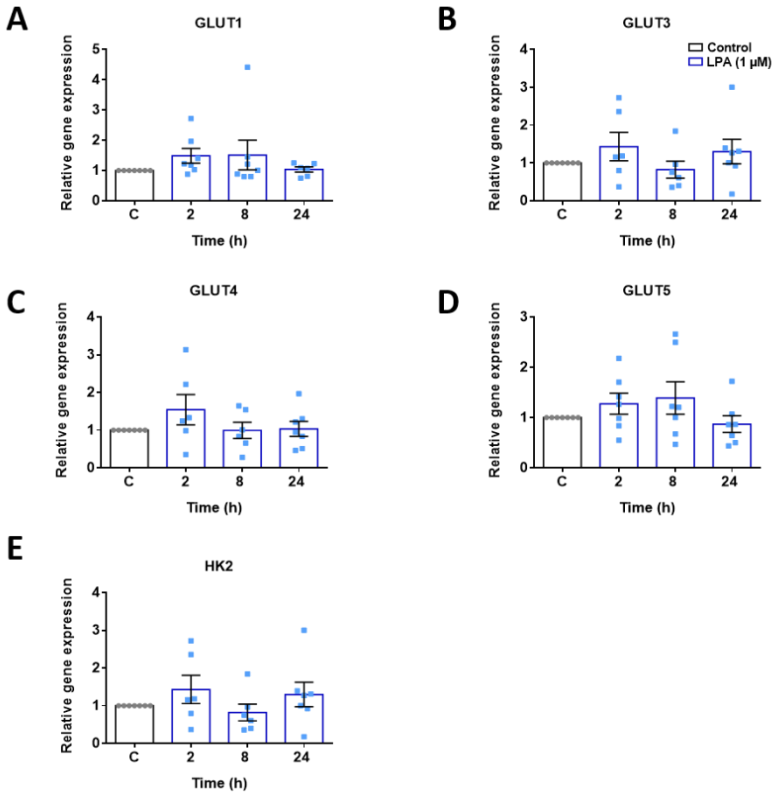

Figure 20: Gene expression of glucose transporters and hexokinase 2 in LPA-treated BV-2 microglia. Serum-starved BV-2 cells were treated with 1 µM LPA for the indicated times and gene expression of glucose transporters (**A**) GLUT1, (**B**) GLUT3, (**C**) GLUT4, and (**D**) GLUT5, and (**E**) hexokinase 2 was evaluated by qPCR analysis. Hypoxanthine-guanine phosphoribosyltransferase (HPRT) was used as housekeeping gene. Expression was calculated

using the 2^{-ddCt} method. Results are presented as mean values ± SEM of 3 independent experiments (one-way ANOVA with Bonferroni correction) (172).

LPA increases extracellular lactate concentrations

Increased glycolytic activity appears to be a core pre-requisite for pro-inflammatory microglia functions (210). Therefore I quantified the levels of extracellular lactate, the major end product of aerobic glycolysis. These analyses demonstrated that the concentration of lactate secreted into the media in response to LPA was significantly higher (6.8 vs 5.2 mM) in response to LPA 1 µM (**Fig. 21**). This further supports a metabolic shift towards aerobic glycolysis.

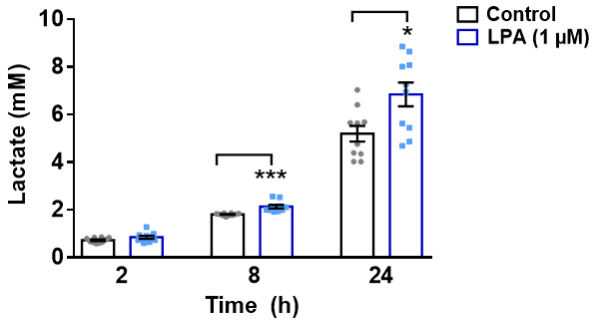

Figure 21: Effect of LPA on lactate content in BV-2 microglia. Lactate content of LPA (1 µM) treated cells was measured by EnzyChrom™ Glycolysis Assay Kit and compared to their appropriate controls. Bar graph represents mean values ± SEM of 3 independent experiments; (*p < 0.05, *** p<0.001 compared to control; unpaired Student's t-test) (172).

LPA induces lipogenesis in BV-2 cells

Microglia engages in lipid metabolism in order to control morphological transitions and cytokine secretion during microglial activation (67). We first investigated signaling pathways involving key regulators of fatty acid turnover (**Fig. 22A**). AMP-activated protein kinase (AMPK), the metabolic master switch regulates Acetyl CoA carboxylase (ACC1) activity, a key enzyme involved in fatty acid synthesis. The phosphorylation of ACC1 at S79 inhibits malonyl-CoA formation and hence, suppresses FA synthesis/elongation (172). Western blot analyses revealed a time dependent reduction of AMPK phosphorylation at S172, concomitant with dephosphorylation of ACC at S79 in response to LPA at incubation times >30 min. Phosphorylation status of sterol regulatory element binding protein (SREBP)-1c was not significantly changed. Densitometric evaluations of band intensity from three independent biological replicates are shown in the bar graph (**Fig. 22B-D**).

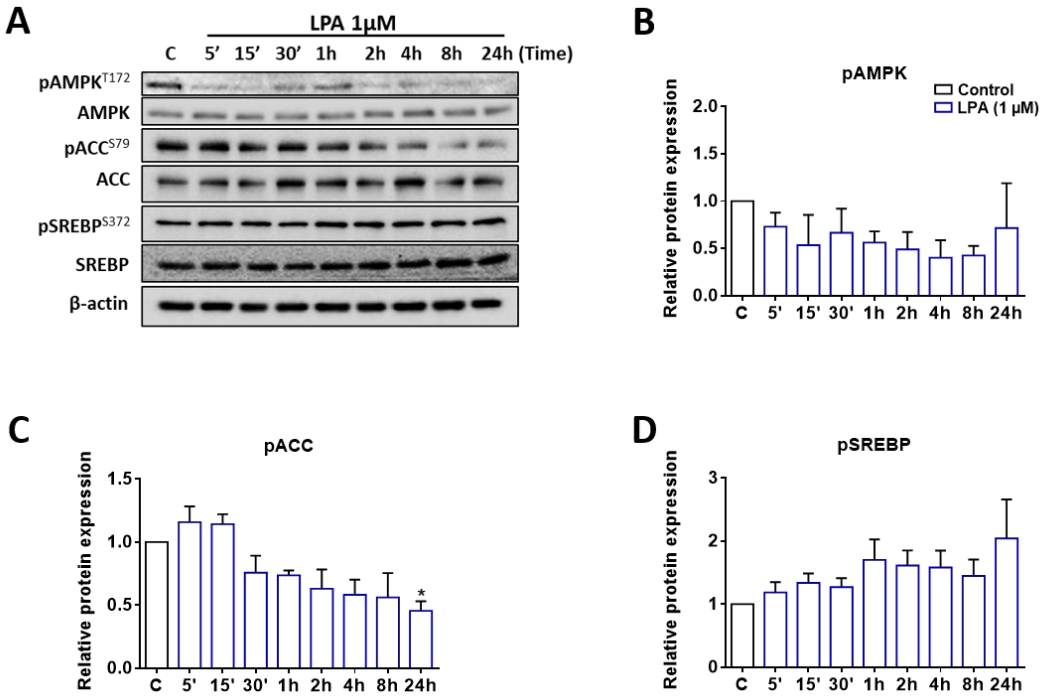

Figure 22: Phosphorylation status of AMPK, ACC, and SREBP in LPA treated BV-2 microglia. BV-2 cells were serum-starved overnight and incubated in the absence ('c') and presence of 1 µM LPA for the indicated times. Phosphorylation states of proteins were detected using western blot analysis, β-actin served as loading control. (**A**) One representative blot out of three is shown. Densitometric analyses of immunoreactive bands of (**B**) phospho AMPK (pAMPK), (**C**) phospho ACC (pACC), and (**D**) phospho SREBP (pSREBP) relative to β-actin are shown. Results are presented as mean values ± SEM of 3 independent experiments. (*p<0.05, compared to control; one-way ANOVA with Bonferroni correction) (172).

To quantitate the FA content in major lipid subclasses (phospholipids, PL; free fatty acids, FFA; diacylglycerols, DAG; triacylglycerols, TAG; and cholesterylesters, CE), gas chromatography was performed with lipid extract from untreated and LPA-treated (8 and 24 h) BV-2 cells. Under basal conditions, the PL fraction (96 µg FA/mg cell protein) was found to be present at highest concentration, while the other lipid subclasses were less abundant. LPA (1 µM) significant increased the concentration of PL and TAG fractions at 8 h, while DAG, FFAs and CE fractions showed an increasing trend (**Fig. 23A**). Within PL subclasses, 16:0, 16:1, 18:0, and 18:1 fractions were significantly increased (**Fig. 23B**). 16:0, 18:0, and 18:1 DAG fractions were the predominating species (**Fig. 23C**), while 18:0 FFA fractions was most abundant (**Fig. 23D**). In the TAG family, 18:0 and 18:1 were detected in abundance (**Fig. 23E**), whereas only 16:1 and 18:1 CE fractions were detectable in the CE fraction (**Fig. 23F**).

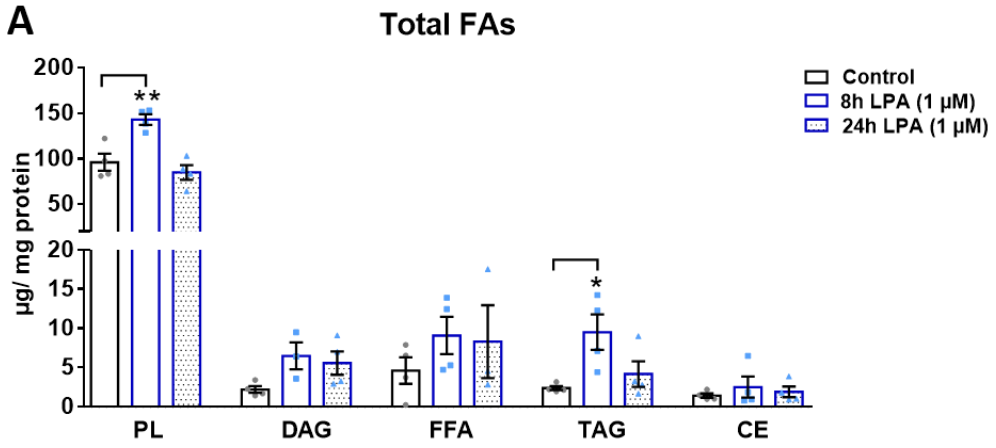
A
Total FAs
Control
8h LPA (1 μM)
24h LPA (1 μM)
μg/ mg protein
PL
DAG
FFA
TAG
CE

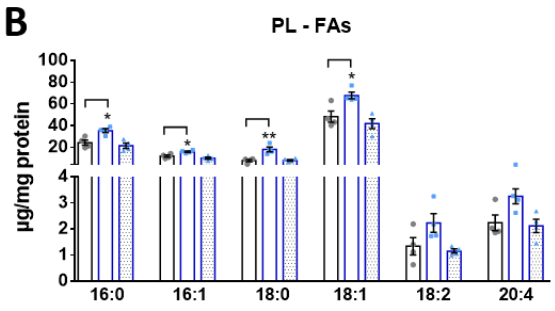
B
PL - FAs
μg/mg protein
16:0
16:1
18:0
18:1
18:2
20:4

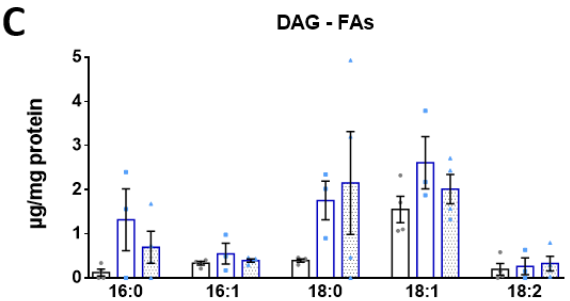
C
DAG - FAs
μg/mg protein
16:0
16:1
18:0
18:1
18:2

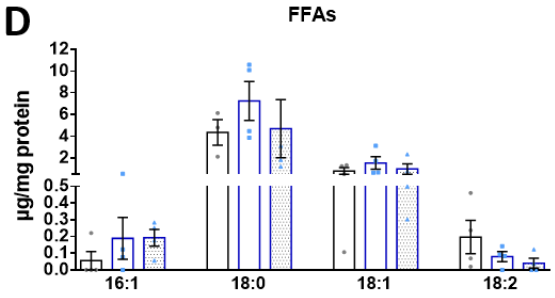
D
FFAs
μg/mg protein
16:1
18:0
18:1
18:2

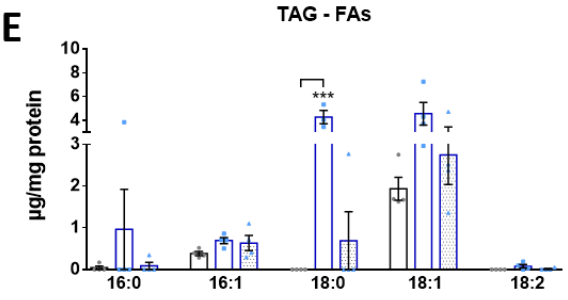
E
TAG - FAs
μg/mg protein
16:0
16:1
18:0
18:1
18:2

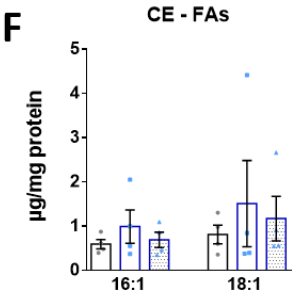
F
CE - FAs
μg/mg protein
16:1
18:1

Figure 23: Quantitation of fatty acid species in lipid subclasses of LPA treated BV-2 microglia. Serum starved BV-2 cells were incubated with 1 µM LPA for the indicated times. (**A**) Quantitation of total FAs present in the indicated lipid species (PL, phospholipids; DG, diacylglycerols; FFA, free fatty acids; TAG, triacylglycerols; CE, cholesterylesters). Individual FA content in each lipid class: (**B**) phospholipids, (**C**) diacylglycerols, (**D**) free fatty acids, (**E**) triacylglycerols, and (**F**) cholesterylesters. Data represent mean ± SEM of four independent experiments; *$p < 0.05$, **$p < 0.01$, compared to control; one-way ANOVA with Bonferroni correction) (172).

LPA increases intracellular amino acid concentrations in BV-2 cells.

LPA induces microglia activation and is marked by proinflammatory cytokine secretion. It is reasonable to assume that de-novo cytokine synthesis results in altered intracellular amino acid concentration/composition. Furthermore, AAs activate mTOR signaling to participate in different metabolic processes including fatty acid synthesis. Hence, we determined time dependent concentration of free amino acids in BV-2 microglia. AAs were separated as OPA derivatives by HPLC and quantified in comparison with external standard mixture. Under basal conditions, Glu and Gln (6 and 10 µg/mg cells protein) were the most abundant AAs, followed by Asp, Asn, Gly and Tyr. The aliphatic AAs Gly, Ala, Val, Leu and Ile significantly increased in response to LPA at different time points (**Fig. 24A**). Similar findings were made for OH-and S-containing AAs; Ser, Thr, and Met (**Fig. 24B**). In addition, aromatic AAs - Phe, Tyr, and Trp, and basic AAs - His and Lys showed a similar trend over the entire time course (**Fig. 24C,D**). Within the class of basic AAs, Arg was almost unaffected (**Fig. 24D**). The most abundant AAs belonging to acidic group - Asp, Asn, Glu, and Gln concentrations significantly increased in response to LPA over time (**Fig. 24E**). The last group of non-proteinogenic AAs – βAla, Tau, and Orn were elevated upon stimulation by LPA (**Fig. 24F**).

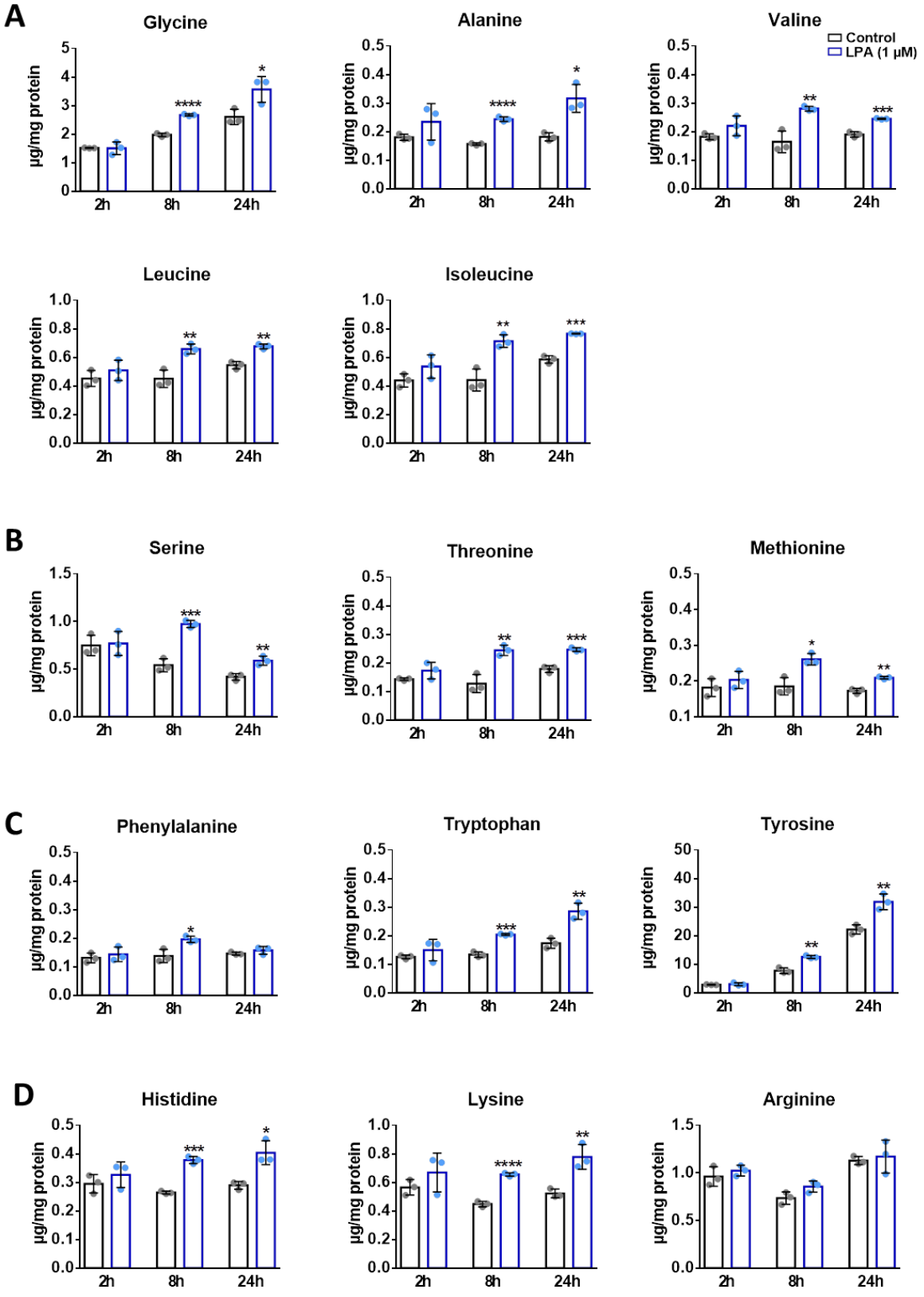
A
Glycine
Alanine
Valine
Control
LPA (1 μM)
Leucine
Isoleucine
B
Serine
Threonine
Methionine
C
Phenylalanine
Tryptophan
Tyrosine
D
Histidine
Lysine
Arginine
μg/mg protein
2h
8h
24h

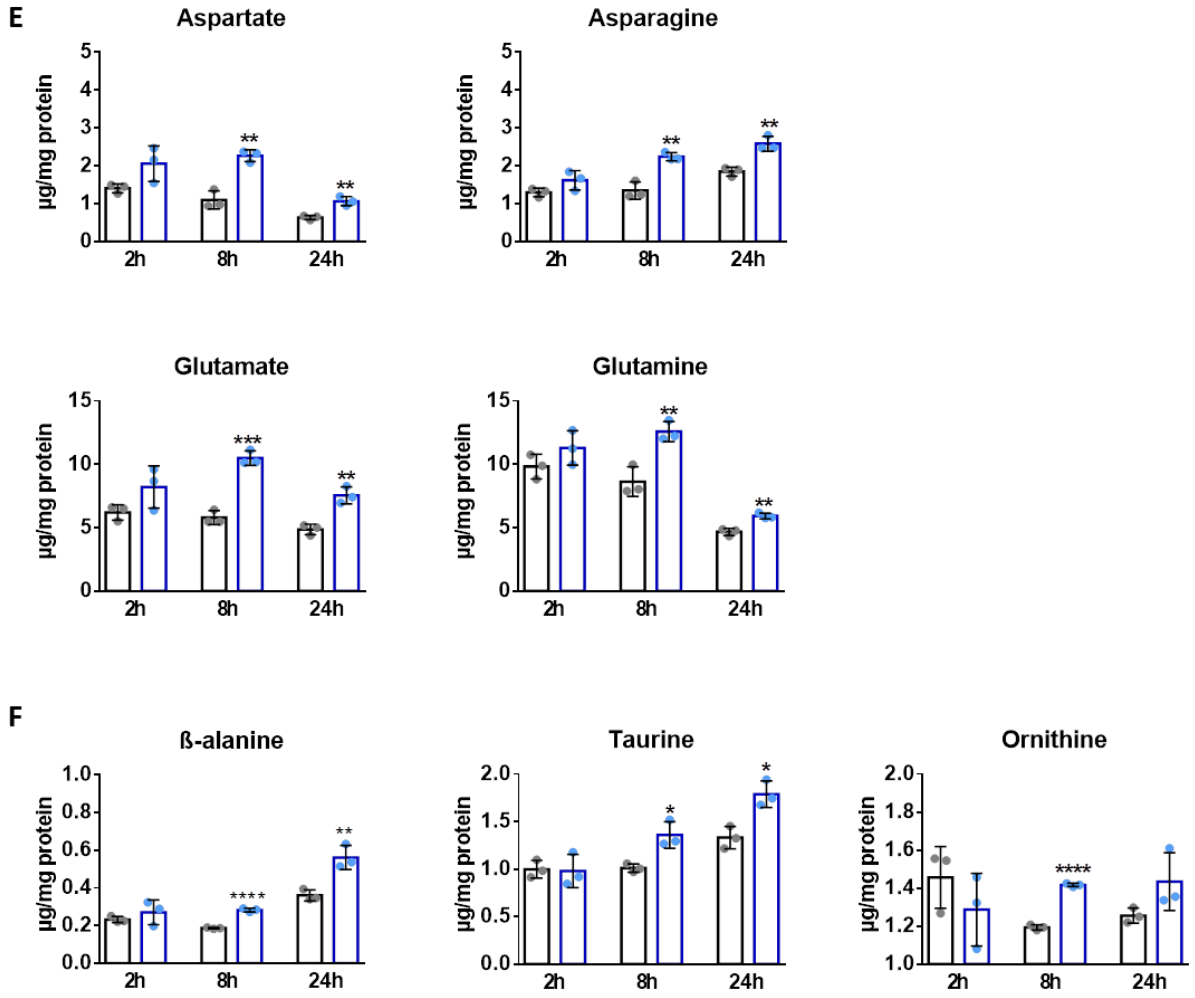

Figure 24: Amino acid analysis of LPA treated BV-2 cells. Serum-starved BV-2 cells were incubated in the absence (control) and presence of LPA (1 µM) for the indicated times. HPLC analysis of OPA derivatized amino acids (AAs) was performed and amino acid concentrations were determined by area comparison with external calibration curves and subsequent normalization to the cellular protein content. Bar graphs indicate mean ± SEM of 3 independent experiments. (*p<0.05, **p<0.01, ***p<0.001, ****p<0.0001 compared to controls; *Student`s* t-test). The amino acids are grouped according to their chemical properties in: (**A**) aliphatic AAs, (**B**) OH- and S-containing AAs, (**C**) aromatic AAs, (**D**) basic AAs, (**E**) acidic AAs, and (**F**) non-proteogenic AAs (172).

Effect of LPA in pentose phosphate pathway utilization

Dysregulation of the pentose phosphate pathway has been associated with the pathogenesis of neurodegenerative diseases (211). Here I observed that BV-2 microglia down-regulated mRNA expression of G6pd2, G6pdx, Tkt, and Pgd following incubation with LPA (**Fig.**

25A-D). In addition, NADPH, a key-product of pentose phosphate pathway was decreased in response to LPA, although statistically not significant (**Fig. 25E**).

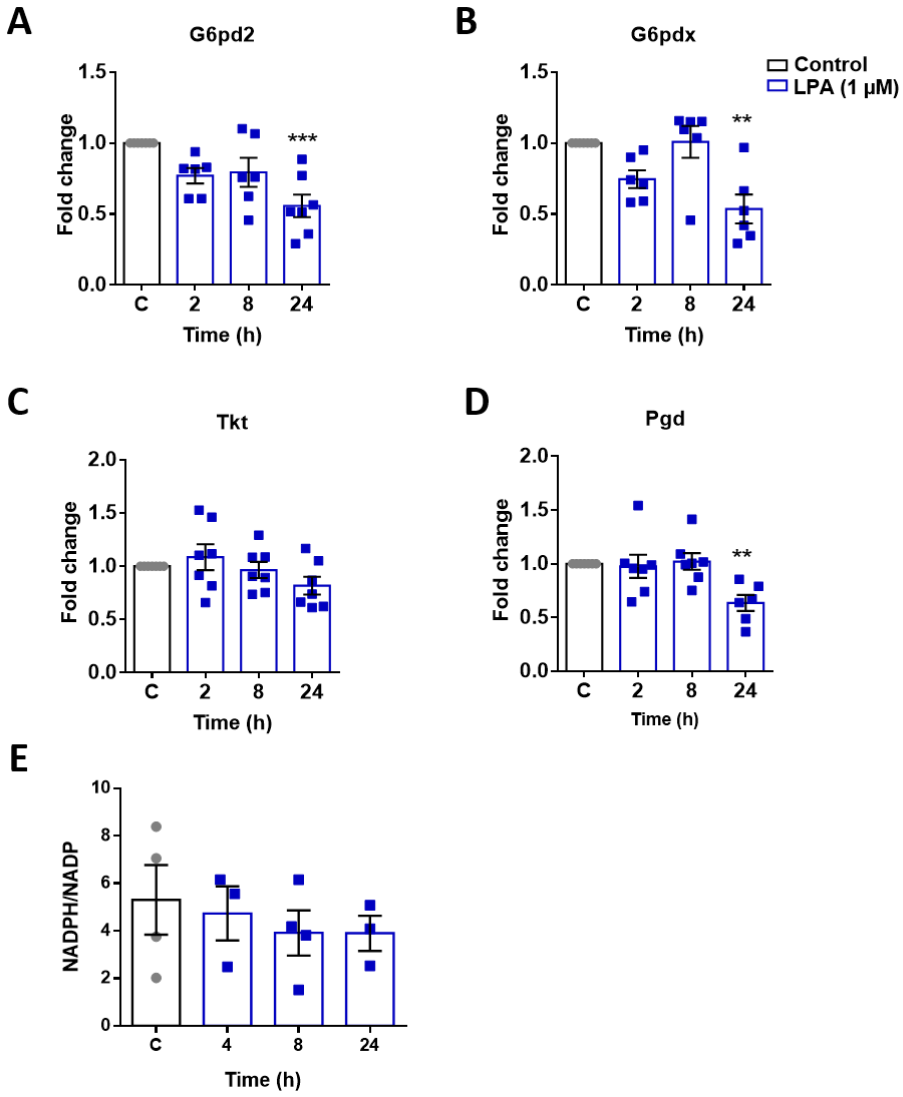

Figure 25: Effect of LPA on pentose phosphate pathway in BV-2 microglia. Serum-starved BV-2 cells were incubated in the absence (c) and presence of LPA (1 µM) for the indicated times and gene expression of (**A**) G6pd2, (**B**) G6pdx, (**C**) Tkt, and (**D**) Pgd, was evaluated by qPCR analysis. Hypoxanthine-guanine phosphoribosyltransferase (HPRT) was used as housekeeping gene. Expression was calculated using the 2^{-ddCt} method. (**E**) NADPH/NADP ratio of the cells were measured by NADP/NADPH assay kit (Abcam), and compared to their control. Results are presented as mean values ± SEM of 3 independent experiments $^{**}p < 0.01$, $^{***}p<0.001$ compared to control; one-way ANOVA with Bonferroni correction).

LPA induces the Nrf2-mediated antioxidant response of BV-2 cells

LPA treatment induces the generation of ROS in BV-2 cells after 2 h (**Fig. 26A**). To understand whether ROS generation leads to an antioxidant response, activation of Nrf2 was studied by western blotting analyses (**Fig. 26B**). LPA induced phosphorylation of Nrf2 at S40 which leads to transcription of antioxidant response elements (AREs) genes. In line, LPA increased the expression of the Nrf2 target, glutamate-cysteine ligase light chain (GCLm; **Fig. 26D**), the rate-limiting enzyme for GSH synthesis. This was reflected on product level by an increase in GSH concentrations at 2 and 8 h (**Fig. 26E**).

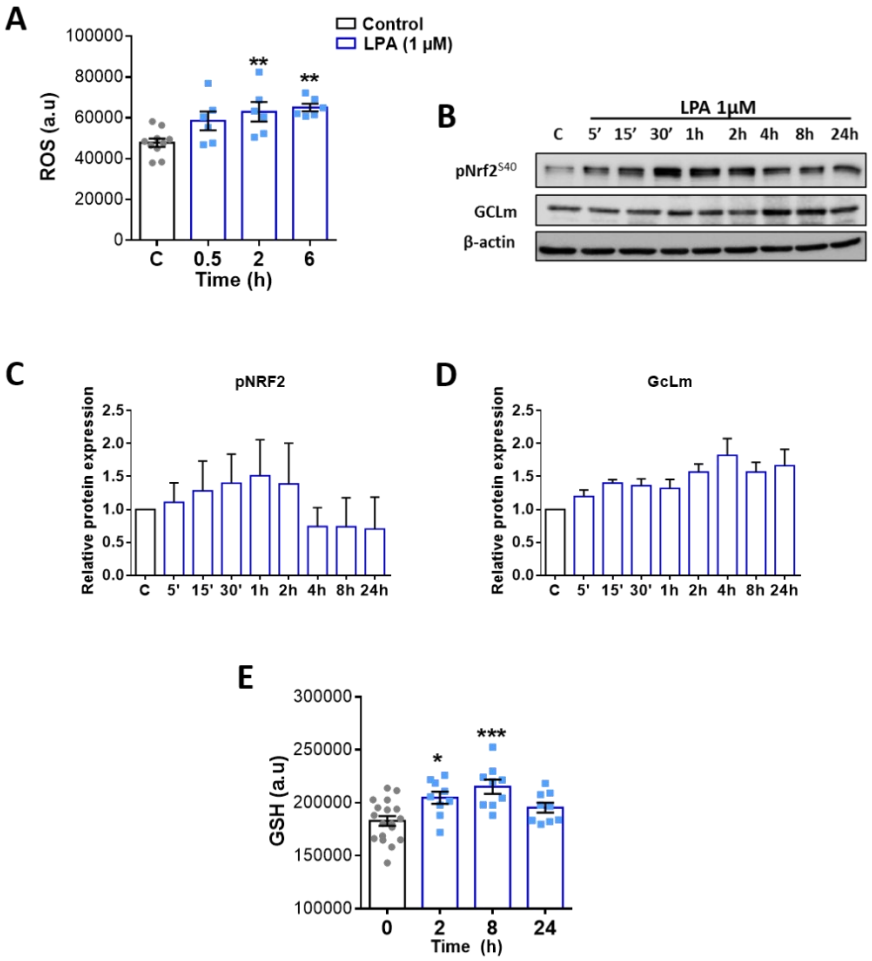

Figure 26: Characterization of the antioxidant response in LPA treated BV-2 microglia. (**A**) Reactive oxygen species (ROS) of control and LPA (1 µM) treated cells was quantified using the ROS-ID® Total ROS Detection kit (a.u. arbitrary units). (**B**) Immunoblot analysis of phospho Nrf2 (Ser40) and GCLm upon treatment with LPA. One representative blot out of three is shown. β-actin was used as loading control. (**C, D**) Densitometric analysis relative to β-actin from three

independent immunoblot experiments are presented. (**E**) Glutathione (GSH) concentration of LPA (1µM) treated cells was quantified with GSH-Glo Assay kit and compared with controls in three independent experiments. Results are presented as mean values ± SEM (*p<0.05, **p<0.01, ***p<0.001, compared to control; one-way ANOVA with Bonferroni correction) (172).

Graphical summary

Key findings of this part of my thesis are summarized in **Fig. 27**.

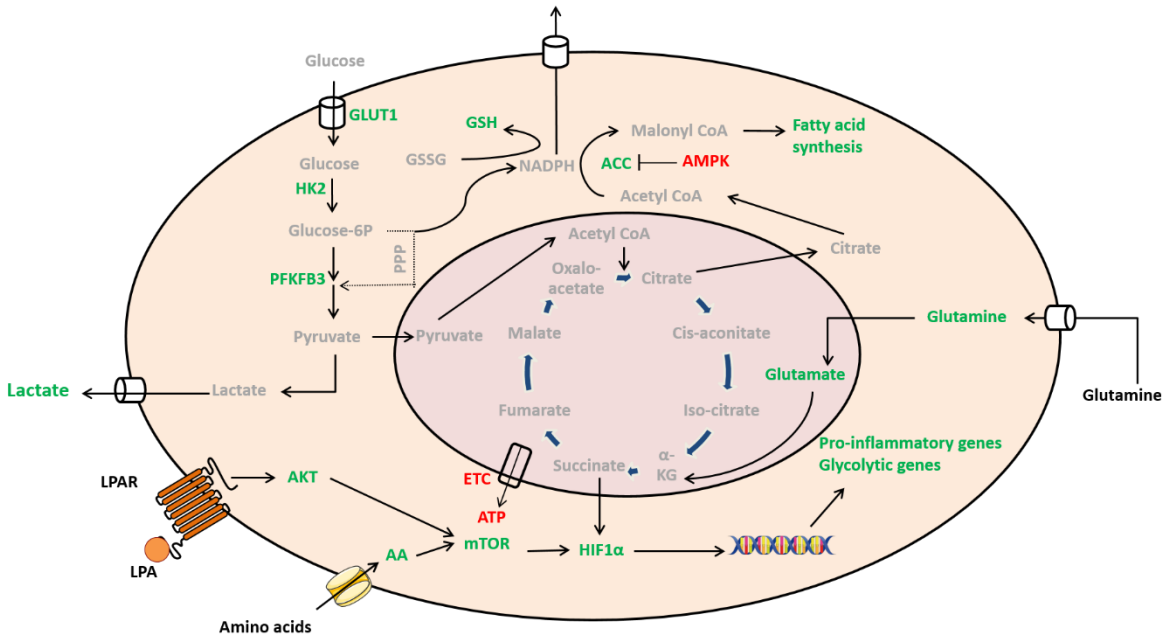

Figure 27: Key metabolic pathways alterations in LPA-activated BV-2 microglia. Graphical summary of findings obtained during a part of my thesis. Stimulation of microglia with LPA reprograms metabolism towards aerobic glycolysis for generation of ATP via the Akt/mTOR/HIF1α/PFKFB3 axis. As a consequence, lactate secretion increases. The activated BV-2 cells switch mitochondrial metabolism to support FA synthesis. Increased AA uptake can further fuel this metabolic program and sustain proinflammatory cytokine synthesis. In response to ROS generation the antioxidant response is initiated and results in higher levels of intracellular GSH to prevent damage of endogenous macromolecules. Red = decreased, green = increased. (Intermediates not experimentally addressed during the present study are grayed out) (172).

3.3. Part III: Effect of genetic LPA5 deletion on microglia inflammation and metabolism

Genetic deletion of LPA5 reduces LPA induced secretion of inflammatory cyto-/chemokines

Evidence indicates that LPA drives BV-2 and primary murine microglia towards a pro-inflammatory phenotype via LPA5 (20). To confirm the role of LPA5 in modulating inflammatory response in microglia, I used global LPA5 knockout mice ($LPA5^{-/-}$) and assessed the effect of LPA5 deletion on microglia inflammation in $LPA5^{-/-}$ microglia. In the first series of experiments, I studied cyto-/chemokine secretion from LPA stimulated PMM and the impact of LPA5 deletion on extracellular accumulation of these analytes. These results revealed that LPA significantly increased the concentration of cytokines TNFα and IL6, chemokines CXCL10, CXCL2 and CCL5 significantly at one or more time point in wildtype microglia (**Fig.28**). This effect was significantly attenuated in $LPA5^{-/-}$ microglia. No significant change was noted in the level of IL-1β in response to LPA in wildtype and $LPA5^{-/-}$ microglia.

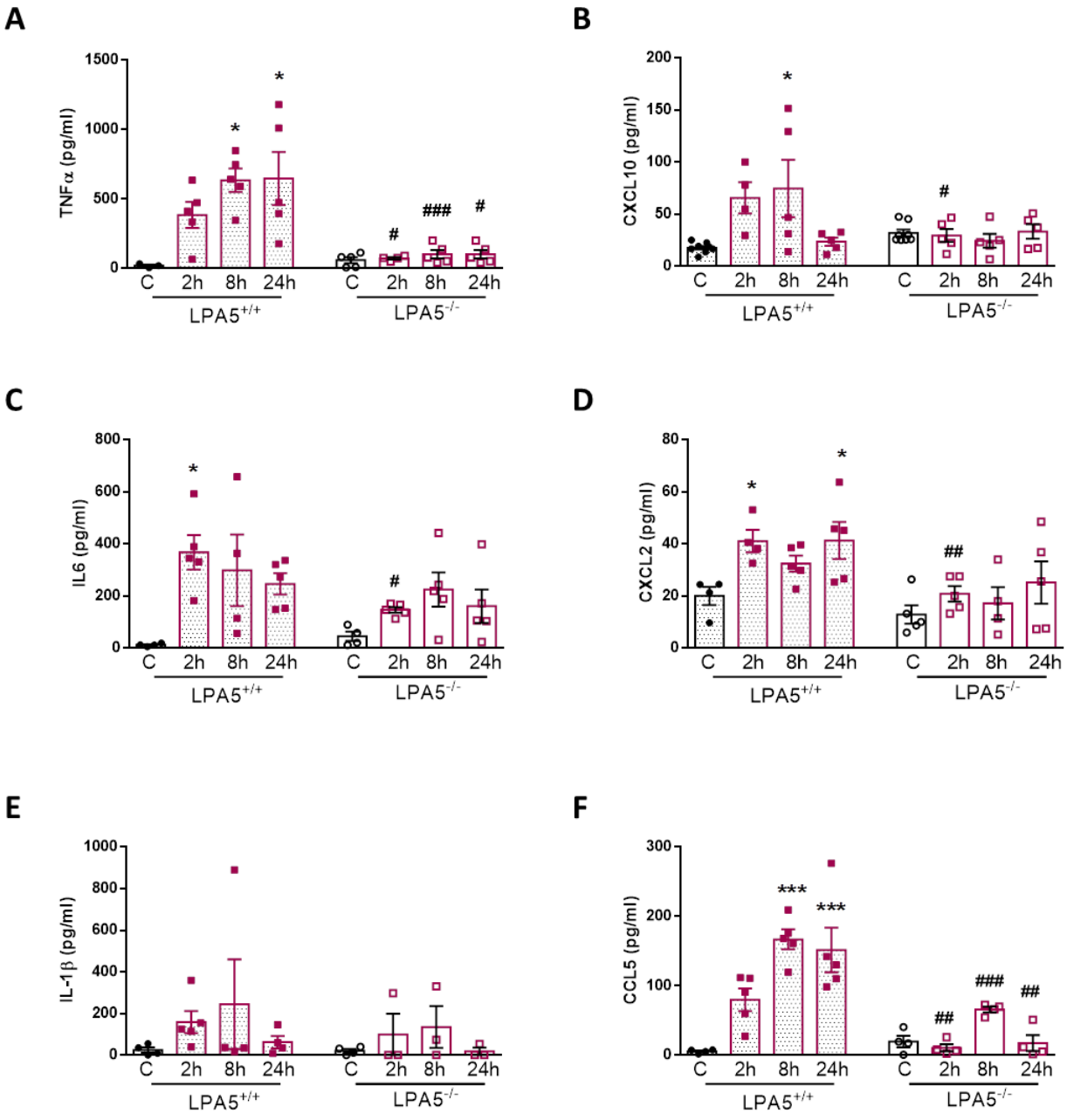

Figure 28: LPA5 regulates LPA-induced secretion of cyto-/chemokines in PMM. LPA5$^{+/+}$ and LPA5$^{-/-}$ microglia were treated with LPA (5 µM) for the indicated time. Supernatants were collected. Concentration of cytokines TNFα, IL6, and IL-1β and chemokines CXCL10, CXCL2, and CCL5 were quantified by ELISA. Values are expressed as mean ± SEM of three independent experiments. (*p < 0.05, ***p < 0.001, **** p < 0.0001 compared to control; # p < 0.05, ## p < 0.01, ### p < 0.001 each LPA5$^{-/-}$ condition compared to LPA-treated LPA5$^{+/+}$ condition (one-way ANOVA with Bonferroni correction)

LPA5 deletion attenuates LPA-induced NO production

Next, we examined the impact of LPA5 deletion on nitric oxide (NO) production in LPA stimulated cells. LPA increased NO production (detected as nitrate) in wildtype microglia. LPA5 deficiency led to a significant reduction in NO production upon incubation with LPA (5 µM) for 24h (**Fig.29**).

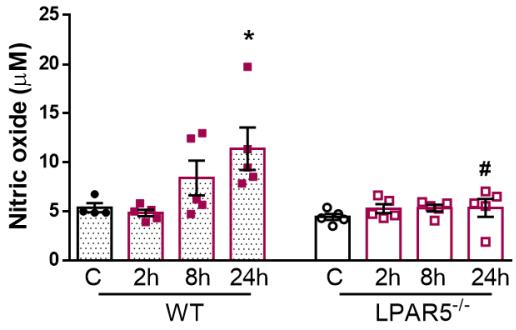

Figure. 29: LPA5 regulates LPA-induced NO production in PMM. LPA5$^{+/+}$ and LPA5$^{-/-}$ microglia were treated with LPA (5 µM) for 24h. Supernatants were collected. The production of NO was determined by measuring the total nitrate concentration in the supernatants. Values are expressed as mean ± SEM of three independent experiments. (# $p < 0.05$ each LPA5$^{-/-}$ condition compared to LPA-treated LPA5$^{+/+}$ condition (one-way ANOVA with Bonferroni correction)

LPA5 deletion increases mitochondrial respiration

Here, I aimed to investigate the mitochondrial respiration of LPA5$^{+/+}$ and LPA$^{-/-}$ microglia in response to LPA using the real time Seahorse Extracellular Flux analyzer mitochondrial stress test as described above. LPA showed a slight decrease in basal and maximal mitochondrial respiration in the wildtype cells (**Fig. 30**). A similar trend was observed in mitochondrial respiration associated with ATP production, and spare respiratory capacity. Interestingly, the maximal respiration rate of untreated and LPA-treated LPA5-/- microglia was nearly 1.5-fold higher as compared to untreated wt cells (**Fig. 30B,D**). Also ATP production and spare respiratory capacity were significantly higher in untreated and LPA-treated LPA5-/- cells as compared to wt (**Fig. 30 E,F**)..

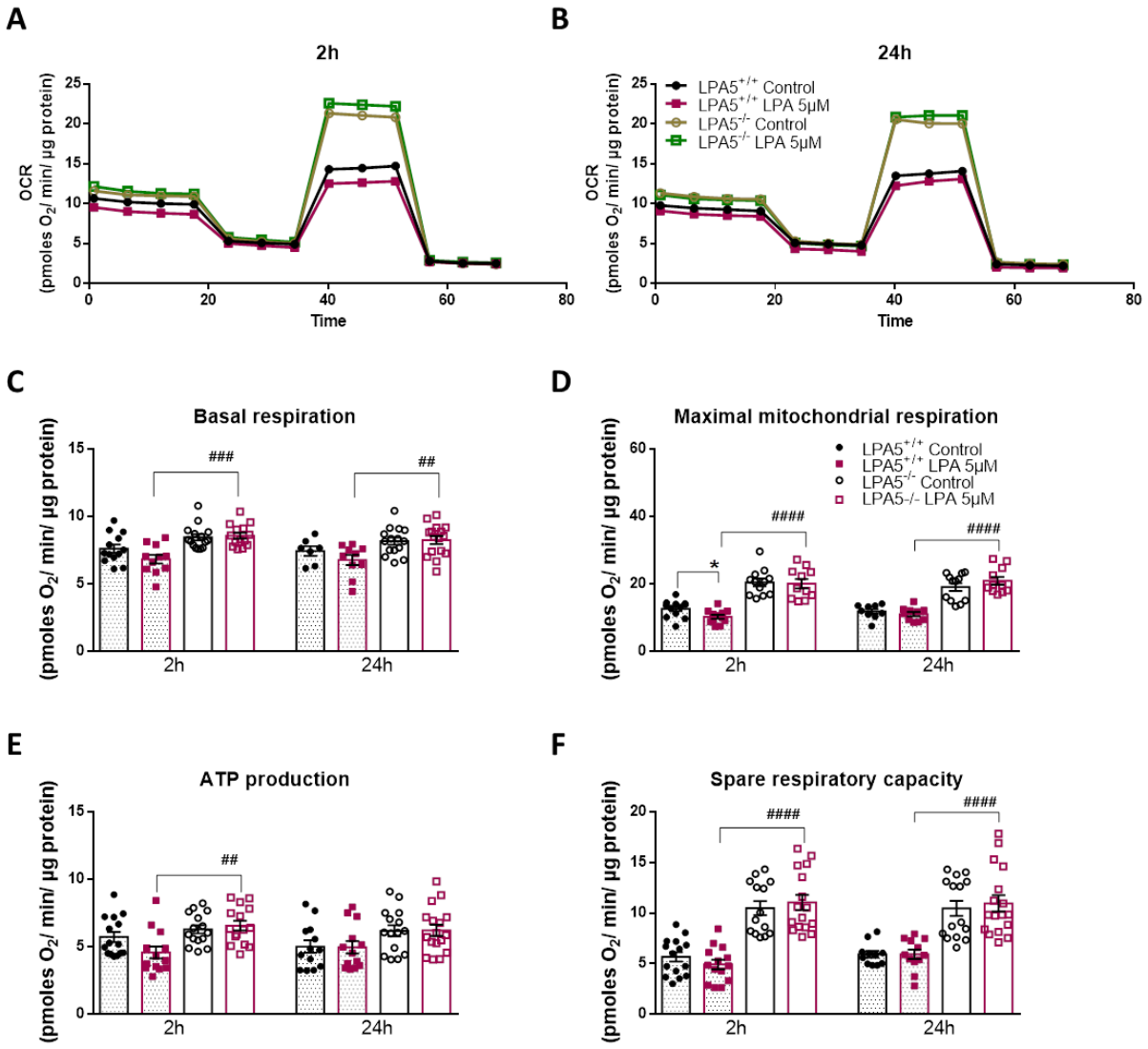

Figure. 30: LPA5 regulates mitochondrial respiration in PMM. (**A-B**) Oxygen consumption rate (OCR) in the absence and presence of LPA (5 µM) for 2h and 24h was detected using the XF Cell Mito Stress Test. LPA5$^{+/+}$ and LPA5$^{-/-}$ microglia were treated with 2 µM oligomycin, 1.75 µM FCCP, and 2.5 µM antimycin A in XF assay medium to assess fundamental parameters of mitochondrial function. Bar graphs show (**C**) basal mitochondrial respiration, (D) maximal mitochondrial respiration, (E) ATP linked respiration, and (**F**) spare respiratory capacity. Values are expressed as mean ± SEM of three independent experiments (** $p < 0.01$ compared to control; ## $p < 0.01$, ### $p < 0.001$ each LPA5$^{-/-}$ condition compared to LPA-treated LPA5$^{+/+}$ condition (one-way ANOVA with Bonferroni correction)

LPA5 deletion attenuates LPA induced lactate secretion

Inflammatory microglia are reported to switch to a glycolytic metabolic profile ((212) and above). Hence, I quantified the levels of extracellular lactate, the major end product of glycolysis. These analyses revealed that the concentration of lactate was significantly increased at 2h with an upward trend at 24h in wildtype microglia. This effect was attenuated by deletion of LPA5 (**Fig. 31**).

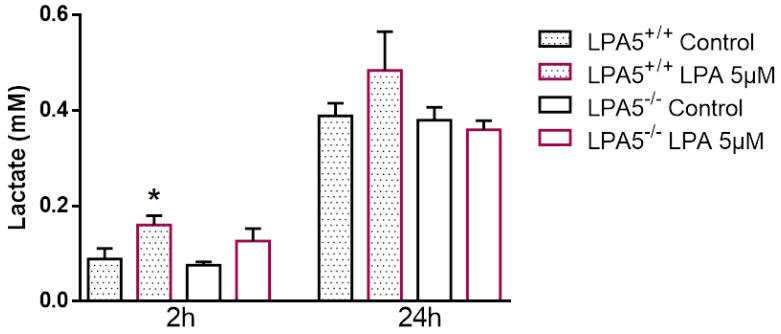

Figure 31: LPA5 regulates extracellular lactate content in PMM. Lactate content of LPA (5 µM) treated LPA5$^{+/+}$ and LPA5$^{-/-}$ microglia was measured by EnzyChrom™ Glycolysis Assay Kit and compared to their appropriate controls. Bar graph represents mean values ± SEM of 3 independent experiments; (*p<0.05 compared to control, unpaired Student's t-test).

LPA5 deletion mitigates utilization of the pentose phosphate pathway

The pentose phosphate pathway (PPP) is an important part of glucose metabolism which runs parallel to glycolysis to supply NADPH. Studies indicate that the activity of the pentose phosphate shunt is enhanced in pro-inflammatory immune cells (213). In response to LPA, NADPH, a key product of the PPP was increased in a time dependent manner in wildtype microglia as indicated by the increase in NADPH/NADP ratio. This utilization of PPP was diminished in LPA5$^{-/-}$ microglia (**Fig. 32**).

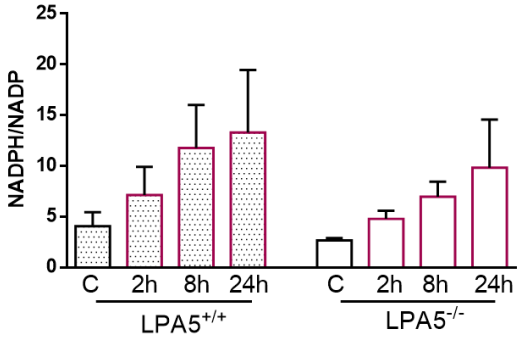

Figure 32: LPA5 regulates the utilization of pentose phosphate pathway in PMM. Serum-starved LPA5$^{+/+}$ and LPA5$^{-/-}$ microglia were incubated in the absence (c) and presence of LPA (5 µM) for the indicated times. NADPH/NADP ratio of the cells were measured by NADP/NADPH assay kit (Abcam), and compared to their control. Results are presented as mean values ± SEM of 3 independent experiments (one-way ANOVA with Bonferroni correction).

LPA5 deletion attenuates glutathione levels

NADPH generated by the PPP has reducing power to reduce glutathione disulfide into antioxidant glutathione (214). The LPA5$^{+/+}$ microglia showed a slight increase in reduced glutathione upon stimulation with LPA. In contrast, GSH levels were significantly lower in untreated or LPA-treated LPA5-/- cells (**Fig. 33**).

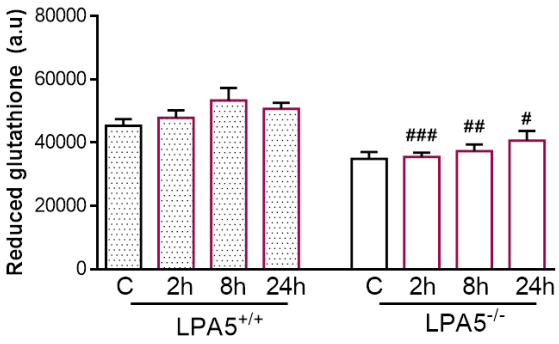

Figure 33: LPA5 regulates the level of reduced glutathione in PMM. Glutathione (GSH) concentration of LPA (5 µM) treated LPA5$^{+/+}$ and LPA5$^{-/-}$ cells was quantified with GSH-Glo Assay kit and compared with controls in three independent experiments. Results are presented as mean values ± SEM (# $p < 0.05$, ## $p < 0.01$, ### $p < 0.001$ each LPA5$^{-/-}$ condition compared to LPA-treated LPA5$^{+/+}$ condition, unpaired Student's t-test).

Graphical abstract

Key findings obtained during this part of my thesis are summarized in **Fig. 34**.

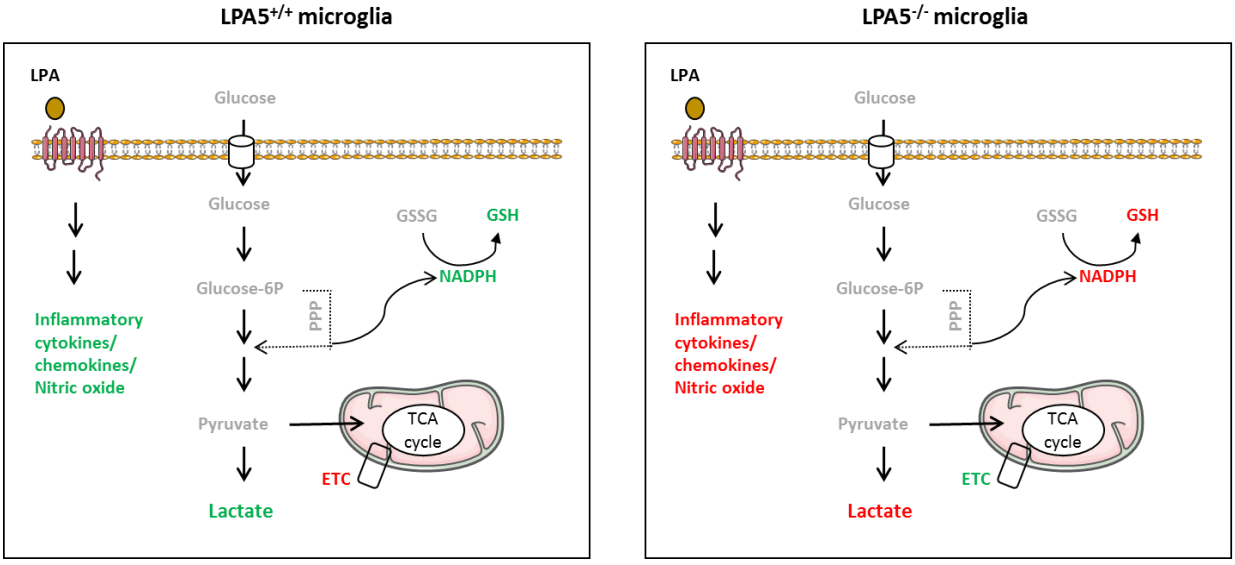

Figure 34: Key metabolic pathways alterations in LPA-activated LPA5$^{+/+}$ and LPA5$^{-/-}$ microglia. Stimulation of microglia with LPA induces metabolic reprograming to switch from oxidative phosphorylation towards glycolysis to increase lactate secretion. The activated PMM increases NADPH, a key metabolite of pentose phosphate pathway, to support the reduction of glutathione. These metabolic changes sustain proinflammatory cytokine synthesis and nitric oxide production. These effects are reversed in LPA5$^{-/-}$ microglia. Red = decreased, green = increased. (Intermediates not experimentally addressed during the present study are grayed out).

4. Discussion

Part I: Targeting the ATX-LPA axis in an endotoxemia model of neuroinflammation

Studies in experimental animal models revealed that a systemic challenge with LPS initiates a complex immunological response in the brain resulting in microglial activation, priming and/or tolerance, memory deficits and loss of brain synapses and neurons (26). Therefore, peripheral administration of LPS in mice is commonly used as experimental model to induce neuroinflammation. Of note, clinical evidence highlights the close and complex connection between systemic inflammation and neuroinflammation. Zhan and colleagues reported that brain

endotoxin levels are elevated two- to three-fold in Alzheimer's disease, with LPS colocalizing with Aβ1-40/42 in amyloid plaques and around vessels in AD brain (32). Studies revealed that the mean blood endotoxin levels are elevated in ALS patients possibly as a result of gut inflammation and microbiome changes (38). Also peripheral diseases that elevate blood endotoxin, such as sepsis and AIDS, are known to lead to neurodegeneration (26). In mice a single systemic injection of LPS results in elevated LPA concentrations in blood and brain, and induces differential regulation of ATX and LPARs in brain and FACS-sorted microglia (168). Therefore, we assessed the potential of an ATX and LPA5 inhibitor to ameliorate neuroinflammatory pathways that are elicited in response to peripheral LPS. For these studies we used the BV-2 microglia cell line (with all their known pros and cons) and a single i.p. injection of LPS in C57Bl/6 mice. Our study revealed that both, ATX and LPA5 antagonism, has potential to dampen the neuroinflammatory response in vitro and in vivo.

The role of the ATX/LPA axis in inflammatory diseases is not entirely clear. In an LPS-induced acute kidney injury mouse model an LPA injection prior to LPS application provided protection (i.e. reduced urea and creatinine levels) and decreased concentrations of circulating pro-inflammatory cytokines (215). In the murine EAE model of multiple sclerosis (MS) and in MS patients concentrations of several LPA species are reduced and subsequent deficiency in LPAR2 signaling in immune cells is promoting disease (216). Also, in ATX-overexpressing BV-2 microglia the LPS-induced inflammatory phenotype was less pronounced as compared to wild-type cells (217). Ciesielska and colleagues reported that binding of LPA to LPA5 and LPAR6 fine-tunes the LPS inflammatory response by activating p38, upregulating IL-10, and down-regulating TNFα production in J774 macrophages (218). Another study demonstrated a potential anti-inflammatory role of LPA in the LPS-mediated inflammatory response in macrophages via p38, Akt and NF-κB (219). In the LPS-induced acute lung injury mouse model, on the other hand, genetic or pharmacologic targeting of ATX had only minor effects on disease severity (187).

In contrast, there is also clear evidence that a dysregulated ATX/LPA axis (decreased LPC, increased ATX expression and LPA concentration) in acute-on chronic liver failure (ACLF) associates with mortality and systemic infection (220). The same group reported that LPS stimulates ATX gene expression and increases the inflammatory phenotype of monocytes isolated from ACLF patients (220). In line, it was demonstrated that LPS induces a massive increase in ATX mRNA and protein expression via autocrine IFN-γ signaling in monocytic THP-1 cells (221). In rodent models of neuropathic and inflammatory pain pharmacological inhibition of

LPA synthesis or downstream signaling has beneficial effects (222), and comparable observations were reported in experimental models of demyelination (223), traumatic brain injury (224), experimental autoimmune encephalomyelitis (225), or focal cerebral ischemia (226). During the present study pharmacological inhibition of ATX and LPA5 showed beneficial effects using in vitro and in vivo LPS models.

During adulthood ATX is highly expressed in adipose tissue and implicated in the development of metabolic disorders like the metabolic syndrome and inflammatory diseases (107). Obesity triggers low-grade inflammation which is associated with 'metabolic endotoxemia' most probably due to the release of low levels of gut derived LPS (227). Here we show, in line with others (217), that LPS modulates ATX and LPAR expression in BV-2 cells. LPS polarized cells exhibited an increase in ATX protein as well as PLD activity and upregulation of LPAR expression. These findings indicate that in BV-2 cells LPS could act as a primary inflammatory stimulus and leads to increased LPA synthesis probably as secondary, autocrine amplifier of the inflammatory response. In line with such a function, pharmacological inhibition of ATX and LPA5 in LPS-primed BV-2 cells reduced several proinflammatory parameters, including TLR4 and COX-2 protein expression, NO production, neurotoxicity, phosphorylation/activation of proinflammatory transcription factors, and cyto-/chemokine secretion.

TLR4 binding of LPS is facilitated in conjunction with LPS binding protein, CD14, and MD-2. As a co-receptor, CD14 sensitizes cells to LPS by transferring LPS molecules to TLR4. An and colleagues have reported CD14 as key mediator of both LPA- and LPS- induced foam cell formation in atherosclerosis (228). Since CD14 transcription and translation is strongly induced in response to LPA (228), LPA could amplify TLR4 signaling induced by LPS. TLR4 activation by LPS triggers two consecutive signaling cascades that rely on (intra)cellular receptor localization: Plasma membrane localized TLR4 triggers the Myd88, while internalized, endosomal TLR4 triggers TRIF-dependent signaling (218). These pathways lead to a synchronized production of pro- and anti-inflammatory mediators. The Myd88 pathway is responsible for COX-2, NOS2, TNFα, and IL-6 production while the TRIF axis contributes to CCL5 and CXCL10 production. In addition, TLR-4 is involved in canonical activation of the NLRP3 inflammasome where caspase 1 contributes to IL-1β synthesis. Our studies indicate that PF8380 and AS2717638 are able to attenuate pro-inflammatory effects in LPS induced inflammation in BV-2 microglia. Our Western blot analysis revealed suppression of TLR4 and COX-2 in PF8380 and AS2717638-treated BV-2 cells. In line, LPA was shown to induce TLR4

expression [52], while AM095, an LPA1 antagonist, suppresses TLR4 expression in mesangial cells [53]. Although both inhibitors used during the present study attenuated cyto-/chemokine concentrations in the cellular supernatant of LPS-treated BV-2 cells, the effects were more clear-cut for the CXCL10, CXCL2 and CCL5 chemokines. These findings could indicate that inhibition of LPA synthesis and/or downstream signaling preferentially attenuates the TLR4-dependent TRIF axis.

Our in vivo studies further demonstrated anti-inflammatory potential of PF8380 and AS2717638 in a murine endotoxemia model. Here it is noteworthy that we have adopted a prophylactic rather than a therapeutic treatment regimen. Using a co-administration protocol of LPS and PF8380 or AS2717638 we found that both compounds reduced iNOS, TNFα, IL-6, and CXCL2 mRNA expression, while IL-1β was only inhibited by PF8380. On protein level both inhibitors reduced LPS-induced TLR4 expression back to baseline levels and normalized several marker proteins being indicative of gliosis (Iba1, GFAP), inflammation (COX-2), apoptosis (Bax/Bcl2), or neuronal death (synaptophysin). This is in line with findings reported by Sapkota and colleagues that demonstrated that TCLPA5 (an LPA5 inhibitor) ameliorated microglia activation and cytokine mRNA expression levels in the tMCAO stroke mouse model (226). Finally, we could show that also peripheral cytokine concentrations were significantly reduced in the peripheral circulation in response to ATX or LPA5 inhibition. These findings indicate that also reduced cytokines in the periphery could contribute to dampened neuroinflammation in inhibitor-treated animals by dampening potential intermediate signals that transmit inflammatory signals across the BBB.

LPA effects in a given cell type or organ will depend on its local concentration, that is regulated by synthesis via ATX or degradation by LPPs, the relative abundance of different receptor subtypes and the presence of potential agonists and/or antagonists (229). Thus, pharmacological targeting of the ATX/LPA axis likely needs some caution. This is based on findings that both, ATX knockout or overexpression are embryonically lethal (115–117) demonstrating the requirement for tight control of LPA levels during development. In contrast, in adult mouse life ATX inhibition using high dose PF8380 for prolonged time appears to be pharmacologically safe (118) indicating that under certain circumstances ATX represents a ‘safe and druggable’ target. Oral administration of PF8380 showed reduced inflammatory hyperalgesia in rat air pouch (230). Also, PF-8380 was found to enhance the radiosensitivity of human and murine glioblastoma (GBM) cell lines suggesting that inhibition of ATX may ameliorate GBM response to radiotherapy (231).

Structural studies revealed that ATX has a tripartite binding site consisting of the catalytic site, a hydrophobic pocket and a hydrophobic channel (191). Based on different binding modes ATX inhibitors were classified into four groups (Type I-IV inhibitors)(232). PF8380, that was used during the present study, belongs to the Type I inhibitors that occupy the catalytic site and mimic binding of LPC. PF8380 is, to the best of our knowledge, is not listed in clinical trials yet (https://clinicaltrials.gov/). The Type IV ATX inhibitor GLPG1690 (ziritaxestat) was the first ATX antagonist used in humans and showed promising results in a phase 2a randomized placebo-controlled trial to treat idiopathic pulmonary fibrosis (233). However, only recently, Galapagos NV announced the discontinuation of the ziritaxestat research program including the ISABELA Phase 3 trials (https://www.glpg.com/IPF) since the benefit-risk profile no longer supports continuing the studies (NCT03733444).

LPA5, the second pharmacological target studied here, is highly expressed in the spinal cord and dorsal root ganglion (234) and shows high expression in BV-2 and primary murine microglia (235). LPA5 is associated with inflammatory and neuropathic pain (93) and induces a proinflammatory microglia phenotype (236). Consequently the LPA5 antagonist AS2717638 showed broad analgesic effects in several animal pain models (93) and inhibited LPA-mediated proinflammatory polarization of BV-2 cells (236).

Different approaches to modulate microglia towards beneficial phenotype have been proposed. One of the possible strategies is targeting the ATX/LPA/LPAR axis by pharmacological interventions to attenuate pro-inflammatory phenotype in microglia. Results from this part of my thesis indicate that inhibition of the ATX/LPA5 axis in endotoxemia inhibits neuroinflammation in vitro (BV-2 cells) and in vivo (C57Bl/6 endotoxemia model). Whether co-inhibition of ATX and LPA5 would provide additional therapeutic benefit due to inhibited chaperoning function of ATX for LPA delivery to LPA5 (perhaps in an interplay between surface integrins and proteoglycans; (237) was not exploited here. Based on the present results, we propose that interference with ATX/LPA/LPA5 signaling axis might provide a potential strategy to pharmacologically shift microglia polarization away from a neurotoxic phenotype.

Part II: LPA induces metabolic reprogramming in BV2 microglia

The results of my metabolic studies in BV-2 cells can be summarized as follows: LPA increased proliferation slightly without inadvertent effects on cell viability. LPA induced a (non-significant) decrease in mitochondrial respiration, as supported by decreased MTT reduction. LPA decreased cellular ATP, ATP/ADP ratio and energy charge ratio. The activated microglia

induced Akt-mTOR-HIF1α- PFKFB3 axis under normoxic conditions to induce glycolytic flux. LPA further showed an upward trend in the mRNA expression of glucose transporters and hexokinase however, these effects were statistically not significant. The increase in extracellular lactate concentration supported a shift towards aerobic glycolysis in LPA-activated microglia. LPA showed a downward trend of pentose phosphate pathway utilization, indicated by by attenuated mRNA expression of G6pd2, G6pdx and Pgd. Of support, LPA reduced NADPH/NADP ratio in BV-2 microglia. Further, LPA induced lipogenesis via de-repression of ACC, and significantly increased FA concentrations in the PL and TAG fraction. The cells showed an increase in free amino acid content in response to LPA. Most pronounced increases were observed for Asp, Asn, Glu, and Ser (≥.2-fold 8h post LPA application). Finally we could show LPA-dependent ROS generation to activate the antioxidant response by phosphorylating Nrf2 followed by upregulation of the antioxidant response element (ARE) target GCLm and increased GSH synthesis (172).

As the first line of host defense, microglia perform constant surveillance of the CNS in an attempt to maintain CNS homeostasis. A recent comprehensive proteomic study revealed early changes in microglia energy metabolism in the pathogenesis of major neurodegenerative diseases (238). In response to exogeneous stimuli, immune cells including T cells, macrophages and microglia undergo metabolic reprogramming to perform energy demanding immune functions. Diverse agents are known to activate microglia to undergo a spectrum of phenotypic changes. In the brain, LPA mediates diverse biological actions on different cell types including neurons, astrocytes, oligodendrocytes and microglia (239). Studies indicate that LPA can have protective (217,240) or detrimental effects (173,235), depending in the context and cellular pre-activation state. The ATX/LPA/LPAR axis has been studied as a signaling hub for inducing metabolic reprograming. This was shown in mice where heterozygous ATX (Enpp2) knockout protected from diet-induced obesity and insulin-resistance and restored mitochondrial function in skeletal muscle (241). Similarly, adipocyte-specific Enpp2$^{-/-}$mice on a high-fat diet, showed smaller body weight gain and less insulin resistance than control mice (242). Previous studies demonstrated that LPA polarizes microglia towards an inflammatory phenotype. In the present study, we investigated energy metabolism in LPA-treated BV-2 microglia in order to explore whether the LPA-induced inflammatory polarization is accompanied by the induction of a specific immunometabolic phenotype in microglia. BV-2 microglia that were used throughout the present study are a well-characterized and widely used in vitro system for microglia studies (243). BV-2

microglia represents murine v-raf/v-myc carrying J2 retrovirus transformed cell line (244,245), however these cells show some but not all features of primary microglia.

Recent studies indicate a crucial role of LPA-modulated metabolism in oncogenesis (246). In ovarian cancer models, LPA induces a shift towards glycolysis (247), upregulates hexokinase 2 (248), and induces metabolic reprograming via a pseudo-hypoxic response that is HIF1α-mediated (249). LPA contributes to development and progression of T cell lymphoma by modulating apoptosis and glucose metabolism via pyruvate kinase, hexokinase, GLUT3, HIF1α and other regulatory molecules (246). LPA treatment of BV-2 and primary murine microglia induces activation of proinflammatory signaling cascades, secretion of cyto-/chemokines, induction of ROS production and expression of M1 plasma membrane marker indicating polarization towards a neurotoxic phenotype (168,173,235).

The highly dynamic nature of microglia is associated with various cellular functions and undergo rapid fluctuations between phenotypic states, all of which affect their energy demand remarkably (59). Transcriptomic studies indicate that microglia expresses all enzymes necessary to undergo major metabolic pathways (46,250). This imparts metabolic flexibility to utilize glucose, glutamine, pyruvate, lactate, ketone bodies or fatty acids as energy substrates (44,251,252), depending on the nutrient availability. Studies indicate that microglia under physiological condition show reliance towards oxidative metabolism, while pro-inflammatory stimuli shifts microglia metabolism towards glycolysis (253). Under aglycemic conditions, microglia can switch to glutaminolysis in an mTOR-dependent manner (44,59). Neurodegeneration is reported to be accompanied by mitochondrial hypometabolism and aberrant cellular redox control, as well as a decrease of ATP levels in brains of experimental AD mouse models (76). In line amyloid-beta acutely triggers inflammatory microglia activation accompanied by a switch from Oxphos towards aerobic glycolysis in an mTOR-HIF1α -mediated pathway (79,172). An earlier proteome study from our lab indicated LPA treatment induced upregulated expression of several enzymes primarily active in the triose branch of glycolysis in a human microglia cell line (71). In the present part of my thesis, I show that this pathway involves activation of Akt/mTOR/HIF1α/PFKFB3 axis in murine microglia cell line. In primary murine microglia, LPA activates Akt via protein kinase D2 (173) and this cascade presumably can lead to downstream activation.

Microglia as surveilling cells, move their ramifications with a constant remodeling of the cytoskeleton. Since these movements are also associated with alterations of the membrane curvatures it is reasonable to assume that the phospholipid synthesis/degradation/remodeling

machinery of this cell type must be able to respond to extracellular cues (172). During the present part of thesis, I found that in response to LPA, AMPK phosphorylation time dependently decreased and was accompanied by dephosphorylation of ACC in response to LPA. This is in line with a previous study, which reported that LPS dose-dependently induced dephosphorylation of AMPK and its target protein ACC, an event accompanied by activation (phosphorylation at T^{172}) of mTOR in lungs of LPS injected animals in a murine endotoxemia model (254). Dephosphorylation of ACC supports synthesis of malonyl-CoA that fuels into *de novo* FA synthesis. This likely provides FA flux into increased PL, DAG/TAG, and CE synthesis as observed here in response to LPA (172). These lipid families form lipid droplets (LD), which is a characteristic feature of aged microglia, or LPS-treated microglia of young mice or BV-2 microglia (255). Of note Marschallinger and colleagues demonstrated that LD formation induces a proinflammatory (increased NO, ROS and cytokine synthesis) microglia phenotype that is dysfunctional in terms of phagocytic capacity (255).

The metabolism of amino acids plays an important role in phenotypic transition of microglia. The present study demonstrated increased intracellular AA concentrations in LPA-treated BV-2 cells. This forms a plausible pathway for replenishing substrate for LPA-induced cyto-/chemokine synthesis (168). mTOR signaling, activated by import of AA in the cytoplasm, has been studied for determining the fate of amino acid, glucose and lipid metabolism (256). Among the AA that mediate full activation of mTORC1 are Leu, Gln, Glu, and Arg (257).

Among AA, the metabolism of glutamate has been associated with microglia function. Microglia are capable of using Gln as anaplerotic energy substrate in a process known as glutaminolysis. The first step in this pathway is catalyzed by one of the two isoforms of glutaminase (GLS1, GLS2), expressed by microglia and converts Gln to Glu. Studies with [U-^{14}C]-labeled Gln and Glu indicates that reductive carboxylation of Glu-derived a-ketoglutarate (a-KG) is funneled into the mitochondria of this microglia cell line (258). The present study revealed that Gln and Glu were quantitatively the most abundant AA in naïve BV-2 cells and the intracellular concentrations were further increased by LPA. Glutamate and Glutamine can serve as anaplerotic energy metabolite in the TCA cycle. Subsequent export of citrate to the cytosol and hydrolysis by ATP-dependent citrate lyase yields AcCoA that serves as substrate for ACC and FASN. Thus, increased AA uptake as observed here can provide AA substrates for de novo cyto-/chemokine synthesis, that contribute to mTOR activation, and fuel AcCoA synthesis that enters fatty acid synthesis (172).

Activation of microglia is coupled to an increase in ROS production to induce altered redox homeostasis (259). The exposure of microglia to ROS activates an antioxidant defense system to limit cell damage. Nrf2 is the master regulator of antioxidant responses and upon translocation to the nucleus, it induces transcription of target genes that contain the antioxidant response element (260). Here I observed that LPA increases phosphorylation of Nrf2 at S40 and induces GCLm expression. GCL is a transcriptional Nrf2 target and an enzyme of central importance for the maintenance of intracellular GSH levels in microglia (261). In agreement with the induction of GCLm protein expression, cellular GSH levels increased in LPA treated cells, a finding indicative of the induction of a protective pathway to counteract damage of endogenous macromolecules (262).

During Part II of my study I could demonstrate i) induction of the Akt/mTOR/HIF1α/ PFKFB3 pathway and a concomitant increase of lactate secretion from LPA-treated cells, ii) de-repression of ACC in LPA-treated BV-2 cells and an associated induction of lipogenesis, iii) higher intracellular concentrations of AAs, and iv) an LPA-mediated induction of the antioxidant response (172). The outcome of these experiments identifies the bioactive lipid LPA as a novel mediator of metabolic pathway reprograming in microglia.

Part III: LPA5 regulates inflammation and metabolism in primary murine microglia

Microglia represent specialized cell population that is conditioned to respond swiftly and aggressively to antigenic and inflammatory signals (263). Activation of microglia leads to changes in morphology, secretion of cytokines and alterations in its phagocytic capacity. During earlier and ongoing studies our group could show that LPA represents an extracellular signal that induces pro-inflammatory phenotype in microglia in vitro (168,235). Many of these inflammatory effects of LPA are mediated via LPA5 (11,168,172).

In the last part of my thesis I used primary microglia isolated from global LPA5-/- mice to provide the evidence that LPA mediates the secretion of inflammatory mediators, cytokines and chemokines and this depends on LPA5 expression. These findings suggest that LPA5 plays a major role in guiding immune response in microglia under conditions where LPA concentrations are high. This is in line with previous studies which indicate that pharmacological intervention with LPA5 specific antagonists (TCLPA5, AS2717638 and Compound 3) attenuates LPA mediated inflammatory immune response of microglia (235,236). Administration of TCLPA5 in tMCAO-challenged mice demonstrated decreased microglia activation, evident by decreased Iba1 immunoreactivities (226).

Emerging studies indicate that metabolic reprograming acts as an underlying factor that regulates immune function and fate of microglia (263,264). It is evident that the highly dynamic nature of microglia is associated with a constant energy-demanding metabolic phenotype (251). The bioenergetic microglia machinery is capable of utilizing glucose, glutamine, pyruvate, lactate, ketone bodies, or fatty acids as energy substrates (44,172,251,252). Previous studies and my own findings indicate that LPA induces aerobic glycolysis, lipogenesis, and increased amino acid uptake in BV-2 microglia. BV-2 microglia represent a murine, v-raf/v-myc carrying J2 retrovirus transformed cell line (244,245). Despite being a good surrogate for microglia studies, it doesn't entirely mimic primary microglia. Hence we investigated the immunometabolic phenotype in primary microglia in response to LPA to establish physiologically more relevant conditions.

My major findings with primary wildtype microglia can be summarized as follows: LPA increased extracellular lactate concentration, the end product of glycolysis, increased the level of NADPH, a key product of pentose phosphate pathway, followed by decreased concentration of reduced glutathione and induced a decrease in mitochondrial respiration. Of note, all of these responses were clearly less pronounced in primary microglia isolated from LPA5$^{-/-}$ mice.

Glucose is the major energy substrate in the brain, and in microglia. The four major pathways of glucose utilization are: i) oxidation to pyruvate to secrete lactate, ii) oxidation of pyruvate to further undergo oxidation in the citric acid cycle (oxidative phosphorylation), iii) an alternative pentose phosphate shunt/hexose monophosphate pathway, and iv) storage as glycogen for rapid utilization at a later time. Microglia in homeostasis show reliance on oxidative metabolism to generate large amounts of ATP required for its dynamic surveillance phenotype (265). When challenged with a pro-inflammatory stimuli, microglia adopt aerobic glycolysis over OXPHOS to rapidly generate ATP despite being less efficient pathway (265,266). In line, we showed that LPA as an inflammatory stimulus increases extracellular lactate and decreases oxygen consumption rate of the mitochondria to switch towards aerobic glycolysis in primary microglia. Of note, glucose uptake by GLUT1 is reported to critically control microglial activation (51). Moreover, the close association of diabetes mellitus and increased risk of Alzheimer's dementia and cognitive decline provides the evidence that glucose fluctuations can alter microglia activity, representing a novel pathogenic mechanism (267)

A disrupted TCA cycle is likely to involve accumulation of TCA metabolites (44). The accumulation of succinate promotes the production of IL-1β, a major pro-inflammatory cytokine (72). The disruption of pyruvate entry into the TCA cycle further supports inflammatory

phenotype by contributing to accumulation of nitric oxide (NO) and IL-1β, which are major pro-inflammatory factors (268,269). NO reacts with oxygen which leads to the formation of peroxynitrite (ONOO-). This reactive nitrogen species irreversibly inhibits the electron transport chain (270). In addition, the enzymatic break points in the TCA cycle leads to the upregulation of the pentose phosphate pathway (PPP), an alternative pathway for glucose metabolism that generates reducing equivalents in form of NADPH, and other substrates required for the synthesis of nucleotides, nucleic acids and aromatic amino acids (269,271,272). NADPH is involved in the production of reactive oxygen species through NADPH oxidase. ROS serve as secondary messengers to activate kinase cascades and transcriptional factors (273–275). This is in line with studies which revealed that LPA induces ROS production. This was accompanied by activation of MAPK pathway with subsequent phosphorylation of proinflammatory transcription factors STAT1, NF-kB and c-Jun (168,172). NADPH serves as an important cofactor for reducing glutathione disulfide into the antioxidant glutathione. Our results reflected that LPA increases the concentration of reduced glutathione in a time dependent manner. Baardman and colleagues have reported a defective pentose phosphate pathway reduces inflammatory response of macrophages in systemic metabolic disorder (213)

It is evident from this part of my study that that LPA induces glucose metabolism mainly via glycolysis and pentose phosphate pathway, with less dependence on mitochondrial respiration in wildtype primary microglia.

To get an indication about the role of LPA5 during these phenotypic transitions I have performed studies with microglia isolated from $LPA5^{-/-}$ mice. Of note, genetic deletion of LPA5 altered the metabolic response of microglia towards LPA. The LPA5 knockout microglia showed reduced levels of extracellular lactate and decreased pentose phosphate pathway flux by reducing NADPH, and in turn decreasing the level of reduced glutathione. In contrast, LPA5 knockout microglia showed a significant increase in mitochondrial respiration as their means of energy production. These effects are similar to microglia facing anti-inflammatory stimuli (269,276).

Based on the present results, we propose that LPA/LPA5 signaling axis might provide an opportunity to modulate inflammatory and metabolic profile of microglia towards beneficial action.

5. References

1. Zengeler KE, Lukens JR. Innate immunity at the crossroads of healthy brain maturation and neurodevelopmental disorders. Nat Rev Immunol [Internet]. 2021 Jan 21 [cited 2021 Feb 2];1–15. Available from: http://www.nature.com/articles/s41577-020-00487-7

2. Ginhoux F, Garel S. The mysterious origins of microglia. Nat Neurosci. 2018;21(7):897–9.

3. Ajami B, Bennett JL, Krieger C, McNagny KM, Rossi FMV. Infiltrating monocytes trigger EAE progression, but do not contribute to the resident microglia pool. Nat Neurosci. 2011;14(9).

4. Ueno M, Fujita Y, Tanaka T, Nakamura Y, Kikuta J, Ishii M, et al. Layer V cortical neurons require microglial support for survival during postnatal development. Nat Neurosci [Internet]. 2013 May 24;16(5):543–51. Available from: http://www.nature.com/articles/nn.3358

5. Colonna M, Butovsky O. Microglia function in the central nervous system during health and neurodegeneration. Annu Rev Immunol. 2017;35(January):441–68.

6. Hoshiko M, Arnoux I, Avignone E, Yamamoto N, Audinat E. Deficiency of the Microglial Receptor CX3CR1 Impairs Postnatal Functional Development of Thalamocortical Synapses in the Barrel Cortex. J Neurosci [Internet]. 2012 Oct 24;32(43):15106–11. Available from: https://www.jneurosci.org/lookup/doi/10.1523/JNEUROSCI.1167-12.2012

7. Lenz KM, Nelson LH. Microglia and beyond: Innate immune cells as regulators of brain development and behavioral function [Internet]. Vol. 9, Frontiers in Immunology. Frontiers Media S.A.; 2018 [cited 2021 Feb 2]. p. 1. Available from: www.frontiersin.org

8. Casano AM, Peri F. Microglia: Multitasking Specialists of the Brain. Dev Cell [Internet]. 2015 Feb 23 [cited 2019 May 16];32(4):469–77. Available from: https://www.sciencedirect.com/science/article/pii/S1534580715000611?via%3Dihub

9. Cai W, Dai X, Chen J, Zhao J, Xu M, Zhang L, et al. STAT6/Arg1 promotes microglia/ macrophage efferocytosis and inflammation resolution in stroke mice. JCI Insight [Internet]. 2019 Oct 17 [cited 2021 Jun 8];4(20). Available from: https://pubmed.ncbi.nlm.nih.gov/31619589/

10. Hickman SE, El Khoury J. Analysis of the Microglial Sensome. In 2019. p. 305–23. Available from: http://link.springer.com/10.1007/978-1-4939-9658-2_23

11. Hickman SE, Kingery ND, Ohsumi TK, Borowsky ML, Wang L, Means TK, et al. The microglial sensome revealed by direct RNA sequencing. Nat Neurosci [Internet]. 2013 Dec 27;16(12):1896–905. Available from: http://www.nature.com/articles/nn.3554

12. Kettenmann H, Hanisch U-K, Noda M, Verkhratsky A. Physiology of Microglia. Physiol Rev [Internet]. 2011 Apr;91(2):461–553. Available from: https://www.physiology.org/doi/10.1152/physrev.00011.2010

13. Ransohoff RM, Perry VH. Microglial Physiology: Unique Stimuli, Specialized Responses. Annu Rev Immunol [Internet]. 2009 Apr;27(1):119–45. Available from: http://www.annualreviews.org/doi/10.1146/annurev.immunol.021908.132528

14. Kierdorf K, Prinz M. Factors regulating microglia activation. Front Cell Neurosci [Internet].

2013;7. Available from: http://journal.frontiersin.org/article/10.3389/fncel.2013.00044/abstract

15. Pocock JM, Kettenmann H. Neurotransmitter receptors on microglia. Trends Neurosci [Internet]. 2007 Oct;30(10):527–35. Available from: https://linkinghub.elsevier.com/retrieve/pii/S0166223607002111

16. Norden DM, Godbout JP. Review: Microglia of the aged brain: primed to be activated and resistant to regulation. Neuropathol Appl Neurobiol [Internet]. 2013 Feb;39(1):19–34. Available from: http://doi.wiley.com/10.1111/j.1365-2990.2012.01306.x

17. Perry VH, Holmes C. Microglial priming in neurodegenerative disease. Nat Rev Neurol [Internet]. 2014 Apr 18;10(4):217–24. Available from: http://www.nature.com/articles/nrneurol.2014.38

18. Sica A, Mantovani A. Macrophage plasticity and polarization: in vivo veritas. J Clin Invest [Internet]. 2012 Mar 1;122(3):787–95. Available from: http://www.jci.org/articles/view/59643

19. Martinez FO, Gordon S. The M1 and M2 paradigm of macrophage activation: time for reassessment. F1000Prime Rep [Internet]. 2014 Mar 3;6. Available from: https://facultyopinions.com/prime/reports/b/6/13/

20. Plastira I, Bernhart E, Goeritzer M, Reicher H, Kumble VB, Kogelnik N, et al. 1-Oleyl-lysophosphatidic acid (LPA) promotes polarization of BV-2 and primary murine microglia towards an M1-like phenotype. J Neuroinflammation [Internet]. 2016 Dec 26 [cited 2019 May 16];13(1):205. Available from: http://jneuroinflammation.biomedcentral.com/articles/10.1186/s12974-016-0701-9

21. Boche D, Perry VH, Nicoll JAR. Review: Activation patterns of microglia and their identification in the human brain. Neuropathol Appl Neurobiol [Internet]. 2013 Feb;39(1):3–18. Available from: http://doi.wiley.com/10.1111/nan.12011

22. Orihuela R, McPherson CA, Harry GJ. Microglial M1/M2 polarization and metabolic states [Internet]. Vol. 173, British Journal of Pharmacology. John Wiley and Sons Inc.; 2016 [cited 2020 Nov 30]. p. 649–65. Available from: /pmc/articles/PMC4742299/?report=abstract

23. Ransohoff RM, El Khoury J. Microglia in health and disease. Cold Spring Harb Perspect Biol [Internet]. 2016 Jan 1 [cited 2020 Oct 19];8(1). Available from: /pmc/articles/PMC4691795/?report=abstract

24. Wes PD, Holtman IR, Boddeke EWGM, Möller T, Eggen BJL. Next generation transcriptomics and genomics elucidate biological complexity of microglia in health and disease. Glia [Internet]. 2016 Feb 4;64(2):197–213. Available from: https://onlinelibrary.wiley.com/doi/10.1002/glia.22866

25. Widmann CN, Heneka MT. Long-term cerebral consequences of sepsis. Lancet Neurol [Internet]. 2014 Jun;13(6):630–6. Available from: https://linkinghub.elsevier.com/retrieve/pii/S1474442214700171

26. Brown GC. The endotoxin hypothesis of neurodegeneration. J Neuroinflammation [Internet]. 2019 Dec 13 [cited 2019 Sep 16];16(1):180. Available from:

https://jneuroinflammation.biomedcentral.com/articles/10.1186/s12974-019-1564-7

27. Nishioku T, Dohgu S, Takata F, Eto T, Ishikawa N, Kodama KB, et al. Detachment of brain pericytes from the basal lamina is involved in disruption of the blood-brain barrier caused by lipopolysaccharide-induced sepsis in mice. Cell Mol Neurobiol [Internet]. 2009 May [cited 2021 May 11];29(3):309–16. Available from: https://pubmed.ncbi.nlm.nih.gov/18987969/

28. Varatharaj A, Galea I. The blood-brain barrier in systemic inflammation. Brain Behav Immun [Internet]. 2017 Feb;60:1–12. Available from: https://linkinghub.elsevier.com/retrieve/pii/S0889159116300551

29. Jaeger LB, Dohgu S, Sultana R, Lynch JL, Owen JB, Erickson MA, et al. Lipopolysaccharide alters the blood–brain barrier transport of amyloid β protein: A mechanism for inflammation in the progression of Alzheimer's disease. Brain Behav Immun [Internet]. 2009 May;23(4):507–17. Available from: https://linkinghub.elsevier.com/retrieve/pii/S0889159109000440

30. Banks WA, Robinson SM. Minimal penetration of lipopolysaccharide across the murine blood-brain barrier. Brain Behav Immun [Internet]. 2010 Jan [cited 2021 May 11];24(1):102–9. Available from: /pmc/articles/PMC2789209/

31. Hoogland ICM, Houbolt C, van Westerloo DJ, van Gool WA, van de Beek D. Systemic inflammation and microglial activation: Systematic review of animal experiments. Vol. 12, Journal of Neuroinflammation. 2015.

32. Zhan X, Stamova B, Jin L-W, DeCarli C, Phinney B, Sharp FR. Gram-negative bacterial molecules associate with Alzheimer disease pathology. Neurology [Internet]. 2016 Nov 29;87(22):2324–32. Available from: http://www.neurology.org/lookup/doi/10.1212/WNL.0000000000003391

33. Lee JW, Lee YK, Yuk DY, Choi DY, Ban SB, Oh KW, et al. Neuro-inflammation induced by lipopolysaccharide causes cognitive impairment through enhancement of beta-amyloid generation. J Neuroinflammation [Internet]. 2008 Aug 29 [cited 2021 May 25];5. Available from: https://pubmed.ncbi.nlm.nih.gov/18759972/

34. Asti A, Gioglio L. Can a bacterial endotoxin be a key factor in the kinetics of amyloid fibril formation? J Alzheimer's Dis [Internet]. 2014 [cited 2021 May 25];39(1):169–79. Available from: https://pubmed.ncbi.nlm.nih.gov/24150108/

35. Gardner LE, White JD, Eimerbrink MJ, Boehm GW, Chumley MJ. Imatinib methanesulfonate reduces hyperphosphorylation of tau following repeated peripheral exposure to lipopolysaccharide. Neuroscience [Internet]. 2016 Sep 7 [cited 2021 May 25];331:72–7. Available from: https://pubmed.ncbi.nlm.nih.gov/27320209/

36. Bhaskar K, Konerth M, Kokiko-Cochran ON, Cardona A, Ransohoff RM, Lamb BT. Regulation of tau pathology by the microglial fractalkine receptor. Neuron [Internet]. 2010 Oct 6 [cited 2021 May 25];68(1):19–31. Available from: https://pubmed.ncbi.nlm.nih.gov/20920788/

37. Forsyth CB, Shannon KM, Kordower JH, Voigt RM, Shaikh M, Jaglin JA, et al. Increased intestinal permeability correlates with sigmoid mucosa alpha-synuclein staining and endotoxin exposure markers in early Parkinson's disease. PLoS One [Internet]. 2011 Dec

1 [cited 2021 May 25];6(12). Available from: https://pubmed.ncbi.nlm.nih.gov/22145021/

38. Rowin J, Xia Y, Jung B, Sun J. Gut inflammation and dysbiosis in human motor neuron disease. Physiol Rep [Internet]. 2017 Sep 1 [cited 2021 May 25];5(18). Available from: https://pubmed.ncbi.nlm.nih.gov/28947596/

39. Tejera D, Mercan D, Sanchez-Caro JM, Hanan M, Greenberg D, Soreq H, et al. Systemic inflammation impairs microglial Aβ clearance through NLRP 3 inflammasome . EMBO J [Internet]. 2019 Sep 2 [cited 2021 Jun 8];38(17):e101064. Available from: https://www.embopress.org/doi/full/10.15252/embj.2018101064

40. Heneka MT, Carson MJ, Khoury J El, Landreth GE, Brosseron F, Feinstein DL, et al. Neuroinflammation in Alzheimer's disease. Lancet Neurol [Internet]. 2015 Apr;14(4):388–405. Available from: https://linkinghub.elsevier.com/retrieve/pii/S1474442215700165

41. Pulido-Salgado M, Vidal-Taboada JM, Barriga GGD, Solà C, Saura J. RNA-Seq transcriptomic profiling of primary murine microglia treated with LPS or LPS + IFNγ. Sci Rep [Internet]. 2018 Dec 1 [cited 2021 May 9];8(1):1–21. Available from: www.nature.com/scientificreports/

42. Bélanger M, Allaman I, Magistretti PJ. Brain Energy Metabolism: Focus on Astrocyte-Neuron Metabolic Cooperation. Cell Metab [Internet]. 2011 Dec;14(6):724–38. Available from: https://linkinghub.elsevier.com/retrieve/pii/S1550413111004207

43. Obel LF, Müller MS, Walls AB, Sickmann HM, Bak LK, Waagepetersen HS, et al. Brain glycogen—new perspectives on its metabolic function and regulation at the subcellular level. Front Neuroenergetics [Internet]. 2012;4. Available from: http://journal.frontiersin.org/article/10.3389/fnene.2012.00003/abstract

44. Bernier LP, York EM, MacVicar BA. Immunometabolism in the Brain: How Metabolism Shapes Microglial Function. Trends in Neurosciences. Elsevier Ltd; 2020.

45. O'Neill LAJ, Kishton RJ, Rathmell J. A guide to immunometabolism for immunologists. Nat Rev Immunol [Internet]. 2016 Sep 11 [cited 2019 Feb 11];16(9):553–65. Available from: http://www.nature.com/articles/nri.2016.70

46. Zhang Y, Chen K, Sloan SA, Bennett ML, Scholze AR, O'Keeffe S, et al. An RNA-sequencing transcriptome and splicing database of glia, neurons, and vascular cells of the cerebral cortex. J Neurosci [Internet]. 2014 Sep 3 [cited 2021 Feb 5];34(36):11929–47. Available from: http://www.ncbi.nlm.nih.gov/tools/primer-blast/

47. Hammond TR, Dufort C, Dissing-Olesen L, Giera S, Young A, Wysoker A, et al. Single-Cell RNA Sequencing of Microglia throughout the Mouse Lifespan and in the Injured Brain Reveals Complex Cell-State Changes. Immunity [Internet]. 2019 Jan;50(1):253-271.e6. Available from: https://linkinghub.elsevier.com/retrieve/pii/S1074761318304850

48. Hwang JJ, Jiang L, Hamza M, Dai F, Belfort-DeAguiar R, Cline G, et al. The human brain produces fructose from glucose. JCI Insight [Internet]. 2017 Feb 23;2(4). Available from: https://insight.jci.org/articles/view/90508

49. Payne J, Maher F, Simpson I, Mattice L, Davies P. Glucose transporter glut 5 expression in microglial cells. Glia [Internet]. 1997 Nov;21(3):327–31. Available from: https://onlinelibrary.wiley.com/doi/10.1002/(SICI)1098-1136(199711)21:3%3C327::AID-

GLIA7%3E3.0.CO;2-1

50. Millet P, Vachharajani V, McPhail L, Yoza B, McCall CE. GAPDH Binding to TNF-α mRNA Contributes to Posttranscriptional Repression in Monocytes: A Novel Mechanism of Communication between Inflammation and Metabolism. J Immunol [Internet]. 2016 Mar 15;196(6):2541–51. Available from: http://www.jimmunol.org/lookup/doi/10.4049/jimmunol.1501345

51. Wang L, Pavlou S, Du X, Bhuckory M, Xu H, Chen M. Glucose transporter 1 critically controls microglial activation through facilitating glycolysis. Mol Neurodegener [Internet]. 2019 Dec 11 [cited 2019 Jan 22];14(1):2. Available from: https://molecularneurodegeneration.biomedcentral.com/articles/10.1186/s13024-019-0305-9

52. Bennett ML, Bennett FC, Liddelow SA, Ajami B, Zamanian JL, Fernhoff NB, et al. New tools for studying microglia in the mouse and human CNS. Proc Natl Acad Sci [Internet]. 2016 Mar 22;113(12):E1738–46. Available from: http://www.pnas.org/lookup/doi/10.1073/pnas.1525528113

53. Gimeno-Bayón J, López-López A, Rodríguez MJ, Mahy N. Glucose pathways adaptation supports acquisition of activated microglia phenotype. J Neurosci Res [Internet]. 2014 Jun;92(6):723–31. Available from: http://doi.wiley.com/10.1002/jnr.23356

54. Rubio-Araiz A, Finucane OM, Keogh S, Lynch MA. Anti-TLR2 antibody triggers oxidative phosphorylation in microglia and increases phagocytosis of β-amyloid. J Neuroinflammation [Internet]. 2018 Dec 31;15(1):247. Available from: https://jneuroinflammation.biomedcentral.com/articles/10.1186/s12974-018-1281-7

55. Piers TM, Cosker K, Mallach A, Johnson GT, Guerreiro R, Hardy J, et al. A locked immunometabolic switch underlies TREM2 R47H loss of function in human iPSC-derived microglia. FASEB J [Internet]. 2020 Feb 23;34(2):2436–50. Available from: https://onlinelibrary.wiley.com/doi/10.1096/fj.201902447R

56. Mela V, Mota BC, Milner M, McGinley A, Mills KHG, Kelly ÁM, et al. Exercise-induced re-programming of age-related metabolic changes in microglia is accompanied by a reduction in senescent cells. Brain Behav Immun [Internet]. 2020 Jul;87:413–28. Available from: https://linkinghub.elsevier.com/retrieve/pii/S0889159119314801

57. Niot I, Poirier H, Tran TTT, Besnard P. Intestinal absorption of long-chain fatty acids: Evidence and uncertainties. Prog Lipid Res [Internet]. 2009 Mar;48(2):101–15. Available from: https://linkinghub.elsevier.com/retrieve/pii/S0163782709000022

58. Kalsbeek MJT, Mulder L, Yi CX. Microglia energy metabolism in metabolic disorder. Mol Cell Endocrinol [Internet]. 2016;438:27–35. Available from: http://dx.doi.org/10.1016/j.mce.2016.09.028

59. Bernier LP, York EM, Kamyabi A, Choi HB, Weilinger NL, MacVicar BA. Microglial metabolic flexibility supports immune surveillance of the brain parenchyma. Nat Commun [Internet]. 2020 Dec 1 [cited 2021 Feb 5];11(1):1–17. Available from: https://doi.org/10.1038/s41467-020-15267-z

60. Schönfeld P, Reiser G. Why does Brain Metabolism not Favor Burning of Fatty Acids to Provide Energy? - Reflections on Disadvantages of the Use of Free Fatty Acids as Fuel

for Brain. J Cereb Blood Flow Metab [Internet]. 2013 Oct 7;33(10):1493–9. Available from: http://journals.sagepub.com/doi/10.1038/jcbfm.2013.128

61. Romano A, Koczwara JB, Gallelli CA, Vergara D, Micioni Di Bonaventura MV, Gaetani S, et al. Fats for thoughts: An update on brain fatty acid metabolism. Int J Biochem Cell Biol [Internet]. 2017 Mar;84:40–5. Available from: https://linkinghub.elsevier.com/retrieve/pii/S1357272516304058

62. Coraci IS, Husemann J, Berman JW, Hulette C, Dufour JH, Campanella GK, et al. CD36, a Class B Scavenger Receptor, Is Expressed on Microglia in Alzheimer's Disease Brains and Can Mediate Production of Reactive Oxygen Species in Response to β-Amyloid Fibrils. Am J Pathol [Internet]. 2002 Jan;160(1):101–12. Available from: https://linkinghub.elsevier.com/retrieve/pii/S0002944010643544

63. Jernberg JN, Bowman CE, Wolfgang MJ, Scafidi S. Developmental regulation and localization of carnitine palmitoyltransferases (CPTs) in rat brain. J Neurochem [Internet]. 2017 Aug;142(3):407–19. Available from: http://doi.wiley.com/10.1111/jnc.14072

64. Infantino V, Iacobazzi V, Menga A, Avantaggiati ML, Palmieri F. A key role of the mitochondrial citrate carrier (SLC25A1) in TNFα- and IFNγ-triggered inflammation. Biochim Biophys Acta - Gene Regul Mech [Internet]. 2014 Nov;1839(11):1217–25. Available from: https://linkinghub.elsevier.com/retrieve/pii/S1874939914002016

65. Schousboe A, Scafidi S, Bak LK, Waagepetersen HS, McKenna MC. Glutamate Metabolism in the Brain Focusing on Astrocytes. In 2014. p. 13–30. Available from: http://link.springer.com/10.1007/978-3-319-08894-5_2

66. Schousboe A. Metabolic signaling in the brain and the role of astrocytes in control of glutamate and GABA neurotransmission. Neurosci Lett [Internet]. 2019 Jan;689:11–3. Available from: https://linkinghub.elsevier.com/retrieve/pii/S0304394018300442

67. Chausse B, Kakimoto PA, Kann O. Microglia and lipids: how metabolism controls brain innate immunity. Seminars in Cell and Developmental Biology. Elsevier Ltd; 2020.

68. Ghosh S, Castillo E, Frias ES, Swanson RA. Bioenergetic regulation of microglia [Internet]. Vol. 66, GLIA. John Wiley and Sons Inc.; 2018 [cited 2021 Jun 1]. p. 1200–12. Available from: /pmc/articles/PMC5903989/

69. Aldana BI. Microglia-Specific Metabolic Changes in Neurodegeneration. J Mol Biol [Internet]. 2019 Mar [cited 2019 Apr 5]; Available from: https://linkinghub.elsevier.com/retrieve/pii/S002228361930124X

70. Ghosh S, Castillo E, Frias ES, Swanson RA. Bioenergetic regulation of microglia. Vol. 66, GLIA. John Wiley and Sons Inc.; 2018. p. 1200–12.

71. Bernhart E, Kollroser M, Rechberger G, Reicher H, Heinemann A, Schratl P, et al. Lysophosphatidic acid receptor activation affects the C13NJ microglia cell line proteome leading to alterations in glycolysis, motility, and cytoskeletal architecture. Proteomics [Internet]. 2010 Jan;10(1):141–58. Available from: http://doi.wiley.com/10.1002/pmic.200900195

72. Galván-Peña S, O'Neill LAJ. Metabolic Reprograming in Macrophage Polarization. Front Immunol [Internet]. 2014 Sep 2;5. Available from:

http://journal.frontiersin.org/article/10.3389/fimmu.2014.00420/abstract

73. Geric I, Schoors S, Claes C, Gressens P, Verderio C, Verfaillie CM, et al. Metabolic Reprogramming during Microglia Activation. 2019;

74. Heneka MT, Golenbock DT, Latz E. Innate immunity in Alzheimer's disease. Nat Immunol [Internet]. 2015 Mar 17;16(3):229–36. Available from: http://www.nature.com/articles/ni.3102

75. Rayaprolu S, Mullen B, Baker M, Lynch T, Finger E, Seeley WW, et al. TREM2 in neurodegeneration: evidence for association of the p.R47H variant with frontotemporal dementia and Parkinson's disease. Mol Neurodegener [Internet]. 2013 Dec 21;8(1):19. Available from: https://molecularneurodegeneration.biomedcentral.com/articles/10.1186/1750-1326-8-19

76. Yin F, Sancheti H, Patil I, Cadenas E. Energy metabolism and inflammation in brain aging and Alzheimer's disease. Free Radic Biol Med [Internet]. 2016 Nov;100:108–22. Available from: https://linkinghub.elsevier.com/retrieve/pii/S0891584916302167

77. Simpson IA, Chundu KR, Davies-Hill T, Honer WG, Davies P. Decreased concentrations of GLUT1 and GLUT3 glucose transporters in the brains of patients with Alzheimer's disease. Ann Neurol [Internet]. 1994 May;35(5):546–51. Available from: http://doi.wiley.com/10.1002/ana.410350507

78. Iwangoff P, Armbruster R, Enz A, Meier-Ruge W. Glycolytic enzymes from human autoptic brain cortex: Normal aged and demented cases. Mech Ageing Dev [Internet]. 1980 Sep;14(1–2):203–9. Available from: https://linkinghub.elsevier.com/retrieve/pii/0047637480901207

79. Baik SH, Kang S, Lee W, Choi H, Chung S, Kim J Il, et al. A Breakdown in Metabolic Reprogramming Causes Microglia Dysfunction in Alzheimer's Disease. Cell Metab [Internet]. 2019;30(3):493-507.e6. Available from: https://doi.org/10.1016/j.cmet.2019.06.005

80. Daniele SG, Béraud D, Davenport C, Cheng K, Yin H, Maguire-Zeiss KA. Activation of MyD88-dependent TLR1/2 signaling by misfolded α-synuclein, a protein linked to neurodegenerative disorders. Sci Signal [Internet]. 2015 May 12;8(376):ra45–ra45. Available from: https://stke.sciencemag.org/lookup/doi/10.1126/scisignal.2005965

81. Edison P, Ahmed I, Fan Z, Hinz R, Gelosa G, Ray Chaudhuri K, et al. Microglia, Amyloid, and Glucose Metabolism in Parkinson's Disease with and without Dementia. Neuropsychopharmacology [Internet]. 2013 May 6;38(6):938–49. Available from: http://www.nature.com/articles/npp2012255

82. Reynolds AD, Kadiu I, Garg SK, Glanzer JG, Nordgren T, Ciborowski P, et al. Nitrated Alpha-Synuclein and Microglial Neuroregulatory Activities. J Neuroimmune Pharmacol [Internet]. 2008 Jun 17;3(2):59–74. Available from: http://link.springer.com/10.1007/s11481-008-9100-z

83. Atallah N, Vasiu R, Boşca AB, Creţu D-I, Georgiu C, Constantin A-M, et al. Microglia-performers of the 21st century. Rom J Morphol Embryol [Internet]. 2014 [cited 2019 May 16];55(3):745–65. Available from: http://www.rjme.ro/

84. Gveric D, Kaltschmidt C, Cuzner ML, Newcombe J. Transcription Factor NF-kB and Inhibitor kBα are Localized in Macrophages in Active Multiple Sclerosis Lesions. J Neuropathol Exp Neurol [Internet]. 1998 Feb;57(2):168–9. Available from: https://academic.oup.com/jnen/article-lookup/doi/10.1097/00005072-199802000-00008

85. Adiele RC, Adiele CA. Metabolic defects in multiple sclerosis. Mitochondrion [Internet]. 2019 Jan;44:7–14. Available from: https://linkinghub.elsevier.com/retrieve/pii/S1567724917300570

86. Mathur D, LÃ³pez-Rodas G, Casanova B, Marti MB. Perturbed Glucose Metabolism: Insights into Multiple Sclerosis Pathogenesis. Front Neurol [Internet]. 2014 Dec 1;5. Available from: http://journal.frontiersin.org/article/10.3389/fneur.2014.00250/abstract

87. Jones HH, Jones Jr HH, Bunch LD. BIOCHEMICAL STUDIES IN MULTIPLE SCLEROSIS. Ann Intern Med [Internet]. 1950 Oct 1;33(4):831. Available from: http://annals.org/article.aspx?doi=10.7326/0003-4819-33-4-831

88. Sapp E, Kegel KB, Aronin N, Hashikawa T, Uchiyama Y, Tohyama K, et al. Early and Progressive Accumulation of Reactive Microglia in the Huntington Disease Brain. J Neuropathol Exp Neurol [Internet]. 2001 Feb 1;60(2):161–72. Available from: https://academic.oup.com/jnen/article-lookup/doi/10.1093/jnen/60.2.161

89. Antonini A, Leenders KL, Spiegel R, Meier D, Vontobel P, Weigell-Weber M, et al. Striatal glucose metabolism and dopamine D 2 receptor binding in asymptomatic gene carriers and patients with Huntington's disease. Brain [Internet]. 1996;119(6):2085–95. Available from: https://academic.oup.com/brain/article-lookup/doi/10.1093/brain/119.6.2085

90. Steiner J, Bielau H, Brisch R, Danos P, Ullrich O, Mawrin C, et al. Immunological aspects in the neurobiology of suicide: Elevated microglial density in schizophrenia and depression is associated with suicide. J Psychiatr Res [Internet]. 2008 Jan;42(2):151–7. Available from: https://linkinghub.elsevier.com/retrieve/pii/S0022395606002184

91. Torres-Platas SG, Cruceanu C, Chen GG, Turecki G, Mechawar N. Evidence for increased microglial priming and macrophage recruitment in the dorsal anterior cingulate white matter of depressed suicides. Brain Behav Immun [Internet]. 2014 Nov;42:50–9. Available from: https://linkinghub.elsevier.com/retrieve/pii/S0889159114001299

92. Tsuda M, Beggs S, Salter MW, Inoue K. Microglia and intractable chronic pain. Glia [Internet]. 2013 Jan;61(1):55–61. Available from: http://doi.wiley.com/10.1002/glia.22379

93. Murai N, Hiyama H, Kiso T, Sekizawa T, Watabiki T, Oka H, et al. Analgesic effects of novel lysophosphatidic acid receptor 5 antagonist AS2717638 in rodents. Neuropharmacology [Internet]. 2017 Nov 1 [cited 2019 Sep 12];126:97–107. Available from: https://www.sciencedirect.com/science/article/pii/S0028390817304112?via%3Dihub

94. Hefendehl JK, Neher JJ, Sühs RB, Kohsaka S, Skodras A, Jucker M. Homeostatic and injury-induced microglia behavior in the aging brain. Aging Cell [Internet]. 2014 Feb;13(1):60–9. Available from: http://doi.wiley.com/10.1111/acel.12149

95. Sierra A, Gottfried-Blackmore AC, McEwen BS, Bulloch K. Microglia derived from aging mice exhibit an altered inflammatory profile. Glia [Internet]. 2007 Mar;55(4):412–24. Available from: http://doi.wiley.com/10.1002/glia.20468

96. Flowers A, Bell-Temin H, Jalloh A, Stevens SM, Bickford PC. Proteomic analysis of aged microglia: shifts in transcription, bioenergetics, and nutrient response. J Neuroinflammation [Internet]. 2017 Dec 3;14(1):96. Available from: https://jneuroinflammation.biomedcentral.com/articles/10.1186/s12974-017-0840-7

97. Mattson MP, Arumugam T V. Hallmarks of Brain Aging: Adaptive and Pathological Modification by Metabolic States. Cell Metab [Internet]. 2018 Jun;27(6):1176–99. Available from: https://linkinghub.elsevier.com/retrieve/pii/S1550413118303188

98. Ivanisevic J, Stauch KL, Petrascheck M, Benton HP, Epstein AA, Fang M, et al. Metabolic drift in the aging brain. Aging (Albany NY) [Internet]. 2016 May 5;8(5):1000–20. Available from: https://www.aging-us.com/lookup/doi/10.18632/aging.100961

99. Svennerholm L, Boström K, Jungbjer B, Olsson L. Membrane Lipids of Adult Human Brain: Lipid Composition of Frontal and Temporal Lobe in Subjects of Age 20 to 100 Years. J Neurochem [Internet]. 2002 Nov 23;63(5):1802–11. Available from: http://doi.wiley.com/10.1046/j.1471-4159.1994.63051802.x

100. Veloso A, Fernández R, Astigarraga E, Barreda-Gómez G, Manuel I, Giralt MT, et al. Distribution of lipids in human brain. Anal Bioanal Chem [Internet]. 2011 Jul 26;401(1):89–101. Available from: http://link.springer.com/10.1007/s00216-011-4882-x

101. Adibhatla RM, Hatcher JF. Role of lipids in brain injury and diseases. Future Lipidol [Internet]. 2007 Aug;2(4):403–22. Available from: https://www.futuremedicine.com/doi/10.2217/17460875.2.4.403

102. Fernandis AZ, Wenk MR. Membrane lipids as signaling molecules. Curr Opin Lipidol. 2007;18(2):121–8.

103. Yung YC, Stoddard NC, Mirendil H, Chun J. Lysophosphatidic Acid Signaling in the Nervous System. Neuron [Internet]. 2015 Feb 18 [cited 2019 May 16];85(4):669–82. Available from: https://www.sciencedirect.com/science/article/pii/S0896627315000355?via%3Dihub

104. Jansen S, Stefan C, Creemers JWM, Waelkens E, Van Eynde A, Stalmans W, et al. Proteolytic maturation and activation of autotaxin (NPP2), a secreted metastasis-enhancing lysophospholipase D. J Cell Sci [Internet]. 2005 Jul 15;118(14):3081–9. Available from: https://journals.biologists.com/jcs/article/118/14/3081/28323/Proteolytic-maturation-and-activation-of-autotaxin

105. Ramesh S, Govindarajulu M, Suppiramaniam V, Moore T, Dhanasekaran M, Ramesh S, et al. Autotaxin–Lysophosphatidic Acid Signaling in Alzheimer's Disease. Int J Mol Sci [Internet]. 2018 Jun 21 [cited 2018 Dec 14];19(7):1827. Available from: http://www.mdpi.com/1422-0067/19/7/1827

106. Perrakis A, Moolenaar WH. Thematic Review Series: Lysophospholipids and their Receptors: Autotaxin: Structure-function and signaling. Vol. 55, Journal of Lipid Research. American Society for Biochemistry and Molecular Biology Inc.; 2014. p. 1010–8.

107. Magkrioti C, Galaris A, Kanellopoulou P, Stylianaki E-A, Kaffe E, Aidinis V. Autotaxin and chronic inflammatory diseases. J Autoimmun [Internet]. 2019 Nov;104:102327. Available from: https://linkinghub.elsevier.com/retrieve/pii/S0896841119305505

108. Dusaulcy R, Rancoule C, Grès S, Wanecq E, Colom A, Guigné C, et al. Adipose-specific disruption of autotaxin enhances nutritional fattening and reduces plasma lysophosphatidic acid. J Lipid Res [Internet]. 2011 Jun;52(6):1247–55. Available from: https://linkinghub.elsevier.com/retrieve/pii/S0022227520313420

109. Kanda H, Newton R, Klein R, Morita Y, Gunn MD, Rosen SD. Autotaxin, an ectoenzyme that produces lysophosphatidic acid, promotes the entry of lymphocytes into secondary lymphoid organs. Nat Immunol [Internet]. 2008 Apr 9;9(4):415–23. Available from: http://www.nature.com/articles/ni1573

110. Perrakis A, Moolenaar WH. Autotaxin: Structure-function and signaling [Internet]. Vol. 55, Journal of Lipid Research. American Society for Biochemistry and Molecular Biology Inc.; 2014 [cited 2021 Jun 27]. p. 1010–8. Available from: http://www.jlr.org

111. Tokumura A, Majima E, Kariya Y, Tominaga K, Kogure K, Yasuda K, et al. Identification of Human Plasma Lysophospholipase D, a Lysophosphatidic Acid-producing Enzyme, as Autotaxin, a Multifunctional Phosphodiesterase. J Biol Chem [Internet]. 2002 Oct;277(42):39436–42. Available from: https://linkinghub.elsevier.com/retrieve/pii/S0021925819723023

112. Umezu-Goto M, Kishi Y, Taira A, Hama K, Dohmae N, Takio K, et al. Autotaxin has lysophospholipase D activity leading to tumor cell growth and motility by lysophosphatidic acid production. J Cell Biol [Internet]. 2002 Jul 22;158(2):227–33. Available from: https://rupress.org/jcb/article/158/2/227/32762/Autotaxin-has-lysophospholipase-D-activity-leading

113. Giganti A, Rodriguez M, Fould B, Moulharat N, Cogé F, Chomarat P, et al. Murine and Human Autotaxin α, β, and γ Isoforms. J Biol Chem [Internet]. 2008 Mar;283(12):7776–89. Available from: https://linkinghub.elsevier.com/retrieve/pii/S0021925820551685

114. Kawagoe H, Soma O, Goji J, Nishimura N, Narita M, Inazawa J, et al. Molecular Cloning and Chromosomal Assignment of the Human Brain-Type Phosphodiesterase I/Nucleotide Pyrophosphatase Gene (PDNP2). Genomics [Internet]. 1995 Nov;30(2):380–4. Available from: https://linkinghub.elsevier.com/retrieve/pii/S0888754385700365

115. van Meeteren LA, Ruurs P, Stortelers C, Bouwman P, van Rooijen MA, Pradère JP, et al. Autotaxin, a Secreted Lysophospholipase D, Is Essential for Blood Vessel Formation during Development. Mol Cell Biol [Internet]. 2006 Jul 1 [cited 2021 May 25];26(13):5015–22. Available from: /pmc/articles/PMC1489177/

116. Tanaka M, Okudaira S, Kishi Y, Ohkawa R, Iseki S, Ota M, et al. Autotaxin Stabilizes Blood Vessels and Is Required for Embryonic Vasculature by Producing Lysophosphatidic Acid. J Biol Chem [Internet]. 2006 Sep;281(35):25822–30. Available from: https://linkinghub.elsevier.com/retrieve/pii/S0021925819352950

117. Yukiura H, Kano K, Kise R, Inoue A, Aoki J. Autotaxin Overexpression Causes Embryonic Lethality and Vascular Defects. Yue J, editor. PLoS One [Internet]. 2015 May 19;10(5):e0126734. Available from: https://dx.plos.org/10.1371/journal.pone.0126734

118. Katsifa A, Kaffe E, Nikolaidou-Katsaridou N, Economides AN, Newbigging S, McKerlie C, et al. The bulk of autotaxin activity is dispensable for adult mouse life. PLoS One [Internet]. 2015 Nov 1 [cited 2021 May 25];10(11):e0143083. Available from:

https://journals.plos.org/plosone/article?id=10.1371/journal.pone.0143083

119. Zimmermann H, Zebisch M, Sträter N. Cellular function and molecular structure of ecto-nucleotidases. Purinergic Signal [Internet]. 2012 Sep 4;8(3):437–502. Available from: http://link.springer.com/10.1007/s11302-012-9309-4

120. Aikawa S, Hashimoto T, Kano K, Aoki J. Lysophosphatidic acid as a lipid mediator with multiple biological actions. J Biochem [Internet]. 2015 Feb 1;157(2):81–9. Available from: https://academic.oup.com/jb/article-lookup/doi/10.1093/jb/mvu077

121. Perrakis A, Moolenaar WH. Autotaxin: structure-function and signaling. J Lipid Res [Internet]. 2014 Jun;55(6):1010–8. Available from: https://linkinghub.elsevier.com/retrieve/pii/S0022227520352652

122. Pagès C, Simon M-F, Valet P, Saulnier-Blache JS. Lysophosphatidic acid synthesis and release. Prostaglandins Other Lipid Mediat [Internet]. 2001 Apr;64(1–4):1–10. Available from: https://linkinghub.elsevier.com/retrieve/pii/S0090698001001101

123. Bektas M, Payne SG, Liu H, Goparaju S, Milstien S, Spiegel S. A novel acylglycerol kinase that produces lysophosphatidic acid modulates cross talk with EGFR in prostate cancer cells. J Cell Biol [Internet]. 2005 Jun 6;169(5):801–11. Available from: https://rupress.org/jcb/article/169/5/801/51690/A-novel-acylglycerol-kinase-that-produces

124. Brindley DN, Pilquil C. Lipid phosphate phosphatases and signaling. J Lipid Res [Internet]. 2009 Apr;50:S225–30. Available from: https://linkinghub.elsevier.com/retrieve/pii/S0022227520306167

125. Fukushima N, Weiner JA, Kaushal D, Contos JJA, Rehen SK, Kingsbury MA, et al. Lysophosphatidic Acid Influences the Morphology and Motility of Young, Postmitotic Cortical Neurons. Mol Cell Neurosci [Internet]. 2002 Jun;20(2):271–82. Available from: https://linkinghub.elsevier.com/retrieve/pii/S1044743102911231

126. Yung YC, Stoddard NC, Chun J. LPA receptor signaling: Pharmacology, physiology, and pathophysiology [Internet]. Vol. 55, Journal of Lipid Research. American Society for Biochemistry and Molecular Biology Inc.; 2014 [cited 2021 May 29]. p. 1192–214. Available from: http://www.jlr.org

127. Ishii I, Fukushima N, Ye X, Chun J. Lysophospholipid Receptors: Signaling and Biology. Annu Rev Biochem [Internet]. 2004 Jun;73(1):321–54. Available from: http://www.annualreviews.org/doi/10.1146/annurev.biochem.73.011303.073731

128. Choi J, W LC, J C. Biological roles of lysophospholipid receptors revealed by genetic null mice: An update. Biochim Biophys Acta - Mol Cell Biol Lipids [Internet]. 2008 Sep;1781(9):531–9. Available from: https://linkinghub.elsevier.com/retrieve/pii/S1388198108000644

129. Xiang H, Lu Y, Shao M, Wu T. Lysophosphatidic acid receptors: Biochemical and clinical implications in different diseases. Vol. 11, Journal of Cancer. Ivyspring International Publisher; 2020. p. 3519–35.

130. Hecht JH, Weiner JA, Post SR, Chun J. Ventricular zone gene-1 (vzg-1) encodes a lysophosphatidic acid receptor expressed in neurogenic regions of the developing cerebral cortex. J Cell Biol [Internet]. 1996 Nov 15;135(4):1071–83. Available from:

https://rupress.org/jcb/article/135/4/1071/56541/Ventricular-zone-gene1-vzg1-encodes-a

131. Contos JJA, Ishii I, Chun J. Lysophosphatidic Acid Receptors. Mol Pharmacol [Internet]. 2000 Dec 1;58(6):1188–96. Available from: http://molpharm.aspetjournals.org/lookup/doi/10.1124/mol.58.6.1188

132. Contos JJA, Fukushima N, Weiner JA, Kaushal D, Chun J. Requirement for the lpA1 lysophosphatidic acid receptor gene in normal suckling behavior. Proc Natl Acad Sci [Internet]. 2000 Nov 21;97(24):13384–9. Available from: http://www.pnas.org/cgi/doi/10.1073/pnas.97.24.13384

133. Choi JW, Herr DR, Noguchi K, Yung YC, Lee C-W, Mutoh T, et al. LPA Receptors: Subtypes and Biological Actions. Annu Rev Pharmacol Toxicol [Internet]. 2010 Feb [cited 2018 Dec 4];50(1):157–86. Available from: http://www.ncbi.nlm.nih.gov/pubmed/20055701

134. Ohuchi H, Hamada A, Matsuda H, Takagi A, Tanaka M, Aoki J, et al. Expression patterns of the lysophospholipid receptor genes during mouse early development. Dev Dyn [Internet]. 2008 Nov;237(11):3280–94. Available from: http://doi.wiley.com/10.1002/dvdy.21736

135. Bandoh K, Aoki J, Hosono H, Kobayashi S, Kobayashi T, Murakami-Murofushi K, et al. Molecular Cloning and Characterization of a Novel Human G-protein-coupled Receptor, EDG7, for Lysophosphatidic Acid. J Biol Chem [Internet]. 1999 Sep;274(39):27776–85. Available from: https://linkinghub.elsevier.com/retrieve/pii/S0021925819521858

136. Im D-S, Heise CE, Harding MA, George SR, O'Dowd BF, Theodorescu D, et al. Molecular Cloning and Characterization of a Lysophosphatidic Acid Receptor, Edg-7, Expressed in Prostate. Mol Pharmacol [Internet]. 2000 Apr 1;57(4):753–9. Available from: http://molpharm.aspetjournals.org/lookup/doi/10.1124/mol.57.4.753

137. Ishii I, Contos JJA, Fukushima N, Chun J. Functional Comparisons of the Lysophosphatidic Acid Receptors, LP A1 /VZG-1/EDG-2, LP A2 /EDG-4, and LP A3 /EDG-7 in Neuronal Cell Lines Using a Retrovirus Expression System. Mol Pharmacol [Internet]. 2000 Nov 1;58(5):895–902. Available from: http://molpharm.aspetjournals.org/lookup/doi/10.1124/mol.58.5.895

138. Ye X, Hama K, Contos JJA, Anliker B, Inoue A, Skinner MK, et al. LPA3-mediated lysophosphatidic acid signalling in embryo implantation and spacing. Nature [Internet]. 2005 May;435(7038):104–8. Available from: http://www.nature.com/articles/nature03505

139. Lee C-W, Rivera R, Dubin AE, Chun J. LPA4/GPR23 Is a Lysophosphatidic Acid (LPA) Receptor Utilizing Gs-, Gq/Gi-mediated Calcium Signaling and G12/13-mediated Rho Activation. J Biol Chem [Internet]. 2007 Feb;282(7):4310–7. Available from: https://linkinghub.elsevier.com/retrieve/pii/S0021925820650013

140. Yanagida K, Ishii S, Hamano F, Noguchi K, Shimizu T. LPA4/p2y9/GPR23 Mediates Rho-dependent Morphological Changes in a Rat Neuronal Cell Line. J Biol Chem [Internet]. 2007 Feb;282(8):5814–24. Available from: https://linkinghub.elsevier.com/retrieve/pii/S0021925820688767

141. Liu Y-B, Kharode Y, Bodine PVN, Yaworsky PJ, Robinson JA, Billiard J. LPA induces osteoblast differentiation through interplay of two receptors: LPA1 and LPA4. J Cell

Biochem [Internet]. 2010;n/a-n/a. Available from: http://doi.wiley.com/10.1002/jcb.22471

142. Sumida H, Noguchi K, Kihara Y, Abe M, Yanagida K, Hamano F, et al. LPA4 regulates blood and lymphatic vessel formation during mouse embryogenesis. Blood [Internet]. 2010 Dec 2;116(23):5060–70. Available from: https://ashpublications.org/blood/article/116/23/5060/28363/LPA4-regulates-blood-and-lymphatic-vessel

143. Kotarsky K, Boketoft Å, Bristulf J, Nilsson NE, Norberg Å, Hansson S, et al. Lysophosphatidic Acid Binds to and Activates GPR92, a G Protein-Coupled Receptor Highly Expressed in Gastrointestinal Lymphocytes. J Pharmacol Exp Ther [Internet]. 2006 Aug;318(2):619–28. Available from: http://jpet.aspetjournals.org/lookup/doi/10.1124/jpet.105.098848

144. Chun J, Hla T, Lynch KR, Spiegel S, Moolenaar WH. International Union of Basic and Clinical Pharmacology. LXXVIII. Lysophospholipid Receptor Nomenclature: TABLE 1. Pharmacol Rev [Internet]. 2010 Dec 15;62(4):579–87. Available from: http://pharmrev.aspetjournals.org/lookup/doi/10.1124/pr.110.003111

145. Lee CW, Rivera R, Gardell S, Dubin AE, Chun J. GPR92 as a New G12/13- and Gq-coupled Lysophosphatidic Acid Receptor That Increases cAMP, LPA5. J Biol Chem [Internet]. 2006 Aug;281(33):23589–97. Available from: https://linkinghub.elsevier.com/retrieve/pii/S0021925819463965

146. Lundequist A, Boyce JA. LPA5 Is Abundantly Expressed by Human Mast Cells and Important for Lysophosphatidic Acid Induced MIP-1β Release. Meuth S, editor. PLoS One [Internet]. 2011 Mar 28;6(3):e18192. Available from: https://dx.plos.org/10.1371/journal.pone.0018192

147. Lee M, Choi S, Halldén G, Yo SJ, Schichnes D, Aponte GW. P2Y5 is a Gα i , Gα 12/13 G protein-coupled receptor activated by lysophosphatidic acid that reduces intestinal cell adhesion. Am J Physiol Liver Physiol [Internet]. 2009 Oct;297(4):G641–54. Available from: https://www.physiology.org/doi/10.1152/ajpgi.00191.2009

148. Yanagida K, Masago K, Nakanishi H, Kihara Y, Hamano F, Tajima Y, et al. Identification and Characterization of a Novel Lysophosphatidic Acid Receptor, p2y5/LPA6. J Biol Chem [Internet]. 2009 Jun;284(26):17731–41. Available from: https://linkinghub.elsevier.com/retrieve/pii/S0021925819820562

149. Taniguchi R, Inoue A, Sayama M, Uwamizu A, Yamashita K, Hirata K, et al. Structural insights into ligand recognition by the lysophosphatidic acid receptor LPA6. Nature [Internet]. 2017 Aug 9;548(7667):356–60. Available from: http://www.nature.com/articles/nature23448

150. Pasternack SM, von Kügelgen I, Aboud K Al, Lee Y-A, Rüschendorf F, Voss K, et al. G protein–coupled receptor P2Y5 and its ligand LPA are involved in maintenance of human hair growth. Nat Genet [Internet]. 2008 Mar 24;40(3):329–34. Available from: http://www.nature.com/articles/ng.84

151. Aaltonen N, Laitinen JT, Lehtonen M. Quantification of lysophosphatidic acids in rat brain tissue by liquid chromatography–electrospray tandem mass spectrometry. J Chromatogr B [Internet]. 2010 May;878(15–16):1145–52. Available from:

https://linkinghub.elsevier.com/retrieve/pii/S1570023210001704

152. Yung YC, Mutoh T, Lin M-E, Noguchi K, Rivera RR, Choi JW, et al. Lysophosphatidic Acid Signaling May Initiate Fetal Hydrocephalus. Sci Transl Med [Internet]. 2011 Sep 7;3(99):99ra87-99ra87. Available from: https://stm.sciencemag.org/lookup/doi/10.1126/scitranslmed.3002095

153. Trimbuch T, Beed P, Vogt J, Schuchmann S, Maier N, Kintscher M, et al. Synaptic PRG-1 Modulates Excitatory Transmission via Lipid Phosphate-Mediated Signaling. Cell [Internet]. 2009 Sep;138(6):1222–35. Available from: https://linkinghub.elsevier.com/retrieve/pii/S0092867409008435

154. Anliker B, Choi JW, Lin M-E, Gardell SE, Rivera RR, Kennedy G, et al. Lysophosphatidic acid (LPA) and its receptor, LPA 1 , influence embryonic schwann cell migration, myelination, and cell-to-axon segregation. Glia [Internet]. 2013 Dec;61(12):2009–22. Available from: http://doi.wiley.com/10.1002/glia.22572

155. Möller T, Contos JJ, Musante DB, Chun J, Ransom BR. Expression and Function of Lysophosphatidic Acid Receptors in Cultured Rodent Microglial Cells. J Biol Chem [Internet]. 2001 Jul;276(28):25946–52. Available from: https://linkinghub.elsevier.com/retrieve/pii/S0021925819301437

156. Frisca F, Sabbadini RA, Goldshmit Y, Pébay A. Biological Effects of Lysophosphatidic Acid in the Nervous System. In 2012. p. 273–322. Available from: https://linkinghub.elsevier.com/retrieve/pii/B9780123943071000059

157. Kingsbury MA, Rehen SK, Contos JJA, Higgins CM, Chun J. Non-proliferative effects of lysophosphatidic acid enhance cortical growth and folding. Nat Neurosci [Internet]. 2003 Dec 16;6(12):1292–9. Available from: http://www.nature.com/articles/nn1157

158. Fukushima N, Shano S, Moriyama R, Chun J. Lysophosphatidic acid stimulates neuronal differentiation of cortical neuroblasts through the LPA1–Gi/o pathway. Neurochem Int [Internet]. 2007 Jan;50(2):302–7. Available from: https://linkinghub.elsevier.com/retrieve/pii/S0197018606002920

159. Tigyi G, Fischer DJ, Sebök Á, Yang C, Dyer DL, Miledi R. Lysophosphatidic Acid-Induced Neurite Retraction in PC12 Cells: Control by Phosphoinositide-Ca2+ Signaling and Rho. J Neurochem [Internet]. 1996 Nov 23;66(2):537–48. Available from: http://doi.wiley.com/10.1046/j.1471-4159.1996.66020537.x

160. Furuta D, Yamane M, Tsujiuchi T, Moriyama R, Fukushima N. Lysophosphatidic acid induces neurite branch formation through LPA3. Mol Cell Neurosci [Internet]. 2012 May;50(1):21–34. Available from: https://linkinghub.elsevier.com/retrieve/pii/S1044743112000462

161. Fukushima N, Morita Y. Actomyosin-dependent microtubule rearrangement in lysophosphatidic acid-induced neurite remodeling of young cortical neurons. Brain Res [Internet]. 2006 Jun;1094(1):65–75. Available from: https://linkinghub.elsevier.com/retrieve/pii/S0006899306010298

162. Herr D, Chun J. Effects of LPA and S1P on the Nervous System and Implications for Their Involvement in Disease. Curr Drug Targets [Internet]. 2007 Jan 1;8(1):155–67. Available from:

http://www.eurekaselect.com/openurl/content.php?genre=article&issn=1389-4501&volume=8&issue=1&spage=155

163. Ramakers GJA, Moolenaar WH. Regulation of Astrocyte Morphology by RhoA and Lysophosphatidic Acid. Exp Cell Res [Internet]. 1998 Dec;245(2):252–62. Available from: https://linkinghub.elsevier.com/retrieve/pii/S0014482798942240

164. Sorensen SD, Nicole O, Peavy RD, Montoya LM, Lee CJ, Murphy TJ, et al. Common Signaling Pathways Link Activation of Murine PAR-1, LPA, and S1P Receptors to Proliferation of Astrocytes. Mol Pharmacol [Internet]. 2003 Nov;64(5):1199–209. Available from: http://molpharm.aspetjournals.org/lookup/doi/10.1124/mol.64.5.1199

165. Spohr TCL de S e, Dezonne RS, Rehen SK, Gomes FCA. Astrocytes treated by lysophosphatidic acid induce axonal outgrowth of cortical progenitors through extracellular matrix protein and epidermal growth factor signaling pathway. J Neurochem [Internet]. 2011 Oct;119(1):113–23. Available from: http://doi.wiley.com/10.1111/j.1471-4159.2011.07421.x

166. Tabuchi S, Kume K, Aihara M, Shimizu T. Expression of lysophosphatidic acid receptor in rat astrocytes: mitogenic effect and expression of neurotrophic genes. Neurochem Res [Internet]. 2000 May;25(5):573–82. Available from: http://www.ncbi.nlm.nih.gov/pubmed/10905618

167. Keller JN, Steiner MR, Mattson MP, Steiner SM. Lysophosphatidic Acid Decreases Glutamate and Glucose Uptake by Astrocytes. J Neurochem [Internet]. 2002 Nov 23;67(6):2300–5. Available from: http://doi.wiley.com/10.1046/j.1471-4159.1996.67062300.x

168. Plastira I, Bernhart E, Joshi L, Koyani CN, Strohmaier H, Reicher H, et al. MAPK signaling determines lysophosphatidic acid (LPA)-induced inflammation in microglia. J Neuroinflammation [Internet]. 2020 Apr 23 [cited 2021 May 27];17(1):1–17. Available from: https://doi.org/10.1186/s12974-020-01809-1

169. Fujita R, Ma Y, Ueda H. Lysophosphatidic acid-induced membrane ruffling and brain-derived neurotrophic factor gene expression are mediated by ATP release in primary microglia. J Neurochem [Internet]. 2008 Oct;107(1):152–60. Available from: http://doi.wiley.com/10.1111/j.1471-4159.2008.05599.x

170. Schilling T, Stock C, Schwab A, Eder C. Functional importance of Ca2+-activated K+ channels for lysophosphatidic acid-induced microglial migration. Eur J Neurosci [Internet]. 2004 Mar;19(6):1469–74. Available from: http://doi.wiley.com/10.1111/j.1460-9568.2004.03265.x

171. Bernhart E, Kollroser M, Rechberger G, Reicher H, Heinemann A, Schratl P, et al. Lysophosphatidic acid receptor activation affects the C13NJ microglia cell line proteome leading to alterations in glycolysis, motility, and cytoskeletal architecture. Proteomics [Internet]. 2010 Jan 1 [cited 2019 May 16];10(1):141–58. Available from: http://doi.wiley.com/10.1002/pmic.200900195

172. Joshi L, Plastira I, Bernhart E, Reicher H, Koyani CN, Madl T, et al. Lysophosphatidic Acid Induces Aerobic Glycolysis, Lipogenesis, and Increased Amino Acid Uptake in BV-2 Microglia. Int J Mol Sci [Internet]. 2021 Feb 17 [cited 2021 Apr 21];22(4):1968. Available

from: https://www.mdpi.com/1422-0067/22/4/1968

173. Plastira I, Bernhart E, Goeritzer M, DeVaney T, Reicher H, Hammer A, et al. Lysophosphatidic acid via LPA-receptor 5/protein kinase D-dependent pathways induces a motile and pro-inflammatory microglial phenotype. J Neuroinflammation [Internet]. 2017 Dec 19 [cited 2019 May 16];14(1):253. Available from: https://jneuroinflammation.biomedcentral.com/articles/10.1186/s12974-017-1024-1

174. Weiner JA, Hecht JH, Chun J. Lysophosphatidic acid receptor gene vzg-1/lpA1/edg-2 is expressed by mature oligodendrocytes during myelination in the postnatal murine brain. J Comp Neurol [Internet]. 1998 Sep 7;398(4):587–98. Available from: http://www.ncbi.nlm.nih.gov/pubmed/9717712

175. Nogaroli L, Yuelling LM, Dennis J, Gorse K, Payne SG, Fuss B. Lysophosphatidic Acid can Support the Formation of Membranous Structures and an Increase in MBP mRNA Levels in Differentiating Oligodendrocytes. Neurochem Res [Internet]. 2009 Jan 2;34(1):182–93. Available from: http://link.springer.com/10.1007/s11064-008-9772-z

176. Möller T, Musante DB, Ransom BR. Lysophosphatidic acid-induced calcium signals in cultured rat oligodendrocytes. Neuroreport [Internet]. 1999 Sep;10(14):2929–32. Available from: http://journals.lww.com/00001756-199909290-00010

177. Greenberg DA, Jin K. From angiogenesis to neuropathology. Nature [Internet]. 2005 Dec 14;438(7070):954–9. Available from: http://www.nature.com/articles/nature04481

178. Eichmann A, Thomas J-L. Molecular Parallels between Neural and Vascular Development. Cold Spring Harb Perspect Med [Internet]. 2013 Jan 1;3(1):a006551–a006551. Available from: http://perspectivesinmedicine.cshlp.org/lookup/doi/10.1101/cshperspect.a006551

179. Lin C-I, Chen C-N, Huang M-T, Lee S-J, Lin C-H, Chang C-C, et al. Lysophosphatidic acid upregulates vascular endothelial growth factor-C and tube formation in human endothelial cells through LPA1/3, COX-2, and NF-κB activation- and EGFR transactivation-dependent mechanisms. Cell Signal [Internet]. 2008 Oct;20(10):1804–14. Available from: https://linkinghub.elsevier.com/retrieve/pii/S0898656808001812

180. Dutta S, Wang F, Wu H, Mukherjee TJ, Fishman DA. The NF-κB pathway mediates lysophosphatidic acid (LPA)-induced VEGF signaling and cell invasion in epithelial ovarian cancer (EOC). Gynecol Oncol [Internet]. 2011 Oct;123(1):129–37. Available from: https://linkinghub.elsevier.com/retrieve/pii/S0090825811004446

181. Lin C-I, Chen C-N, Lin P-W, Chang K-J, Hsieh F-J, Lee H. Lysophosphatidic acid regulates inflammation-related genes in human endothelial cells through LPA1 and LPA3. Biochem Biophys Res Commun [Internet]. 2007 Nov;363(4):1001–8. Available from: https://linkinghub.elsevier.com/retrieve/pii/S0006291X07020694

182. Schleicher SM, Thotala DK, Linkous AG, Hu R, Leahy KM, Yazlovitskaya EM, et al. Autotaxin and LPA Receptors Represent Potential Molecular Targets for the Radiosensitization of Murine Glioma through Effects on Tumor Vasculature. Bauer JA, editor. PLoS One [Internet]. 2011 Jul 20;6(7):e22182. Available from: https://dx.plos.org/10.1371/journal.pone.0022182

183. Ren Y, Guo L, Tang X, Apparsundaram S, Kitson C, Deguzman J, et al. Comparing the

differential effects of LPA on the barrier function of human pulmonary endothelial cells. Microvasc Res [Internet]. 2013 Jan;85:59–67. Available from: https://linkinghub.elsevier.com/retrieve/pii/S0026286212001677

184. English D, Kovala AT, Welch Z, Harvey KA, Siddiqui RA, Brindley DN, et al. Induction of Endothelial Cell Chemotaxis by Sphingosine 1-Phosphate and Stabilization of Endothelial Monolayer Barrier Function by Lysophosphatidic Acid, Potential Mediators of Hematopoietic Angiogenesis. J Hematother Stem Cell Res [Internet]. 1999 Dec;8(6):627–34. Available from: https://www.liebertpub.com/doi/10.1089/152581699319795

185. Ruisanchez É, Dancs P, Kerék M, Németh T, Faragó B, Balogh A, et al. Lysophosphatidic acid induces vasodilation mediated by LPA 1 receptors, phospholipase C, and endothelial nitric oxide synthase. FASEB J [Internet]. 2014 Feb 18;28(2):880–90. Available from: https://onlinelibrary.wiley.com/doi/abs/10.1096/fj.13-234997

186. Li S, Zhang J. Lipopolysaccharide induces autotaxin expression in human monocytic THP-1 cells. Biochem Biophys Res Commun [Internet]. 2009;378(2):264–8. Available from: http://dx.doi.org/10.1016/j.bbrc.2008.11.047

187. Mouratis MA, Magkrioti C, Oikonomou N, Katsifa A, Prestwich GD, Kaffe E, et al. Autotaxin and endotoxin-induced acute lung injury. PLoS One [Internet]. 2015 Jul 21 [cited 2021 May 16];10(7):e0133619. Available from: https://journals.plos.org/plosone/article?id=10.1371/journal.pone.0133619

188. Herr DR, Ong JH-J, Ong W-Y. Potential Therapeutic Applications for Inhibitors of Autotaxin, a Bioactive Lipid-Producing Lysophospholipase D, in Disorders Affecting the Nervous System. ACS Chem Neurosci [Internet]. 2018 Mar 21;9(3):398–400. Available from: https://pubs.acs.org/doi/10.1021/acschemneuro.8b00057

189. Prestwich G. Phosphatase-resistant analogues of lysophosphatidic acid: Agonists promote healing, antagonists and autotaxin inhibitors treat cancer. Biochim Biophys Acta - Mol Cell Biol Lipids [Internet]. 2008 Sep;1781(9):588–94. Available from: https://linkinghub.elsevier.com/retrieve/pii/S1388198108000693

190. Ferry G, Moulharat N, Pradère JP, Desos P, Try A, Genton A, et al. S32826, a nanomolar inhibitor of autotaxin: Discovery, synthesis and applications as a pharmacological tool. J Pharmacol Exp Ther. 2008;327(3):809–19.

191. Hausmann J, Kamtekar S, Christodoulou E, Day JE, Wu T, Fulkerson Z, et al. Structural basis of substrate discrimination and integrin binding by autotaxin. Nat Struct Mol Biol [Internet]. 2011 Feb 16;18(2):198–204. Available from: http://www.nature.com/articles/nsmb.1980

192. Gierse J, Thorarensen A, Beltey K, Bradshaw-Pierce E, Cortes-Burgos L, Hall T, et al. A novel autotaxin inhibitor reduces lysophosphatidic acid levels in plasma and the site of inflammation. J Pharmacol Exp Ther [Internet]. 2010 Jul [cited 2021 May 25];334(1):310–7. Available from: https://pubmed.ncbi.nlm.nih.gov/20392816/

193. Fells JI, Tsukahara R, Fujiwara Y, Liu J, Perygin DH, Osborne DA, et al. Identification of non-lipid LPA3 antagonists by virtual screening. Bioorg Med Chem [Internet]. 2008 Jun;16(11):6207–17. Available from: https://linkinghub.elsevier.com/retrieve/pii/S0968089608003635

194. Sardar VM, Bautista DL, Fischer DJ, Yokoyama K, Nusser N, Virag T, et al. Molecular basis for lysophosphatidic acid receptor antagonist selectivity. Biochim Biophys Acta - Mol Cell Biol Lipids [Internet]. 2002 May;1582(1–3):309–17. Available from: https://linkinghub.elsevier.com/retrieve/pii/S1388198102001853

195. Fujiwara Y, Sardar V, Tokumura A, Baker D, Murakami-Murofushi K, Parrill A, et al. Identification of Residues Responsible for Ligand Recognition and Regioisomeric Selectivity of Lysophosphatidic Acid Receptors Expressed in Mammalian Cells. J Biol Chem [Internet]. 2005 Oct;280(41):35038–50. Available from: https://linkinghub.elsevier.com/retrieve/pii/S0021925820639448

196. Chrencik JE, Roth CB, Terakado M, Kurata H, Omi R, Kihara Y, et al. Crystal Structure of Antagonist Bound Human Lysophosphatidic Acid Receptor 1. Cell [Internet]. 2015 Jun;161(7):1633–43. Available from: https://linkinghub.elsevier.com/retrieve/pii/S0092867415006856

197. Murai N, Hiyama H, Kiso T, Sekizawa T, Watabiki T, Oka H, et al. Analgesic effects of novel lysophosphatidic acid receptor 5 antagonist AS2717638 in rodents. Neuropharmacology [Internet]. 2017 Nov 1 [cited 2020 Dec 9];126:97–107. Available from: https://linkinghub.elsevier.com/retrieve/pii/S0028390817304112

198. Lin ME, Rivera RR, Chun J. Targeted deletion of LPA5 identifies novel roles for lysophosphatidic acid signaling in development of neuropathic pain. J Biol Chem [Internet]. 2012;287(21):17608–17. Available from: http://dx.doi.org/10.1074/jbc.M111.330183

199. Fürst W, Hallström S. Simultaneous determination of myocardial nucleotides, nucleosides, purine bases and creatine phosphate by ion-pair high-performance liquid chromatography. J Chromatogr B Biomed Sci Appl. 1992 Jul 1;578(1):39–44.

200. Pelzmann B, Hallström S, Schaffer P, Lang P, Nadlinger K, Birkmayer GD, et al. NADH supplementation decreases pinacidil-primed I K(ATP) in ventricular cardiomyocytes by increasing intracellular ATP. Br J Pharmacol [Internet]. 2003 Jun [cited 2020 Nov 30];139(4):749–54. Available from: /pmc/articles/PMC1573896/?report=abstract

201. Livak KJ, Schmittgen TD. Analysis of relative gene expression data using real-time quantitative PCR and the 2-ΔΔCT method. Methods. 2001;25(4):402–8.

202. Sattler W, Puhl H, Hayn M, Kostner GM, Esterbauer H. Determination of fatty acids in the main lipoprotein classes by capillary gas chromatography: BF3/methanol transesterification of lyophilized samples instead of folch extraction gives higher yields. Anal Biochem. 1991 Oct 1;198(1):184–90.

203. Wu G, Meininger CJ. Analysis of Citrulline, Arginine, and Methylarginines Using High-Performance Liquid Chromatography. Vol. 440, Methods in Enzymology. Academic Press; 2008. p. 177–89.

204. Kumari M, Schoiswohl G, Chitraju C, Paar M, Cornaciu I, Rangrez AY, et al. Adiponutrin functions as a nutritionally regulated lysophosphatidic acid acyltransferase. Cell Metab. 2012 May 2;15(5):691–702.

205. Triebl A, Trötzmüller M, Eberl A, Hanel P, Hartler J, Köfeler HC. Quantitation of phosphatidic acid and lysophosphatidic acid molecular species using hydrophilic

interaction liquid chromatography coupled to electrospray ionization high resolution mass spectrometry. J Chromatogr A [Internet]. 2014 Jun 20 [cited 2021 Mar 5];1347:104–10. Available from: /pmc/articles/PMC6013042/

206. Hartler J, Trötzmüller M, Chitraju C, Spener F, Köfeler HC, Thallinger GG. Lipid data analyzer: Unattended identification and quantitation of lipids in LC-MS data. Bioinformatics [Internet]. 2011 Feb [cited 2021 Mar 5];27(4):572–7. Available from: https://pubmed.ncbi.nlm.nih.gov/21169379/

207. Whitmarsh AJ. Regulation of gene transcription by mitogen-activated protein kinase signaling pathways. Vol. 1773, Biochimica et Biophysica Acta - Molecular Cell Research. Elsevier; 2007. p. 1285–98.

208. Kawamoto Y, Seo R, Murai N, Hiyama H, Oka H. Identification of potent lysophosphatidic acid receptor 5 (LPA5) antagonists as potential analgesic agents. Bioorganic Med Chem [Internet]. 2018 Jan 1 [cited 2021 May 27];26(1):257–65. Available from: https://pubmed.ncbi.nlm.nih.gov/29208511/

209. van Corven EJ, van Rijswijk A, Jalink K, van der Bend RL, van Blitterswijk WJ, Moolenaar WH. Mitogenic action of lysophosphatidic acid and phosphatidic acid on fibroblasts. Dependence on acyl-chain length and inhibition by suramin. Biochem J [Internet]. 1992 Jan 1;281(1):163–9. Available from: https://portlandpress.com/biochemj/article/281/1/163/27588/Mitogenic-action-of-lysophosphatidic-acid-and

210. Devanney NA, Stewart AN, Gensel JC. Microglia and macrophage metabolism in CNS injury and disease: The role of immunometabolism in neurodegeneration and neurotrauma. Vol. 329, Experimental Neurology. Academic Press Inc.; 2020. p. 113310.

211. Tu D, Gao Y, Yang R, Guan T, Hong JS, Gao HM. The pentose phosphate pathway regulates chronic neuroinflammation and dopaminergic neurodegeneration. J Neuroinflammation [Internet]. 2019 Dec 5 [cited 2021 May 25];16(1):1–17. Available from: https://doi.org/10.1186/s12974-019-1659-1

212. Holland R, McIntosh AL, Finucane OM, Mela V, Rubio-Araiz A, Timmons G, et al. Inflammatory microglia are glycolytic and iron retentive and typify the microglia in APP/PS1 mice. Brain Behav Immun [Internet]. 2018 Feb;68:183–96. Available from: https://linkinghub.elsevier.com/retrieve/pii/S0889159117304737

213. Baardman J, Verberk SGS, Prange KHM, van Weeghel M, van der Velden S, Ryan DG, et al. A Defective Pentose Phosphate Pathway Reduces Inflammatory Macrophage Responses during Hypercholesterolemia. Cell Rep [Internet]. 2018 Nov 20 [cited 2018 Dec 14];25(8):2044-2052.e5. Available from: https://linkinghub.elsevier.com/retrieve/pii/S2211124718316966

214. Pålsson-McDermott EM, O'Neill LAJ. Targeting immunometabolism as an anti-inflammatory strategy. Cell Res [Internet]. 2020 Apr 4;30(4):300–14. Available from: http://www.nature.com/articles/s41422-020-0291-z

215. Mirzoyan K, Denis C, Casemayou A, Gilet M, Marsal D, Goudounéche D, et al. Lysophosphatidic Acid Protects Against Endotoxin-Induced Acute Kidney Injury. Inflammation [Internet]. 2017 Oct 30;40(5):1707–16. Available from:

http://link.springer.com/10.1007/s10753-017-0612-7

216. Schmitz K, Brunkhorst R, de Bruin N, Mayer CA, Häussler A, Ferreiros N, et al. Dysregulation of lysophosphatidic acids in multiple sclerosis and autoimmune encephalomyelitis. Acta Neuropathol Commun [Internet]. 2017 Dec 2;5(1):42. Available from: http://actaneurocomms.biomedcentral.com/articles/10.1186/s40478-017-0446-4

217. Awada R, Saulnier-Blache JS, Grès S, Bourdon E, Rondeau P, Parimisetty A, et al. Autotaxin Downregulates LPS-Induced Microglia Activation and Pro-Inflammatory Cytokines Production. J Cell Biochem [Internet]. 2014 Dec 1 [cited 2019 Sep 12];115(12):2123–32. Available from: http://doi.wiley.com/10.1002/jcb.24889

218. Ciesielska A, Hromada-Judycka A, Ziemlińska E, Kwiatkowska K. Lysophosphatidic acid up-regulates IL-10 production to inhibit TNF-α synthesis in Mϕs stimulated with LPS. J Leukoc Biol [Internet]. 2019 Dec 1 [cited 2021 Jan 8];106(6):1285–301. Available from: https://pubmed.ncbi.nlm.nih.gov/31335985/

219. Chien HY, Lu CS, Chuang KH, Kao PH, Wu YL. Attenuation of LPS-induced cyclooxygenase-2 and inducible NO synthase expression by lysophosphatidic acid in macrophages. Innate Immun [Internet]. 2015 Aug 3 [cited 2021 Mar 9];21(6):635–46. Available from: http://journals.sagepub.com/doi/10.1177/1753425915576345

220. Trovato FM, Zia R, Napoli S, Wolfer K, Huang X, Morgan PE, et al. Dysregulation of the Lysophosphatidylcholine/Autotaxin/Lysophosphatidic Acid Axis in Acute-on-Chronic Liver Failure Is Associated With Mortality and Systemic Inflammation by Lysophosphatidic Acid–Dependent Monocyte Activation. Hepatology [Internet]. 2021 Jun 15;hep.31738. Available from: https://onlinelibrary.wiley.com/doi/10.1002/hep.31738

221. Song J, Guan M, Zhao Z, Zhang J. Type I Interferons Function as Autocrine and Paracrine Factors to Induce Autotaxin in Response to TLR Activation. Jin D-Y, editor. PLoS One [Internet]. 2015 Aug 27;10(8):e0136629. Available from: https://dx.plos.org/10.1371/journal.pone.0136629

222. Ueda H, Matsunaga H, Olaposi OI, Nagai J. Lysophosphatidic acid: Chemical signature of neuropathic pain. Biochim Biophys Acta - Mol Cell Biol Lipids [Internet]. 2013 Jan;1831(1):61–73. Available from: https://linkinghub.elsevier.com/retrieve/pii/S1388198112001850

223. Santos-Nogueira E, Lopez-Serrano C, Hernandez J, Lago N, Astudillo AM, Balsinde J, et al. Activation of Lysophosphatidic Acid Receptor Type 1 Contributes to Pathophysiology of Spinal Cord Injury. J Neurosci [Internet]. 2015 Jul 15;35(28):10224–35. Available from: https://www.jneurosci.org/lookup/doi/10.1523/JNEUROSCI.4703-14.2015

224. Crack PJ, Zhang M, Morganti-Kossmann M, Morris AJ, Wojciak JM, Fleming JK, et al. Anti-lysophosphatidic acid antibodies improve traumatic brain injury outcomes. J Neuroinflammation [Internet]. 2014;11(1):37. Available from: http://jneuroinflammation.biomedcentral.com/articles/10.1186/1742-2094-11-37

225. Thirunavukkarasu K, Tan B, Swearingen CA, Rocha G, Bui HH, McCann DJ, et al. Pharmacological Characterization of a Potent Inhibitor of Autotaxin in Animal Models of Inflammatory Bowel Disease and Multiple Sclerosis. J Pharmacol Exp Ther [Internet]. 2016 Sep 15;359(1):207–14. Available from:

http://jpet.aspetjournals.org/cgi/doi/10.1124/jpet.116.234013

226. Sapkota A, Lee C-H, Park SJ, Choi JW. Lysophosphatidic Acid Receptor 5 Plays a Pathogenic Role in Brain Damage after Focal Cerebral Ischemia by Modulating Neuroinflammatory Responses. Cells [Internet]. 2020 Jun 10;9(6):1446. Available from: https://www.mdpi.com/2073-4409/9/6/1446

227. Guevara-Cruz M, Flores-López AG, Aguilar-López M, Sánchez-Tapia M, Medina-Vera I, Díaz D, et al. Improvement of Lipoprotein Profile and Metabolic Endotoxemia by a Lifestyle Intervention That Modifies the Gut Microbiota in Subjects With Metabolic Syndrome. J Am Heart Assoc [Internet]. 2019 Sep 3;8(17). Available from: https://www.ahajournals.org/doi/10.1161/JAHA.119.012401

228. An D, Hao F, Zhang F, Kong W, Chun J, Xu X, et al. CD14 is a key mediator of both lysophosphatidic acid and lipopolysaccharide induction of foam cell formation. J Biol Chem [Internet]. 2017 Sep 1 [cited 2021 May 16];292(35):14391–400. Available from: http://www.jbc.org/article/S0021925820341806/fulltext

229. Ninou I, Magkrioti C, Aidinis V. Autotaxin in Pathophysiology and Pulmonary Fibrosis. Front Med [Internet]. 2018 Jun 13;5. Available from: https://www.frontiersin.org/article/10.3389/fmed.2018.00180/full

230. Gierse J, Thorarensen A, Beltey K, Bradshaw-Pierce E, Cortes-Burgos L, Hall T, et al. A novel autotaxin inhibitor reduces lysophosphatidic acid levels in plasma and the site of inflammation. J Pharmacol Exp Ther. 2010;334(1):310–7.

231. Bhave SR, Dadey DYA, Karvas RM, Ferraro DJ, Kotipatruni RP, Jaboin JJ, et al. Autotaxin inhibition with PF-8380 enhances the radiosensitivity of human and murine glioblastoma cell lines. Front Oncol [Internet]. 2013 Sep 17 [cited 2021 May 25];3 SEP:236. Available from: www.frontiersin.org

232. Joncour A, Desroy N, Housseman C, Bock X, Bienvenu N, Cherel L, et al. Discovery, Structure–Activity Relationship, and Binding Mode of an Imidazo[1,2- a]pyridine Series of Autotaxin Inhibitors. J Med Chem [Internet]. 2017 Sep 14;60(17):7371–92. Available from: https://pubs.acs.org/doi/10.1021/acs.jmedchem.7b00647

233. Maher TM, van der Aar EM, Van de Steen O, Allamassey L, Desrivot J, Dupont S, et al. Safety, tolerability, pharmacokinetics, and pharmacodynamics of GLPG1690, a novel autotaxin inhibitor, to treat idiopathic pulmonary fibrosis (FLORA): a phase 2a randomised placebo-controlled trial. Lancet Respir Med [Internet]. 2018 Aug;6(8):627–35. Available from: https://linkinghub.elsevier.com/retrieve/pii/S2213260018301814

234. Lin M-E, Rivera RR, Chun J. Targeted deletion of LPA5 identifies novel roles for lysophosphatidic acid signaling in development of neuropathic pain. J Biol Chem [Internet]. 2012 May 18 [cited 2019 May 16];287(21):17608–17. Available from: http://www.ncbi.nlm.nih.gov/pubmed/22461625

235. Plastira I, Bernhart E, Goeritzer M, Reicher H, Kumble VB, Kogelnik N, et al. 1-Oleyl-lysophosphatidic acid (LPA) promotes polarization of BV-2 and primary murine microglia towards an M1-like phenotype. J Neuroinflammation [Internet]. 2016 Dec 26 [cited 2019 Feb 8];13(1):205. Available from: http://jneuroinflammation.biomedcentral.com/articles/10.1186/s12974-016-0701-9

236. Plastira I, Joshi L, Bernhart E, Schoene J, Specker E, Nazare M, et al. Small-Molecule Lysophosphatidic Acid Receptor 5 (LPAR5) Antagonists: Versatile Pharmacological Tools to Regulate Inflammatory Signaling in BV-2 Microglia Cells. Front Cell Neurosci [Internet]. 2019 Nov 29 [cited 2021 May 25];13:531. Available from: www.frontiersin.org

237. Salgado-Polo F, Perrakis A. The Structural Binding Mode of the Four Autotaxin Inhibitor Types that Differentially Affect Catalytic and Non-Catalytic Functions. Cancers (Basel) [Internet]. 2019 Oct 16;11(10):1577. Available from: https://www.mdpi.com/2072-6694/11/10/1577

238. Jurga AM, Paleczna M, Kuter KZ. Overview of General and Discriminating Markers of Differential Microglia Phenotypes. Front Cell Neurosci [Internet]. 2020 Aug 6;14. Available from: https://www.frontiersin.org/article/10.3389/fncel.2020.00198/full

239. Herr DR, Chew WS, Satish RL, Ong W-Y. Pleotropic Roles of Autotaxin in the Nervous System Present Opportunities for the Development of Novel Therapeutics for Neurological Diseases. Mol Neurobiol [Internet]. 2020 Jan 30;57(1):372–92. Available from: http://link.springer.com/10.1007/s12035-019-01719-1

240. Awada R, Rondeau P, Grès S, Saulnier-Blache JS, Lefebvre d'Hellencourt C, Bourdon E. Autotaxin protects microglial cells against oxidative stress. Free Radic Biol Med [Internet]. 2012 Jan;52(2):516–26. Available from: https://linkinghub.elsevier.com/retrieve/pii/S0891584911012019

241. D'Souza K, Nzirorera C, Cowie AM, Varghese GP, Trivedi P, Eichmann TO, et al. Autotaxin-LPA signaling contributes to obesity-induced insulin resistance in muscle and impairs mitochondrial metabolism. J Lipid Res [Internet]. 2018 Oct;59(10):1805–17. Available from: https://linkinghub.elsevier.com/retrieve/pii/S0022227520341742

242. Nishimura S, Nagasaki M, Okudaira S, Aoki J, Ohmori T, Ohkawa R, et al. ENPP2 Contributes to Adipose Tissue Expansion and Insulin Resistance in Diet-Induced Obesity. Diabetes [Internet]. 2014 Dec 1;63(12):4154–64. Available from: http://diabetes.diabetesjournals.org/cgi/doi/10.2337/db13-1694

243. Henn A. The suitability of BV2 cells as alternative model system for primary microglia cultures or for animal experiments examining brain inflammation. ALTEX [Internet]. 2009;83–94. Available from: https://www.altex.org/index.php/altex/article/view/623

244. Timmerman R, Burm SM, Bajramovic JJ. An Overview of in vitro Methods to Study Microglia. Front Cell Neurosci [Internet]. 2018 Aug 6;12. Available from: https://www.frontiersin.org/article/10.3389/fncel.2018.00242/full

245. Blasi E, Barluzzi R, Bocchini V, Mazzolla R, Bistoni F. Immortalization of murine microglial cells by a v-raf / v-myc carrying retrovirus. J Neuroimmunol [Internet]. 1990 May;27(2–3):229–37. Available from: https://linkinghub.elsevier.com/retrieve/pii/016557289090073V

246. Gupta VK, Jaiswara PK, Sonker P, Rawat SG, Tiwari RK, Kumar A. Lysophosphatidic acid promotes survival of T lymphoma cells by altering apoptosis and glucose metabolism. Apoptosis [Internet]. 2020;25(1–2):135–50. Available from: https://doi.org/10.1007/s10495-019-01585-1

247. Radhakrishnan R, Ha JH, Jayaraman M, Liu J, Moxley KM, Isidoro C, et al. Ovarian cancer cell-derived lysophosphatidic acid induces glycolytic shift and cancer-associated

fibroblast-phenotype in normal and peritumoral fibroblasts. Cancer Lett [Internet]. 2019 Feb;442:464–74. Available from: https://linkinghub.elsevier.com/retrieve/pii/S030438351830689X

248. Mukherjee A, Ma Y, Yuan F, Gong Y, Fang Z, Mohamed EM, et al. Lysophosphatidic Acid Up-Regulates Hexokinase II and Glycolysis to Promote Proliferation of Ovarian Cancer Cells. Neoplasia [Internet]. 2015 Sep;17(9):723–34. Available from: https://linkinghub.elsevier.com/retrieve/pii/S1476558615001165

249. Ha JH, Radhakrishnan R, Jayaraman M, Yan M, Ward JD, Fung K-M, et al. LPA Induces Metabolic Reprogramming in Ovarian Cancer via a Pseudohypoxic Response. Cancer Res [Internet]. 2018 Apr 15;78(8):1923–34. Available from: http://cancerres.aacrjournals.org/lookup/doi/10.1158/0008-5472.CAN-17-1624

250. Butovsky O, Jedrychowski MP, Moore CS, Cialic R, Lanser AJ, Gabriely G, et al. Identification of a unique TGF-β–dependent molecular and functional signature in microglia. Nat Neurosci [Internet]. 2014 Jan 8;17(1):131–43. Available from: http://www.nature.com/articles/nn.3599

251. Paolicelli RC, Angiari S. Microglia immunometabolism: From metabolic disorders to single cell metabolism. Semin Cell Dev Biol [Internet]. 2019 Oct;94:129–37. Available from: https://linkinghub.elsevier.com/retrieve/pii/S1084952118300910

252. Nagy AM, Fekete R, Horvath G, Koncsos G, Kriston C, Sebestyen A, et al. Versatility of microglial bioenergetic machinery under starving conditions. Biochim Biophys Acta - Bioenerg. 2018 Mar 1;1859(3):201–14.

253. Lynch MA. Can the emerging field of immunometabolism provide insights into neuroinflammation? Prog Neurobiol. 2019 Nov;101719.

254. Fan K, Lin L, Ai Q, Wan J, Dai J, Liu G, et al. Lipopolysaccharide-Induced Dephosphorylation of AMPK-Activated Protein Kinase Potentiates Inflammatory Injury via Repression of ULK1-Dependent Autophagy. Front Immunol [Internet]. 2018 Jun 25;9. Available from: https://www.frontiersin.org/article/10.3389/fimmu.2018.01464/full

255. Marschallinger J, Iram T, Zardeneta M, Lee SE, Lehallier B, Haney MS, et al. Lipid-droplet-accumulating microglia represent a dysfunctional and proinflammatory state in the aging brain. Nat Neurosci [Internet]. 2020 Feb 20;23(2):194–208. Available from: http://www.nature.com/articles/s41593-019-0566-1

256. Kim J, Guan K-L. mTOR as a central hub of nutrient signalling and cell growth. Nat Cell Biol [Internet]. 2019 Jan 2;21(1):63–71. Available from: http://www.nature.com/articles/s41556-018-0205-1

257. Mossmann D, Park S, Hall MN. mTOR signalling and cellular metabolism are mutual determinants in cancer. Nat Rev Cancer [Internet]. 2018 Dec 13;18(12):744–57. Available from: http://www.nature.com/articles/s41568-018-0074-8

258. Brose SA, Marquardt AL, Golovko MY. Fatty acid biosynthesis from glutamate and glutamine is specifically induced in neuronal cells under hypoxia. J Neurochem [Internet]. 2014 May;129(3):400–12. Available from: http://doi.wiley.com/10.1111/jnc.12617

259. Rojo AI, McBean G, Cindric M, Egea J, López MG, Rada P, et al. Redox Control of

Microglial Function: Molecular Mechanisms and Functional Significance. Antioxid Redox Signal [Internet]. 2014 Oct 20;21(12):1766–801. Available from: http://www.liebertpub.com/doi/10.1089/ars.2013.5745

260. Cuadrado A, Rojo AI, Wells G, Hayes JD, Cousin SP, Rumsey WL, et al. Therapeutic targeting of the NRF2 and KEAP1 partnership in chronic diseases. Nat Rev Drug Discov [Internet]. 2019 Apr 4 [cited 2019 May 17];18(4):295–317. Available from: http://www.nature.com/articles/s41573-018-0008-x

261. Rosito M, Testi C, Parisi G, Cortese B, Baiocco P, Di Angelantonio S. Exploring the Use of Dimethyl Fumarate as Microglia Modulator for Neurodegenerative Diseases Treatment. Antioxidants [Internet]. 2020 Aug 3;9(8):700. Available from: https://www.mdpi.com/2076-3921/9/8/700

262. Vilhardt F, Haslund-Vinding J, Jaquet V, McBean G. Microglia antioxidant systems and redox signalling. Br J Pharmacol [Internet]. 2017 Jun;174(12):1719–32. Available from: http://doi.wiley.com/10.1111/bph.13426

263. Palmer CS, Ostrowski M, Balderson B, Christian N, Crowe SM. Glucose Metabolism Regulates T Cell Activation, Differentiation, and Functions. Front Immunol [Internet]. 2015 Jan 22;6. Available from: http://journal.frontiersin.org/article/10.3389/fimmu.2015.00001/abstract

264. Lauro C, Limatola C. Metabolic Reprograming of Microglia in the Regulation of the Innate Inflammatory Response. Front Immunol | www.frontiersin.org [Internet]. 2020 [cited 2020 Jul 10];1:493. Available from: www.frontiersin.org

265. Lynch MA. Can the emerging field of immunometabolism provide insights into neuroinflammation? Prog Neurobiol [Internet]. 2020 Jan;184:101719. Available from: https://linkinghub.elsevier.com/retrieve/pii/S0301008219303375

266. Van den Bossche J, Baardman J, Otto NA, van der Velden S, Neele AE, van den Berg SM, et al. Mitochondrial Dysfunction Prevents Repolarization of Inflammatory Macrophages. Cell Rep [Internet]. 2016 Oct;17(3):684–96. Available from: https://linkinghub.elsevier.com/retrieve/pii/S221112471631213X

267. Hsieh C-F, Liu C-K, Lee C-T, Yu L-E, Wang J-Y. Acute glucose fluctuation impacts microglial activity, leading to inflammatory activation or self-degradation. Sci Rep [Internet]. 2019 Dec 29;9(1):840. Available from: http://www.nature.com/articles/s41598-018-37215-0

268. Mills EL, Kelly B, Logan A, Costa ASH, Varma M, Bryant CE, et al. Succinate Dehydrogenase Supports Metabolic Repurposing of Mitochondria to Drive Inflammatory Macrophages. Cell [Internet]. 2016 Oct;167(2):457-470.e13. Available from: https://linkinghub.elsevier.com/retrieve/pii/S009286741631162X

269. Yang S, Qin C, Hu ZW, Zhou LQ, Yu HH, Chen M, et al. Microglia reprogram metabolic profiles for phenotype and function changes in central nervous system. Vol. 152, Neurobiology of Disease. Academic Press Inc.; 2021. p. 105290.

270. Bolanos J, Garcia-Nogales P, Almeida A. Provoking Neuroprotection by Peroxynitrite. Curr Pharm Des [Internet]. 2004 Mar 1;10(8):867–77. Available from: http://www.eurekaselect.com/openurl/content.php?genre=article&issn=1381-

6128&volume=10&issue=8&spage=867

271. Mehla K, Singh PK. Metabolic Regulation of Macrophage Polarization in Cancer. Trends in Cancer [Internet]. 2019 Dec;5(12):822–34. Available from: https://linkinghub.elsevier.com/retrieve/pii/S2405803319302006

272. Peruzzotti-Jametti L, Pluchino S. Targeting Mitochondrial Metabolism in Neuroinflammation: Towards a Therapy for Progressive Multiple Sclerosis. Trends Mol Med [Internet]. 2018 Oct;24(10):838–55. Available from: https://linkinghub.elsevier.com/retrieve/pii/S1471491418301461

273. Kim J-H, Na H-J, Kim C-K, Kim J-Y, Ha K-S, Lee H, et al. The non-provitamin A carotenoid, lutein, inhibits NF-κB-dependent gene expression through redox-based regulation of the phosphatidylinositol 3-kinase/PTEN/Akt and NF-κB-inducing kinase pathways: Role of H2O2 in NF-κB activation. Free Radic Biol Med [Internet]. 2008 Sep;45(6):885–96. Available from: https://linkinghub.elsevier.com/retrieve/pii/S0891584908003729

274. Pawate S, Shen Q, Fan F, Bhat NR. Redox regulation of glial inflammatory response to lipopolysaccharide and interferon? J Neurosci Res [Internet]. 2004 Aug 15;77(4):540–51. Available from: https://onlinelibrary.wiley.com/doi/10.1002/jnr.20180

275. Torres M. Mitogen-activated protein kinase pathways in redox signaling. Front Biosci [Internet]. 2003;8(4):999. Available from: https://fbscience.com/Landmark/articles/10.2741/999

276. Nagy C, Haschemi A. Time and Demand are Two Critical Dimensions of Immunometabolism: The Process of Macrophage Activation and the Pentose Phosphate Pathway. Front Immunol [Internet]. 2015 [cited 2019 Jan 22];6:164. Available from: http://www.ncbi.nlm.nih.gov/pubmed/25904920

Appendix I

Reagent	**Company**
1-Oleoyl-2-hydroxy-sn-glycero-3-phosphate (LPA)	Sigma Aldrich, St. Louis, MO, USA (Cat: L7260)
Acrylamide	Thermo Fisher Scientific, Waltham, USA
Ammoniumpersulfate (APS)	Sigma Aldrich, St. Louis, MO, USA
Aprotinin	Sigma Aldrich, St. Louis, MO, USA
Bis-Acrylamide	Sigma Aldrich, St. Louis, MO, USA
Dimethyl sulfoxide (DMSO)	Sigma Aldrich, St. Louis, MO, USA
DMEM (Dulbecco's modified Eagle's medium) + GlutaMAX	Invitrogen, Waltham, MA, USA (Cat: 61965-026)
Ethylenediaminetetraacetic Acid	Sigma Aldrich, St. Louis, MO, USA
Fetal Calf Serum (FCS)	Sigma Aldrich, St. Louis, MO, USA
Glutamine	Invitrogen, Waltham, MA, USA
Glycerol	Sigma Aldrich, St. Louis, MO, USA
HaltTM Phosphatase Inhibitor	Thermo Fisher Scientific, Waltham, MA, USA

Cocktail	
KCl	Sigma Aldrich, St. Louis, MO, USA
KH2PO4	Sigma Aldrich, St. Louis, MO, USA
Leupeptin	Sigma Aldrich, St. Louis, MO, USA
LPS from E. coli (O111:B4)	Sigma Aldrich, St. Louis, MO, USA (Cat: L2630)
Mercaptoethanol	Sigma Aldrich, St. Louis, MO, USA
Methanol	New England Biolabs, Ipswich, MA, USA
Na2HPO4	Sigma Aldrich, St. Louis, MO, USA
Penicillin	Invitrogen, Waltham, MA, USA
Pepstatin	Sigma Aldrich, St. Louis, MO, USA
PF 8380	Echelon (Cat: B-0702)
Phenylmethylsulfonylfluorid (PMSF)	Sigma Aldrich, St. Louis, MO, USA
Recombinant murine IL-4	Peprotech, Rocky Hill, NJ, USA
RPMI 1640 Cell Culture Medium	Invitrogen, Waltham, MA, USA (Cat: 21875-034)
Sodium Chloride (NaCl)	Sigma Aldrich, St. Louis, MO, USA
Sodium Dodecyl Sulfate (SDS)	Sigma Aldrich, St. Louis, MO, USA
Sodium Fluoride (NaF)	Sigma Aldrich, St. Louis, MO, USA
Sodium Orthovanadate (Na3VO4)	Sigma Aldrich, St. Louis, MO, USA
Streptomycin	Invitrogen, Waltham, MA, USA
Tetramethylethylenediamine (Temed)	New England Biolabs, Ipswich, MA, USA
Tris-HCl	Sigma Aldrich, St. Louis, MO, USA
TritonX	Sigma Aldrich, St. Louis, MO, USA
Trypsin 0.05%, phenol red (for BV2)	Thermo Fisher Scientific, Waltham, USA (Cat: 2530054)
Trypsin 0.25% (for PMM)	Thermo Fisher Scientific, Waltham, USA (Cat: 15050065)
Tween 20	Sigma Aldrich, St. Louis, MO, USA

Antibodies

Antibody	Company	Cat no	Dilution
ACC	Cell Signaling Technology	cs-3676	1:1000
Akt	Cell Signaling Technology	cs-9272	1:1000
AMPK	Cell Signaling Technology	cs-2532	1:1000
Arg1	Cell signaling technologies	cs9879	1:1000
Autotaxin (E-12)	Santa Cruz Biotechnology Inc	sc374222	1:500
Bax	Cell signaling technologies	cs2772	1:1000
Bcl2 (D17C4)	Cell signaling technologies	cs3498	1:1000
c-Jun	Santa Cruz Biotechnology Inc	sc1694	1:500
COX2	Cell signaling technologies	cs12282	1:500
GCLm	Santa Cruz Biotechnology Inc	sc166603	1:1000
GFAP	Cell signaling technologies	cs80788	1:1000
HIF1α	Cell Signaling Technology	cs-14179	1:1000
Iba1	Fujifilm Wako Chemicals	019-19741	1:1000
JNK	Cell signaling technologies	cs9252	1:1000
LPAR1	Cayman Chemicals	10005280	1:250

LPAR2	Abgent	AP6140a	1:250
LPAR3	Cayman Chemicals	10004840	1:400
LPAR4	Santa Cruz Biotechnology Inc	sc46021	1:500
LPAR5	Merck Millipore	ABT114	1:500
LPAR6	Abcam, Cambridge, UK	ab85894	1:500
mTOR	Cell Signaling Technology	cs-2972	1:1000
p38	Cell signaling technologies	cs9212	1:1000
p65	Cell signaling technologies	cs4764	1:1000
pc-Jun Ser63	Cell signaling technologies	cs9261	1:500
PFKFB3	Cell signaling technologies	cs13123	1:1000
Phosho mTOR (Ser 2448)	Cell Signaling Technology	cs5536	1:1000
Phospho ACC (Ser 79)	Cell Signaling Technology	cs-3661	1:1000
Phospho Akt (Ser 473)	Cell Signaling Technology	cs-4060	1:1000
Phospho AMPK (Thr 172)	Cell Signaling Technology	cs-2535	1:500
Phospho NRF2 (Ser40)	Abcam, Cambridge, UK	ab76026	1:1000
Phospho SREBP (Ser 372)	Cell Signaling Technology	cs-9874	1:1000
pJNK Thr183/Tyr185	Cell signaling technologies	cs9251	1:500
pp38 Thr180/Tyr182	Cell signaling technologies	cs4511	1:500
pp65 Ser536	Cell signaling technologies	cs3033	1:500
pSTAT1 Ser727	Cell signaling technologies	cs8826	1:1000
pSTAT6	Cell signaling technologies	cs56554	1:1000
SREBP1	Abcam, Cambridge, UK	ab44153	1:1000
STAT1	Cell signaling technologies	cs14994	1:1000
STAT6	Cell signaling technologies	cs9362	1:1000
Synaptophysin	Agilent Dako	GA660	1:3000
TLR4	Santa Cruz Biotechnology Inc	sc293072	1:500
β-actin	Santa Cruz Biotechnology Inc	sc47778	1:5000

Assay kits

Assay kit	Company	Cat no
ABTS ELISA buffer kit	Peprotech, Rocky Hill, NJ, USA	900-K00
Elisa Development Kit ABTS Murine IL-1 beta	Peprotech, Rocky Hill, NJ, USA	900-M47
Elisa Development Kit ABTS Murine IP-10 (CXCL10)	Peprotech, Rocky Hill, NJ, USA	900-M153
Elisa Development Kit ABTS Murine MIP-2 (CXCL2)	Peprotech, Rocky Hill, NJ, USA	900-M152
Elisa Development Kit Murine IL-6 (TMB EDK)	Peprotech, Rocky Hill, NJ, USA	900-M50
Elisa Development Kit Murine Rantes (CCL5) (TMB EDK)	Peprotech, Rocky Hill, NJ, USA	900-M124
Elisa Development Kit Murine TNF alpha (TMB EDK)	Peprotech, Rocky Hill, NJ, USA	900-M54
EnzyChrom Glycolysis kit	BioAssay Systems, USA	ECGL100

Immobilon Western Chemiluminescent Substrate	Merck Millipore	WBKLS0500
LDH Cytotoxicity Assay Kit	Cayman Chemical, MI, USA	Cay601170-480
NADP/NADPH Assay Kit	Abcam, Cambridge, UK	ab65349
Nitric Oxide (Total) Detection Kit	Enzo Life Sciences (ELS) AG, Lausen, Switzerland	ADI-917-020
Phospholipase D Activity assay kit	Sigma Aldrich, St. Louis, MO, USA	MAK137-1KT
Pierce BCA Protein Assay Kit	Thermo Fisher Scientific, Waltham, USA	1074-1395
Pierce ECL Plus Western Blotting Substrate	Thermo Fisher Scientific, Waltham, USA	32132
Pierce ECL Western Blotting Substrate	Thermo Fisher Scientific, Waltham, USA	10455145

Solutions / Buffers/ WB gel

Acrylamide-Bis (100mL)	Acrylamide 30g, Bis-Acrylamide 0.8g
Blocking Solution	Low-fat Milk Powder 5g, Wash Buffer 100mL
Blotting Buffer (1L)	Tris 1.21g, Glycine 3.0g, Methanol 200mL
PAGE Running Gel (per Gel)	Acrylamide-Bis 2.9mL, 1.5M Tris Buffer pH 8.8 2.17mL, H2O 3.53mL, SDS 10% 86µL, Temed 4.36µL, APS 10% 76 µL
PAGE Stacking Gel (per Gel)	Acrylamide-Bis 0.326mL, 0.5M Tris-Buffer pH 6.8 0.5mL, Glycerol 50% 1.65mL, SDS 10 % 21.5µL, Temed 1.25µL, APS10% 19µL
PBS buffer (1L)	NaCl 8g, KCl 0.2g, Na2HPO4 2.2g, KH2PO4 0.2g
Ripa Buffer pH 7.4 (100mL)	Tris 605.7mg, NaCl 876.6mg, EDTA 37.22mg, NP-40 1% 1g, Na3VO4 [200mM] 500µL, NaF [200mM] 500µL
Sample Buffer pH 6.8	Glycerol 10mL, SDS 2.15g, Tris 0.76g, Mercaptoethanol 2.25mL, Bromphenol Blue
SDS-PAGE Running Buffer (1L)	Tris 3.03g, Glycine 15.01g, SDS 1g
Stripping Buffer pH 6.8 (0.5L)	Tris HCl 3.63g, SDS 10g, Mercaptoethanol 3.5mL
TBST Buffer pH 7.5 (1L)	Tris 3.03g, NaCl 8.77g, Tween 20 0.5g,
Wash Buffer pH 7.4 (1L)	Tween 20 0.5g, NaCl 9g, Tris 1.21g
Lysis buffer for brain (1ml /100mg tissue)	100mM Tris (pH 7.4), 150 mM NaCl, 1mM EGTA, 1mM EDTA, 1% Triton X-100, Phosphatase inhibitor cocktail, protease inhibitor cocktail, PMSF

Primers

Gene	**Company**	**Catalogue number**
iNOS	Qiagen	QT00100275
Glut2	Qiagen	QT00103537
Glut3	Qiagen	QT00159691
Glut5	Qiagen	QT00148267
HPRT	Qiagen	QT00166768

Gene	Company	Forward/Reverse Primers
Arg-1	Invitrogen	F: TGGCTTGCGAGACGTAGAC R: GCTCAGGTGAATCGGCCTTTT
TNFα	Invitrogen	F: ACTTCGGGGTGATCGGTCC R: GGCTACAGGCTTGTCACTCG
IL6	Invitrogen	F: TGTTCTCTGGGAAATCGTGGA R: CAAGTGCATCATCGTTGTTCAT
IL1β	Invitrogen	F: CTCTCCACCTCAATGGACAGA R: CGTTGCTTGGTTCTCCTTGT
CXCL10	Invitrogen	F: TTCTGCCTCATCCTGCTG R: AGACATCTCTGCTCATCATTC
CXCL2	Invitrogen	F: AGTGAACTGCGCTGTCAATG R: GCCCTTGAGAGTGGCTATGA
CCL5	Invitrogen	F: GCTGCTTTGCCTACCTCTCC R: TCGAGTGACAAACACGACTGC
GLUT1	Invitrogen	F: CCGTTCTCCGTCTCGCAG R: CTCCCACAGCCAACATGAGG
GLUT4	Invitrogen	F: ATTGTCGGCATGGGTTTCCA R: AGCAGGAGGACGGCAAATAG
Hexokinase 2	Invitrogen	F: ATCGCCTGCTTATTCACGGAG R: TCTGAGAGACGCATGTGGTAG